1

Measurement report: Impact of domestic heating on dust deposition sources in hyper-arid Qaidam Basin, northern Qinghai-Xizang Plateau

Haixia Zhu[abc], Lufei Zhen[abc], Suping Zhao[d*], Xiying Zhang[ab*]

6

7

8

9

10

11

12

[a] *Key Laboratory of Green and High-end Utilization of Salt Lake Resources, Qinghai Institute of Salt Lakes, Chinese Academy of Sciences, Xining, 810008, China.*

[b] *Qinghai Provincial Key Laboratory of Geology and Environment of Salt Lakes, Qinghai Institute of Salt Lakes, Chinese Academy of Sciences, Xining, 810008, China.*

[c] *University of the Chinese Academy of Sciences, Beijing, 100049, China*

[d] *Key Laboratory of Cryospheric Science and Frozen Soil Engineering, Northwest Institute of Eco-Environment and Resources, Chinese Academy of Sciences, Lanzhou, 730000, China*

[*] *Corresponding author. E-mail address: xyzhchina@isl.ac.cn (Xiying Zhang) and zhaosp@lzb.ac.cn (Suping Zhao)*

Highlights

1. The temporal and spatial distribution of carbonaceous aerosols was analyzed using various carbon indicators.

2. Domestic heating significantly increased atmospheric pollutants in rural areas.

3. The unique energy structure in Qaidam Basin significantly influenced the glaciers of the Qinghai-Xizang Plateau and should not be overlooked.

Abstract

Given the unique energy structure of the Qaidam Basin (QDB), this study systematically reveals the spatiotemporal variations in the chemical composition of atmospheric dust deposition and clarifies the key contributions of coal and biomass burning to carbonaceous aerosols, as well as their potential impacts on the Qinghai-Xizang Plateau (QXP) and global atmospheric systems. Monthly dust deposition samples were collected at six sites in the southern QDB between 2020 and 2023. Results indicated heightened carbon emissions and the higher char/soot ratio during the heating period (HP, 5.06 ± 4.08) than the non-heating period (NHP, 4.42 ± 3.09), indicating intensified seasonal solid fuel consumption. Spatially, the organic carbon (OC) and elemental carbon (EC) ratio was significantly lower in urban (3.97 ± 2.04) than that in rural areas (10.99 ± 10.00). Char-EC dominated EC (80.44%), especially in urban areas (85.00%), while secondary organic carbon (SOC) dominated OC (72.61%), particularly in rural areas (87.32%). The coal combustion (15.19%) and biomass burning (33.55%) as major contributors in rural areas, strongly associated with domestic heating, whereas urban dust predominantly originated from traffic (46.83%) and industrial emissions (16.41%). Coal consumption in QDB was greater during the HP relative to other dust sources on the QXP leads to increased atmospheric pollutant emissions, which may accelerate regional glacier melting. Consequently, integrating QDB carbonaceous aerosols into future environmental policies and climate models for the QXP is essential. This study provides a reference for investigating carbonaceous aerosols in climatically similar hyper-arid basins with intensive human activity and salt lake regions.

Keywords: Qinghai-Xizang Plateau; Qaidam Basin; Biomass burning; carbonaceous elements; atmospheric dust deposition.

Short summary

This study collected dust samples from six sites in the Qaidam Basin over three years to investigate the impact of domestic heating on atmospheric dust in hyper-arid region. Our results indicate that rural dust is significantly influenced by heating, particularly from coal and biomass burning, which accounts for over 70% of total sources. The unique energy structure here has resulted in distinct environmental effects from the emitted carbonaceous aerosols and useful for similar dry areas.

1. Introduction

Atmospheric dust comprises solid particles, typically ranging in size from below 1 μm to 100 μm, which may become airborne, depending on their origin, physical characteristics and ambient conditions (Xu, 2014). It is a key component of particulate matter (PM). Within this size spectrum, larger particles (10-100 μm) that settle under gravity are defined as atmospheric dust deposition. Notably, during long-distance transport, these coarse particles can undergo fragmentation into fine particles ($PM_{2.5}$) and subsequently actively participate in atmospheric chemical and climatic processes (Noll and Fang, 1989). As the dominant natural component of PM, atmospheric dust deposition serves not only a crucial indicator of regional air quality but also a key biogeochemical process linking the atmosphere, cryosphere, hydrosphere, and biosphere, with global-scale influences that significantly shape environmental and climate systems (Feng et al., 2019).

Arid and semi-arid regions are the primary global sources of atmospheric dust (Griffin et al., 2002; Schepanski, 2018). Long-distance transport of this dust via wind currents exerts multi-faceted impacts on the environment and human society. A particularly critical effect is the alteration of the cryosphere: dust deposition on snow and ice lowers surface albedo and modifies ice crystal structure, thereby accelerating glacier and snowpack melt (Tuzet et al., 2017). This process disrupts regional snow energy balance, which is directly linked to glacier retreat and water resource security. Dust deposition also influences the atmospheric energy budget by attenuating solar radiation reaching the surface and participates in the global carbon cycle through biogeochemical pathways, such as delivering nutrients to oceans and affecting marine primary productivity (Mahowald et al., 2009; Parajuli et al., 2022). For human health, harmful components associated with dust can induce respiratory and cardiovascular diseases and even damage cellular DNA (Shahram et al., 2016). For terrestrial ecosystems, the shading effect of dust on leaves can inhibit plant photosynthesis and reduce biological productivity.

Given the complexity and regional variability of atmospheric dust impacts, identifying dust sources (source apportionment) is fundamental for understanding its environmental behavior and effects. Recent advancements in understanding PM characteristics, particularly chemical composition (e.g. water-soluble ions, carbonaceous components, and trace elements) and source apportionment, have been driven by the integrated application of methodological tools. These

88   receptor models include principal component analysis (PCA), chemical mass balance (CMB), and

89   positive matrix factorization (PMF) models, are used to quantify source contributions. Specifically,

90   the PMF model mathematically deconstructs the chemical composition matrix of ambient samples

91   to achieve this. Additionally, multivariate statistical approaches like backward trajectory simulations

92   (e.g., the HYSPLIT model) trace air mass transport pathways to identify potential source regions

93   (Lai et al., 2016; Yao et al., 2016; Zhang et al., 2015a). This multi-method approach has greatly

94   enhanced the precision of dust deposition source analysis. For instance, PMF analysis of

95   atmospheric dust in urban areas such as Lanzhou, Taiyuan, and Jinan have identified diverse sources,

96   including coal combustion, industrial emissions, construction dust, windblown dust, vehicle

97   emissions, and resuspended road dust. Seasonal variations indicate that coal combustion during the

98   domestic heating period and regional meteorological conditions significantly influence dust

99   deposition (Hu and Liu, 2022; Chen et al., 2024; Yang et al., 2024; Zhang et al., 2022). These

100 findings underscore the urgency of region-specific pollution control strategies. When considering

101 the global scale, arid and semi-arid regions are unequivocally the dominant sources, contributing

102 over 60% of the global atmospheric dust flux (Zan et al., 2025). Therefore, a comprehensive

103 investigation of atmospheric dust processes in these key regions, encompassing emission intensity,

104 physicochemical properties, transport pathways, and environmental effects, is indispensable for

105 elucidating global dust cycle mechanisms and assessing their profound impacts on the cryosphere

106 (e.g., glacial melting) and regional climate.

107   The Qinghai-Xizang Plateau (QXP) often referred to as the "Roof of the World" due to its

108 immense elevation, plays a crucial role in regulating the regional and global climate by altering

109 large-scale atmospheric circulation. Its vast glaciers and snow cover influence regional energy

110 balance through the albedo effect, and as the source of many major Asian rivers, it is known as the

111 "Asian Water Tower" (Liu et al., 2019; Liu et al., 2020b). However, rapid glacier retreat on the

112 plateau poses risks to the Asian hydrological cycle and the monsoon system, with potential adverse

113 impacts if unchecked (Luo et al., 2020). Beyond climate warming and moistening, black carbon

114 (BC), a light-absorbing carbonaceous aerosol component emitted from incomplete combustion

115 processes of solid and liquid fuels during household cooking, heating, and coke production (Bond

116 et al., 2013), significantly accelerates glacial melt. By depositing on ice, BC reduces surface albedo,

117 enhances radiative absorption and thus raises it temperatures, promoting glacial melt (Bond and

118 Bergstrom, 2006; Chen et al., 2015). Notably, biomass burning in South and Central Asia during

119 winter serves as a major source of BC, further exacerbating glacier decline on the plateau (Zhang et

120 al., 2015b; Zheng et al., 2017; Xu et al., 2018b). In addition to these external sources, local dust

121 sources within the QXP itself remain significant. Among these, the Qaidam Basin (QDB) in the

122 northeastern plateau is a particularly important contributor, identified as a key dust source for the

123 plateau (Wei et al., 2017; Zheng et al., 2021) and a critical, unique arid dust source area.

124   The QDB, known as the "Treasure Basin" of the QXP, is rich in mineral resources (e.g., copper,

125 iron, and tin) as well as abundant oil and gas reserves. It serves as a key economic development

126 zone in northwest China, accounting for approximately 30% of the plateau's industrial and

127 agricultural output despite comprising only about 8% of its registered population (Fu, 2023).

128 Extensive resource extraction has rendered its ecosystem fragile (Li and Sha, 2022), exacerbating

129 the impact of atmospheric pollution. The region is also highly sensitive and vulnerable to climate

130 change, with severe and extreme vulnerability zones covering 45.98% of its area (Xu et al., 2024).

131 Unlike South Asia, Central Asia, and Xizang, where biomass fuels dominate, the QDB relies

132 primarily on distinct mix of coal (about 60%) and biomass fuels like yak dung, firewood (about

133 35%) for winter domestic heating, reflecting a unique energy structure (Liu et al., 2008; Xiao et al.,

134 2015; Behera et al., 2015; Kerimray et al., 2018; Jiang et al., 2020; Shen et al., 2021). The

135 combustion of coal releases significant pollutants, including light-absorbing aerosols like BC and

136 brown carbon (BrC) (Munawer, 2018; Ye et al., 2020; Zhou et al., 2025). Brown carbon refers to

137 organic compounds that can absorb light, particularly at shorter wavelengths, resulting in a reddish

138 orange or brown appearance (Donahue, 2018). Both BC and BrC can influence solar radiation

139 absorption and cloud properties, exerting a positive radiative forcing on climate (Ramanathan and

140 Carmichael, 2008; Bond et al., 2013). When deposited on snow and ice, they further accelerate

141 glacial melt (Qian et al., 2015; Kang et al., 2020a). Additionally, BC and BrC are significant

142 contributors to global warming and can exacerbate adverse health effects by carrying toxic

143 components (Ramanathan and Carmichael, 2008; Shrivastava et al., 2017). Notably, QDB's

144 widespread use of yak dung as a fuel, a practice less common in other coal-intensive heating regions

145 of northern China, releases pollutants like carbon monoxide (CO), volatile organic compounds

146 (VOCs), and polycyclic aromatic hydrocarbons (PAHs), further affecting local air quality and health

147 (Zhang et al., 2022). Consequently, we posit that seasonal carbon emissions in QDB, particularly

7

during winter domestic heating, could exert a unique influence on the climate and ecological stability of the QXP.

The QDB, as a representative arid region with intensive human activity, exhibits climatic and environmental conditions comparable to other hyper-arid basins (e.g., the Tarim and Junggar Basins in Xinjiang, the Great Basin in the United States) and high-altitude salt lake regions (e.g., Uyuni in Bolivia, Atacama in Chile). These regions are characterized by low precipitation, rich mineral resources subject to significant anthropogenic impact, and abundant salt lakes. Research in the Tarim and Junggar Basins has predominantly focused on dust events, their sources, and associated gas emissions (Gao and Washington, 2010; Liu et al., 2016b; Filonchyk et al., 2018; Yu et al., 2019; Zhou et al., 2023). In the Great Basin, studies largely address ozone and dust sources (Hahnenberger and Nicoll, 2012; Vancuren and Gustin, 2015; Miller et al., 2015). Research on salt lake atmospheres has predominantly focused on high-salinity dust emissions resulting from lakebed desiccation due to resource extraction (Löw et al., 2013; Gholampour et al., 2015; Moravek et al., 2019; Christie et al., 2025), with limited research on atmospheric carbon components, their sources, and environmental impacts. Therefore, this research aims to investigate atmospheric carbonaceous aerosols in arid basins with intensive human activity and climates comparable to the QDB, as well as in salt lakes environments.

From January 2020 to March 2023, monthly dust deposition samples were collected at six urban and rural monitoring sites in the southern QDB. Samples were categorized into two seasonal periods: the domestic heating period (HP) and the non-domestic heating period (NHP). Measured parameters included dust deposition flux, soluble ions, trace elements, and key carbonaceous components. The objectives of this study were: (1) to clarify the variation trends of carbonaceous components in atmospheric dust deposition under the unique energy structure of the QDB, and to quantify the contribution of domestic heating; and (2) to identify the major sources of atmospheric dust deposition in the basin and to evaluate their associated environmental impacts. To achieve these aims, we applied OC/EC and char/soot ratios, the HYSPLIT trajectory, and PMF model for source apportionment. Furthermore, these findings offer a scientific basis and reference for examining atmospheric carbonaceous aerosols in arid basins with similar climates and human activities to the QDB, as well as in salt lake regions.

2. Materials and methods

2.1 Sampling

The QDB, situated in the northeastern part of the QXP, is bordered by the Altyn-Tagh, Kunlun, and Qilian mountains, making it one of China's largest intermontane basins (Zhang, 1987). With an average elevation of 3,000 m, the basin features an extremely arid climate characterized by less than 20 mm of annual precipitation in the northwestern region, while evaporation rates exceed 2,000 mm (Feng et al., 2022). The QDB is rich in salt lakes, non-ferrous metals, and hydrocarbon resources, with significant coal deposits. It leads China in reserves of halite, potash, magnesium, lithium, strontium, asbestos, earning it the nickname "Treasure Basin". As a major salt lake resource area, it hosts 33 lakes, including Qarhan, Dachaidan, and Caka Salt Lake, and faces notable conflicts between resource extraction and ecological preservation. Agriculturally, it cultivates crops like goji berries, quinoa, and forage grass, and hosts China's largest resource-rich circular economy pilot zone. The permanent population of the basin is approximately 400,000, primarily using coal, yak dung, and firewood for domestic heating (Jiang et al., 2020). Additionally, annual tourism peaks from May to September, attracting around 17 million visitors (Qinghai Statistical Yearbook, 2023), which likely amplifies atmospheric pollutant emissions.

From January 2020 to March 2023, monthly dust deposition samples were collected from six monitoring stations in the southern QDB. The stations included Xiao Zaohuo (XZH), Golmud (GEM), Da Gele (LTC), Nuo Muhong (NMH), Balong (BLX), and Dulan station (DLX) (Figure 1). Dry deposition collection employed the glass ball method using Marble dust collector (MDCO) designed dust collection cylinders (Sow et al., 2006). The MDCO sampler operates on the principle of gravitational settling. It uses a collection vessel with a known opening to capture particulate matter that settles naturally from the air. In field measurements, surrogate surfaces or deposition traps are commonly employed to better quantify atmospheric deposition. These surfaces mimic the original ground surface, are easy to deploy, and can be integrated without significantly disturbing airflow. Examples include glass beads (Ganor, 1975; Offer et al., 1992), moist filter paper (Goossens and Offer, 1993), plastic surfaces (Gregory, 1961), and water or antifreeze solutions (Smith and Twiss, 1965). The MDCO deposition vessel is based on the original concept of Ganor (1975), using glass beads as a surrogate collection surface. Due to their very low microscopic roughness, the beads

207   help prevent the resuspension of particles once they have been captured (Goossens and Offer, 1993).

208   The stainless steel collection device (50×30×30 cm) contained a plastic sieve container of

209   identical dimensions, with the sieve base positioned 10 cm above the opening and perforated with

210   0.5 cm diameter holes (Figure S1). To minimize dust resuspension during high wind events (Qian

211   and Dong, 2004), two layers of 16 mm glass balls were placed within the sieve container. A high-

212   density polyethylene bag was attached to the base for sample collection. According to Sow et al

213   (2006), the collection efficiency of the MDCO decreases with increasing wind speed, dropping

214   below 20% when wind speed exceeds 3 m/s, and it preferentially collects the finer fraction of

215   atmospheric dust particles ranging from 10 to 31 μm in size (Chow, 1995). Furthermore, collection

216   efficiency decreases significantly as the size of dust-fall increases. Based on our findings, more than

217   50% of the collected dust particles are below 40 μm (Figure S2), whereas the mean particle size of

218   atmospheric dust deposition reported in other studies is approximately 80 μm (Lin et al., 2022a; Lin

219   et al., 2022b). This confirms that the MDCO sampler preferentially collects relatively finer particles.

220   Consequently, this study may place greater emphasis on analyzing the chemical activity of the finer

221   fraction of atmospheric dust, thereby enhancing the detection sensitivity for components such as

222   secondary ions and carbonaceous species in deposited dust. However, this particle-size selectivity

223   introduces a sampling bias that can amplify inter-site differences in deposition flux between sites,

224   complicate local source apportionment, strengthen signals from distant sources (e.g., combustion

225   and vehicle emissions), and weaken the contribution from local, coarse-particle-dominated sources

226   (e.g., resuspended dust and construction dust). These factors may affect the accuracy of both

227   deposition flux estimates and source apportionment. Future research should enhance data

228   comparability and the reliability of ecological assessments through efficiency correction and the

229   combined application of multiple methods. The collection efficiency at each site was calculated

230   based on local dust grain-size distribution and wind speed; details are provided in Supplementary

231   Text S1. This type of collector has been widely used in many studies to evaluate local dust conditions

232   (Abdollahi et al., 2021; Barjoee et al., 2021; Alzahrani et al., 2024).

233   In this study, dust samples were collected monthly, with each sampling period lasting 30 or 31

234   days. The installation height and environment of the samplers are provided in Table S1. To ensure

235   only dry dust was collected, collection devices were manually-operated covered during rain or

236   snowfall. A total of 37, 39, 23, 30, 16, and 29 samples were obtained from XZH, GEM, LTC, NMH,

BLX, and DLX stations, respectively, and no duplicate samples were collected during the sampling period. Laboratory protocols incorporated biannual analyses with negative controls and appropriate control samples. As continuous dust monitoring commenced in 2020, site blanks were evaluated during initial sampling. Stations were classified as Urban (GEM, NMH, DLX) and Rural (XZH, LTC, BLX) based on location characteristics. Consistent with the cold-arid climate in QDB, the HP was defined as October-April, while the NHP spanned May-September.

Materials such as plant remnants, microfauna, and bird droppings were removed from the sample bags with tweezers. The samples were then measured on a balance (0.0001 g) to determine the total dust deposition flux (DF) (Eq. 1) (Yu et al., 2016):

$$M = \frac{m \times 30}{S \times K}, \tag{1}$$

where M is dust deposition [g/(m²·30d)]; m is the sample mass (g); S is the area of the dust collection device (m²); and K is the actual number of sampling days per month (d).
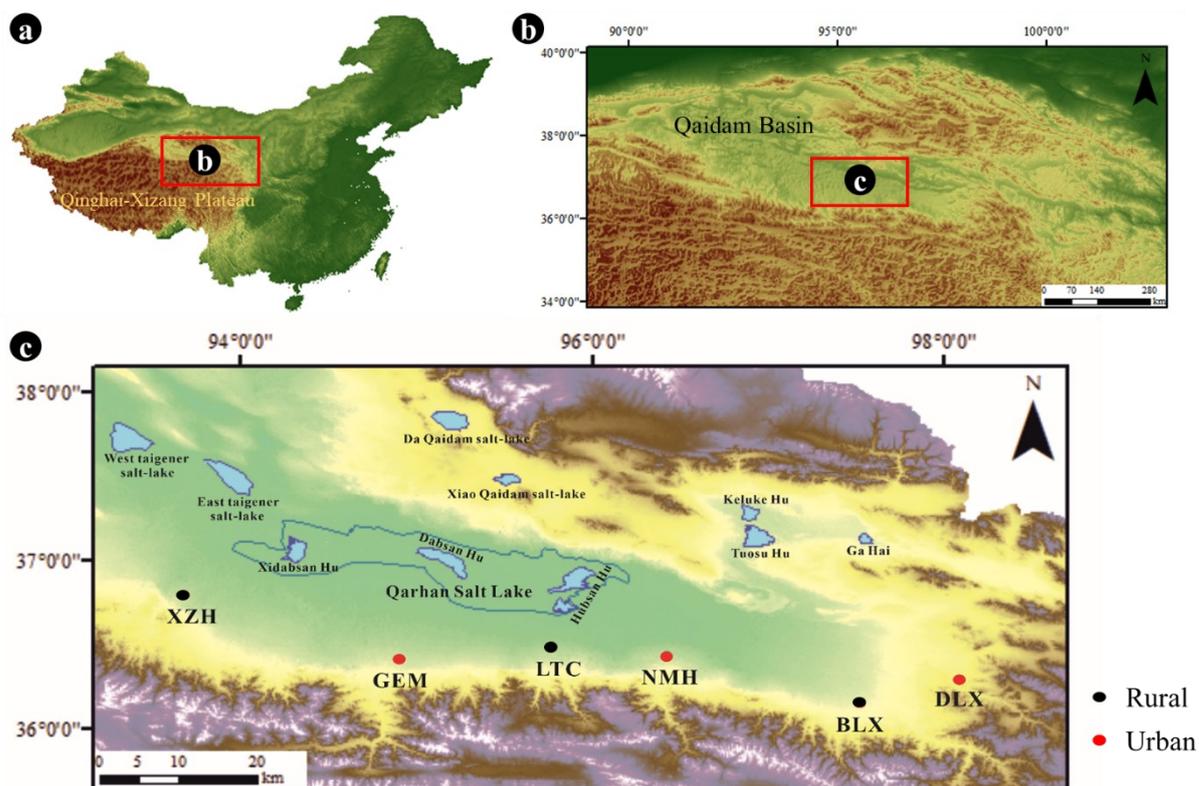
Figure 1. Spatial distribution of monitoring stations in the southern Qaidam Basin. Urban stations (red) and rural stations (black) are labeled as follows: XZH (Xiao Zaohuo), GEM (Golmud), LTC (Da Gele), NMH (Nuo Muhong), BLX (Balong), DLX (Dulan).

2.2 Water-soluble inorganic ions

A 100 mg sample was weighed and transferred into a 250 mL bottle. The mixture underwent ultrasonic extraction for 20 minutes to ensure complete solubilization. The resulting supernatant was then filtered through a 0.45 μm filter for analysis. Based on preliminary experimental results, the concentrations of major ions (K^+, Na^+, Mg^{2+}, and Ca^{2+}) were measured using Inductively Coupled Plasma Optical Emission Spectrometer (ICP-OES, NexIon 2000). Anions (Cl^-, SO_4^{2-}, and NO_3^-) were quantified using ion chromatography (IC). To ensure measurement accuracy, samples were organized in sets of twenty, with one randomly selected sample from each group serving as a replicate, achieving an error margin of less than 10%. The detection limits for the various components were as follows: K^+ (0.0560 mg/L), Na^+ (0.0100 mg/L), Ca^{2+} (0.0037 mg/L), Mg^{2+} (0.0390 mg/L), SO_4^{2-} (0.0090 mg/L), NO_3^- (0.0125 mg/L), Cl^- (0.0100 mg/L). All standard solutions employed in the analysis were sourced from the National Standard Material Center.

2.3 Trace element analysis

According to the Chinese State Standard "Ambient air and waste gas from stationary sources emission-determination of metal elements in ambient particles" (HJ 777-2015), the concentrations of elements such as iron (Fe), aluminum (Al), silicon (Si), titanium (Ti), copper (Cu), cadmium (Cd), chromium (Cr), manganese (Mn), nickel (Ni), zinc (Zn), lead (Pb), and vanadium (V) were quantified using Inductively Coupled Plasma Mass Spectrometry (ICP-MS) and ICP-OES. A dust sample weighing 0.100 g was placed in a Teflon cup, to which 20.0 mL of a nitric acid-hydrochloric acid digestion solution was added. The sample was heated to reflux at $100 \pm 5°C$ for 2 h under a watch glass, then cooled. Following this, the inner walls of the cup were rinsed with water, and approximately 10 mL of water was added, allowing the mixture to stand for 30 minutes for extraction. The extract was then filtered into a 100 mL volumetric flask and diluted to volume with distilled water for analysis. In cases where organic matter content was high, an appropriate amount of hydrogen peroxide was introduced during digestion to decompose the organic materials. Prior to sample analysis, the system was flushed with a rinse solution until the blank intensity value reached a minimum, and samples were analyzed only after the signal stabilized. If the concentration of any element exceeded the calibration range, the sample was diluted and reanalyzed.

2.4 Carbon analysis

This study utilized a combination of wet chemical treatment and thermal/optical reflection (TOR) to analyze carbon elements in dust deposition (Han et al., 2007b; Han et al., 2007a; Han et al., 2016). Dust samples were digested stepwise to remove inorganic materials: first samples were treated with 10 mL of 2 N hydrochloric acid (HCl) for 24 h at room temperature to dissolve carbonates and partial metals, followed by centrifugation (4500 rpm, 12 min) to separate the residue; then with 15 mL of a 1:2 (v/v) mixture of 6 N HCl and 48% hydrofluoric acid (HF) for 24 h at room temperature to dissolve silicates and residual metals; and finally with 15 mL of 4 N HCl for 24 h at 60 °C to remove minerals such as fluorite formed during demineralization. After each step, the mixture was centrifuged, and the supernatant was collected. The solid residue was diluted with 200 mL of deionized water and filtered through a pre-combusted quartz fiber filter (Whatman, 450°C for 4 h, diameter 47 mm) (Han et al., 2007a). This method has been widely applied to measure OC and EC contents in lake sediments and urban soils (Han et al., 2009; Khan et al., 2009; Han et al., 2011). Studies have shown that the EC collection efficiency of this method is approximately 99.6% (Zhan et al., 2013). However, because OC includes polar, basic, and mineral-bound compounds that may dissolve in HCl/HF and be lost during filtration, the supernatant from all three acid-digestion steps was collected and analyzed for water-soluble OC using a carbon-nitrogen analyzer (Shimadzu, TOCN-4200, Japan). Total OC was obtained by summing the dissolved OC and the particulate OC measured by TOR.

The filtered samples were air-dried and analyzed for carbon content using a DRI 2001 thermal/optical carbon analyzer (Atmoslytic Inc., Calabasas, CA) at the Institute of Earth Environment, Chinese Academy of Sciences, adhering to the Interagency Monitoring of Protected Visual Environments (IMPROVE) protocol. A 0.544 cm² disc was extracted from the filter and placed in a quartz boat for analysis. During the carbon analysis, the samples were initially heated in a 100% helium atmosphere, resulting in the production of four organic carbon (OC) fractions (OC1, OC2, OC3, and OC4) at four different temperature levels (140, 280, 480, and 580°C). The atmosphere was subsequently changed to 2% O_2/98% He, generating three elemental carbon (EC) fractions (EC1, EC2, and EC3) at three temperatures (580, 740, and 840 °C). Volatile carbon

underwent carbonization in an anaerobic environment, indicated by a decrease in laser reflectance, and is referred to as pyrolyzed organic carbon (OPC). In the oxidative atmosphere, OPC was emitted along with the original EC from the filter. The amount of OPC is defined as the carbon evolved until the laser reflectance returned to its baseline value (Han et al., 2007b). According to the IMPROVE protocol, EC is calculated as the total of the three EC subfractions minus OPC (i.e., EC is defined as the sum of EC1, EC2, and EC3, with OPC subtracted). The method enables differentiation between soot and char, as determined by the gradual oxidation of these black carbon subtypes in standard reference materials during the EC1 and the EC2 plus EC3 steps, where char is defined as EC1 minus OPC and soot as the sum of EC2 and EC3 (Han et al., 2007a; Han et al., 2016).

Please note that in this manuscript, we interchangeably use the terms "EC" and "BC". While these terms do not strictly refer to the same component, they serve as an adequate approximation within the scope of this study (Seinfeld et al., 1998; Bond et al., 2004). We use "EC" when discussing emissions and modeling components, reserving "BC" for climate-related discussions. Throughout this manuscript, the term "OC" refers to the total organic carbon (sum of the dissolved OC and the particulate OC).

2.5 The particle size analysis

The grain size of dust-fall samples was measured using a laser particle analyzer (Malvern Mastersizer 2000, UK). The particle size distribution was calculated for 100 grain size classes within a range of 0.02-2000 μm. Sample preparation for grain size analysis included wet oxidation of organic matter by adding 10 mL of 30% hydrogen peroxide (H_2O_2) per 1.5 g dry sample. Carbonates were dissolved by boiling with 10 mL (10% HCl) over 10 min. The glass beakers were filled with 150 mL distilled water and suspended particles were left to deposit. After siphoning the supernatant water, 10 mL of 0.05 N sodium hexametaphosphat [$(NaPO_3)_6$] were added, and the residue was dispersed for 5 min in an ultrasonic bath before measurement (Lu and An, 1997). And the results are expressed as volume percentages.

2.6 Collection of Meteorological Factors

Meteorological data used in this study were obtained from the Qinghai Meteorological Bureau

during the sampling period. Monthly meteorological parameters, including wind speed (WS), wind direction (WD), temperature (Temp), relative humidity (RH), Precipitation (RF), sunshine duration (SUN), and the frequency of visibility ≤10 km (VIS), were collected from four national-level meteorological stations: XZH, GEM, DLX, and NMH. All of these stations are standard meteorological observatories established by the state, equipped with standardized monitoring capabilities, and provided continuous and reliable data for this study (https://data.cma.cn). In addition, two atmospheric dust deposition sampling sites (LTC and BLX) were established specifically for collecting dust samples. Due to field-monitoring constraints and research-budget limitations, no meteorological instruments were deployed at these two sites.

2.7 Statistical analysis

2.7.1 Estimation of Secondary Organic Carbon

Organic carbon consists of primary organic carbon (POC) and secondary organic carbon (SOC). Due to the intricate physical and chemical processes involved, SOC in urban atmospheres cannot be directly measured. Therefore, an indirect estimation method, known as the EC tracer method, has been developed (Turpin and Huntzicker, 1991). If the concentrations of OC and EC are available and primary OC from non-combustion sources ($OC_{non-comb}$) can be disregarded, EC can be utilized as a tracer for POC from combustion sources, facilitating the estimation of SOC (Turpin and Huntzicker, 1995):

$$POC=EC\times(OC/EC)_{pri}, \tag{2}$$

$$SOC=OC_{total}-POC, \tag{3}$$

where OC_{total} represents total organic carbon.

Traditional methods for determining $(OC/EC)_{pri}$ involve regressing OC and EC within a fixed percentile range of the lowest (OC/EC) ratio data (typically 5-20%) or relying on sampling days characterized by low photochemical activity and local emissions (Castro et al., 1999; Lim and Turpin, 2002). However, these approaches are limited by their empirical nature, lacking clear quantitative criteria for selecting the data subsets used to establish $(OC/EC)_{pri}$, defined as the hypothetical primary OC/EC ratio. In this study, we employed the minimum R squared (MRS) method (Millet et al., 2005; Wu and Yu, 2016; Wu et al., 2018a) to determine $(OC/EC)_{pri}$. This

method calculates a set of hypothetical $(OC/EC)_{pri}$ and SOC values to identify the minimum correlation coefficient (R^2) between SOC and EC, allowing for the accurate derivation of $(OC/EC)_{pri}$. The computational procedure followed the algorithm developed by Wu and Yu (2016) (available at: https://sites.google.com/site/wuchengust), implemented within the Igor Pro environment (WaveMetrics, Inc., Lake Oswego, OR, USA). Due to the limited dataset size and low temporal resolution, the MRS analysis was performed collectively across all sampling sites. In this approach, the R^2 between SOC and EC was calculated iteratively for a range of $(OC/EC)_{pri}$ values spanning 0 to 10. The minimum R^2 value of 1.33 (Figure S3) identified the optimal $(OC/EC)_{pri}$ representative of the true primary ratio.

2.7.2 Quantifying the contributions of playa salt (ps) and non-playa salt (nps) sources

To differentiate the contributions of salt lake sources to water-soluble ions in atmospheric deposition, we adopted a methodology similar to that used for marine aerosols. This approach relies on the ratio of water-soluble ions (SO_4^{2-}, Ca^{2+}, K^+, Mg^{2+}, Cl^-) to Na^+ in the salt lakes of the QDB, enabling us to assess the contribution of ps-Na^+ components to nps (Zhang, 1987); details in Zhu (2025).

$$nps\text{-}SO_4^{2-}=[SO_4^{2-}]\text{-}0.333\times ps\text{-}Na^+, \tag{4}$$

$$nps\text{-}Ca^{2+}=[Ca^{2+}]\text{-}0.062\times ps\text{-}Na^+, \tag{5}$$

$$nps\text{-}K^+=[K^+]\text{-}0.087\times ps\text{-}Na^+, \tag{6}$$

$$nps\text{-}Mg^{2+}=[Mg^{2+}]\text{-}0.051\times ps\text{-}Na^+, \tag{7}$$

$$nps\text{-}Cl^-=[Cl^-]\text{-}2.287\times ps\text{-}Na^+, \tag{8}$$

This was accomplished using equations that incorporate total Na^+, total Ca^{2+}, the average crustal ratio $(Na^+/Ca^{2+})_{crust} = 0.56$ w/w (Bowen, 1979), and the average (Ca^{2+}/Na^+) ratio for Qaidam salt lakes, $(Ca^{2+}/Na^+)_{salt\ lake} = 0.06$ w/w (Zhang, 1987). Among these, the mass concentration of $[SO_4^{2-}]$, $[Ca^{2+}]$, $[K^+]$, $[Mg^{2+}]$, $[Na^+]$ and $[Cl^-]$ were identified as constituents of dust-fall.

$$ps\text{-}Na^+=[Na^+]\text{-}nps\text{-}Na^+, \tag{9}$$

$$nps\text{-}Na^+=nps\text{-}Ca^{2+}\times(Na^+/Ca^{2+})_{crust}, \tag{10}$$

$$nps\text{-}Ca^{2+}=[Ca^{2+}]\text{-}ps\text{-}Ca^{2+}, \tag{11}$$

$$ps\text{-}Ca^{2+}=ps\text{-}Na^+\times(Ca^{2+}/Na^+)_{salt\ lake}, \tag{12}$$

16

400   2.7.3 HYSPLIT backward trajectory model

401   Backward trajectory clustering analysis was conducted on sampling points using the TrajStat

402   plugin within Meteoinfo software. Daily backward trajectories for 48 hours were calculated from

403   January 2020 to March 2023 and classified monthly based on differences in the horizontal

404   movement direction and velocity of air masses. The trajectories were initiated at Universal Time

405   (UTC) 00:00, with a 6-hour increment, originating from 500 m above sea level (Yang et al., 2014).

406   Meteorological data utilized in this research were obtained from the Global Data Assimilation

407   System (GDAS) provided by the U.S. National Centers for Environmental Prediction (NCEP),

408   covering the period from December 2019 to February 2023 (Meteoinfo software website:

409   http://meteothink.org).

410

411   2.7.4 PMF model

412   The PMF is a multivariate factor analysis tool that decomposes a matrix of speciated sample

413   data into two matrices: factor contributions (G) and factor profiles (F). The goal of the PMF model

414   is to solve the chemical mass balance between measured species concentrations and the respective

415   source profiles, with the purpose of minimizing the objective function Q (Eq. 13) based upon the

416   uncertainties (uij) of measured species (Paatero and Tapper, 1994).

417    $$e_{ij} = x_{ij} - \sum_{h=1}^{p} g_{ih} f_{hj}; \quad Q = \sum_{i=1}^{m} \sum_{j=1}^{n} (e_{ij}/h_{ij}s_{ij})^2, \tag{13}$$

418   where x_{ij} is the measured concentration of the j_{th} species in the i_{th} sample at receptor sites. f_{kj} is the

419   source profile of the j_{th} species in the k_{th} factor and g_{ik} is the mass contribution of the k_{th} factor in

420   the i_{th} sample. e_{ij} is the difference between modeled concentrations and measured concentrations.

421   The uncertainty for individual species (u_{ij}) was defined as the sum of two components: the x_{ij}

422   multiplied by an error fraction, and one-third of the method detection limit (MDL). For data below

423   the MDL, concentrations were replaced by 1/2 MDL and the corresponding uncertainty was set to

424   5/6 MDL (Reff et al., 2007). An extended description of the PMF parameters used in this study and

425   error estimate based on the model's Q value, displacement (DISP), and bootstrapping (BS) tests

426   (DISP-BS) are provided in the Supplementary Information. The error assessment and uncertainty

427   data for the PMF source apportionment can be found in Tables S2 and S3, respectively.

428

429   2.7.5 Statistical Analysis

430   A one-way analysis of variance (One-Way ANOVA) was performed to examine the differences

431   in dust deposition flux, soluble ions, carbonaceous components, and trace elements among various

432   monitoring sites and periods. All statistical analyses were conducted in SPSS (IBM SPSS Statistics

433   26.0.0), with the significance level (P) set at 0.05. Prior to ANOVA, the normality and homogeneity

434   of variance were tested for each dataset. The Shapiro-Wilk test was used to assess normality. If the

435   data met the normality assumption ($P > 0.05$), parametric ANOVA was applied directly. If not, the

436   data were log-transformed and retested; if the transformed data still violated this assumption, the

437   non-parametric Kruskal-Wallis H test was used instead. In this study, all datasets were confirmed to

438   follow a normal distribution. Homogeneity of variance was verified using Levene's test; meeting

439   this assumption ($P < 0.05$) is a prerequisite for conducting ANOVA. When the overall ANOVA

440   result was significant ($P < 0.05$), indicating that at least two group means differed statistically, a

441   post-hoc test was performed. Given the potentially unequal sample sizes among groups, Tukey's

442   Honestly Significant Difference test was used for pairwise comparisons to identify specific inter-

443   group differences. Data in this study are presented as mean ± 1 standard deviation (Mean ± 1 SD).

444   Furthermore, to investigate the influence of meteorological conditions on the chemical

445   composition of atmospheric dust, Pearson correlation analysis was applied to quantitatively assess

446   the linear relationships between meteorological factors (e.g., wind speed and direction, relative

447   humidity) and chemical components in dust (e.g., OC, EC, water-soluble ions). The underlying

448   assumptions of the Pearson correlation (continuous variables, bivariate normal distribution, and

449   linearity) were verified. All variables were tested for normality using the Shapiro-Wilk test and

450   screened for outliers. For data that did not meet the normality assumption, log transformation was

451   applied. The significance of correlation coefficients was tested using the t-test, with $P < 0.05$

452   considered statistically significant.

453

454   **3. Results and discussion**

455   **3.1 Atmospheric dust deposition flux and water soluble ions concentration**

456   The DF in the southern QDB is 5.41 ± 5.33 g/m^2·30d, slightly lower than that of the Lake Aibi

457   Basin (10.77 g/m^2·30d) (Li et al., 2022), but higher than the surrounding areas of Akatama Salt Lake

458   (2.93 g/m²·30d) (Wang et al., 2014). Specifically, DF was 4.67 ± 4.96 g/m²·30d in rural and 5.97 ±

459   5.73 g/m²·30d in urban areas. During the HP, DF in rural and urban areas were 4.62 ± 4.15 g/m²·30d

460   and 4.95 ± 5.25 g/m²·30d, respectively. In contrast, NHP showed increased DF values of 4.77 ± 4.42

461   g/m²·30d (rural) and 7.66 ± 6.09 g/m²·30d (urban) (Figure 2). Notably, Urban DF during NHP

462   demonstrated a 54.6% increase relative to HP, while rural DF rose by 7.1% (not statistically

463   significant), contrasting previous findings that associated elevated DF with HP coal combustion

464   (Cheng et al., 2009; Gao et al., 2013; Guo et al., 2010; Qi et al., 2018). We hypothesize that the

465   increase in DF during the NHP is attributed to seasonal meteorological variations such as wind speed

466   (Yang et al., 2024), and heightened anthropogenic emissions associated with tourism (Zhang et al.,

467   2011). The NHP coincides with the peak tourist season (May-September) in the QDB, which

468   receives about 17 million visitors annually, a number that continues to rise (Qinghai Statistical

469   Yearbook, 2023). This elevated human activity likely enhances local emissions, contributing to

470   increased dust deposition during this period. The influence of meteorological factors on dust

471   deposition will be further examined in Section 3.5.

472
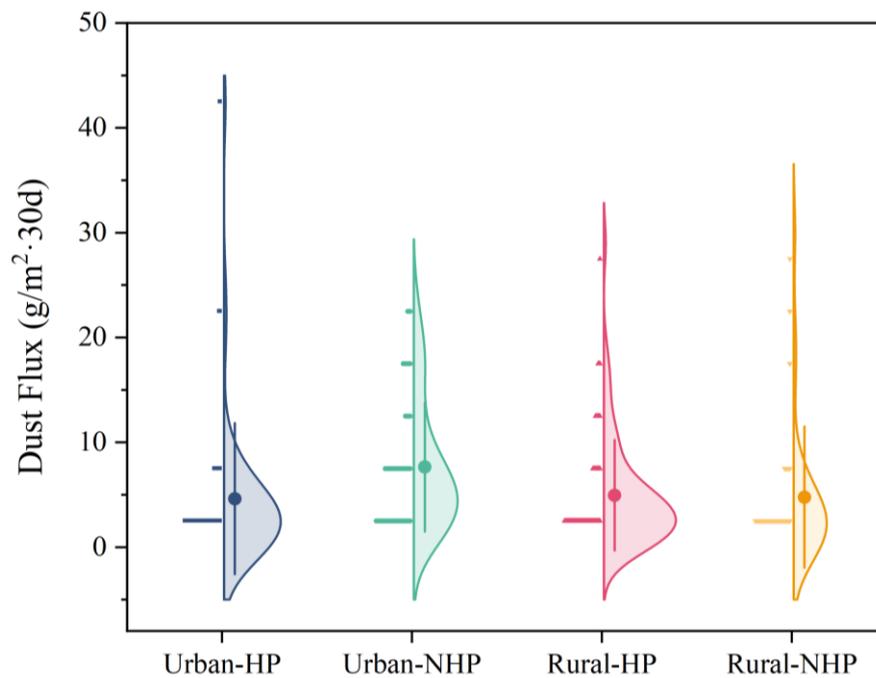
473   **Figure 2** Dust flux distribution in urban and rural. The distribution of dust flux in four contexts:

474   Urban with domestic heating period (Urban-HP), Urban with non-HP (Urban-NHP), Rural with

475   domestic heating period (Rural-HP), and Rural with non-HP (Rural-NHP). Each violin plot

476   illustrates the density distribution of dust flux values, with the central dot representing the mean,

477   and the vertical lines indicating the interquartile range.

478

479   Water-soluble ion concentrations differed between rural (115.31 mg/g) and urban (72.81 mg/g)

480   areas (not statistically significant). In rural, water-soluble ion content was greater during the HP

481   than in the NHP, while the opposite trend was observed in urban areas (not statistically significant)

482   (Figure 3 and S5). We categorized the water-soluble ions in dust deposits into ps and nps based on

483   their sources, following the model of marine aerosols (Zhu et al., 2025). Playa salt content

484   consistently surpassed nps in rural areas across both periods, while urban areas showed the opposite

485   trend (not statistically significant). Notably, during the NHP, ps content in urban and rural increased

486   by 54.46 and 36.86% respectively (not statistically significant). Backward trajectory analysis

487   indicated that airflow in both rural and urban areas primarily originated from the northwest QDB

488   and the eastern Tarim Basin during the HP, while during the NHP, it was influenced more broadly

489   by the salt lake of the QDB (Figure S6 and S7), aligning with the observed variations in ps content.

490   A similar increase in summer sea salt and non-sea salt ions has been reported in Rajkot, India,

491   attributed to ocean wind direction (Gupta and Dhir, 2022).

492   The ratio of nps-SO_4^{2-}/NO_3^- in soluble ions is used to differentiate between coal combustion

493   (fixed sources) and vehicular emissions (mobile sources) (Arimoto et al., 1996; Shen et al., 2008).

494   The higher nps-SO_4^{2-}/NO_3^- ratio in urban areas compared to rural areas (Figure S8) indicates that

495   during the study period, stationary sources (e.g., industrial emissions, coal, and biomass combustion)

496   contributed more significantly to the ionic composition of urban dust-fall (Pipal et al., 2019). In

497   contrast, the ratio was considerably lower during the NHP than during HP, suggesting that mobile

498   sources likely played a more important role in the dust ionic composition during the NHP. Generally,

499   emissions from coal combustion and biomass burning was intensified in northern China during the

500   HP (Liu et al., 2016), while vehicle emissions dominate during the NHP (Xu et al., 2012), supporting

501   the reliability of this analysis. Nevertheless, further investigation integrating atmospheric emission

502   inventories, source tracers, aerosol physicochemical processes, and meteorological conditions is

503   warranted.

504
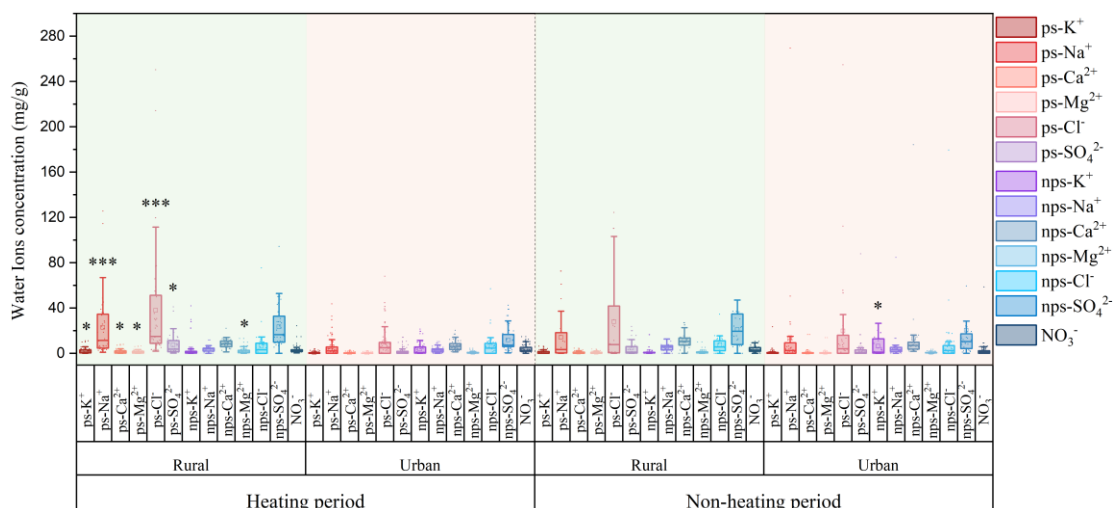
Figure 3 Concentrations of water ions in rural and urban across different seasonal periods (domestic heating and non-domestic heating periods). Asterisks indicate statistically significant differences between sites, with *, $P < 0.05$; **, $P < 0.01$; ***, $P < 0.001$.

3.2 Carbonaceous element compositions

3.2.1 Organic carbon and elemental carbon

The average total carbon (TC) concentration in the southern QDB was 4.87 ± 4.18 mg/g, significantly lower than that of Huangshi, Hubei province (25.15 ± 11.79 mg/g) and Washington (157 ± 3.2 mg/g), Kumasi in West Africa (28 mg/g) and Xi'an (14.6 ± 5.8 mg/g) (Han et al., 2007a; Han et al., 2009b; Zhan et al., 2016; Bandowe et al., 2019), suggesting relatively low carbon emissions in the southern QDB. Average OC and EC levels in QDB (3.48 and 1.41 mg/g, respectively) are markedly lower than those in Xi'an (7.4 and 7.2 mg/g, respectively), Wuhu (33.26 and 22.49mg/g, respectively), and Nanchang (25.15 and 11.46 mg/g, respectively) (Han et al., 2009a; Deng et al., 2014; Zhang, 2014), but significantly higher, particularly for EC, than in Nam Co (0.35 mg/g) (Chen et al., 2015).

In urban, TC content (4.75 ± 4.47 mg/g) was marginally lower than the rural level (5.02 ± 3.79 mg/g), although this difference was not statistically significant. Contrasting spatial patterns emerged for carbon components: EC dominated urban areas (1.46 ± 1.60 mg/g), while OC prevailed in rural (2.25 ± 1.92 mg/g) (not statistically significant) (Figure 4 and S9). This disparity may be attributed to the long-term combustion of biomass, coal, and wood in rural settings (Na et al., 2004). It may also be associated with meteorological conditions, particularly heightened solar radiation resulting

21

527 from reduced primary emissions in rural areas, which facilitates the formation of SOC (Xu et al.,

528 2018a; Wang et al., 2019). Overall, the contents of OC and EC showed small difference between

529 rural (3.73 and 1.33 mg/g, respectively) and urban aeras (3.28 and 1.47 mg/g, respectively).

530
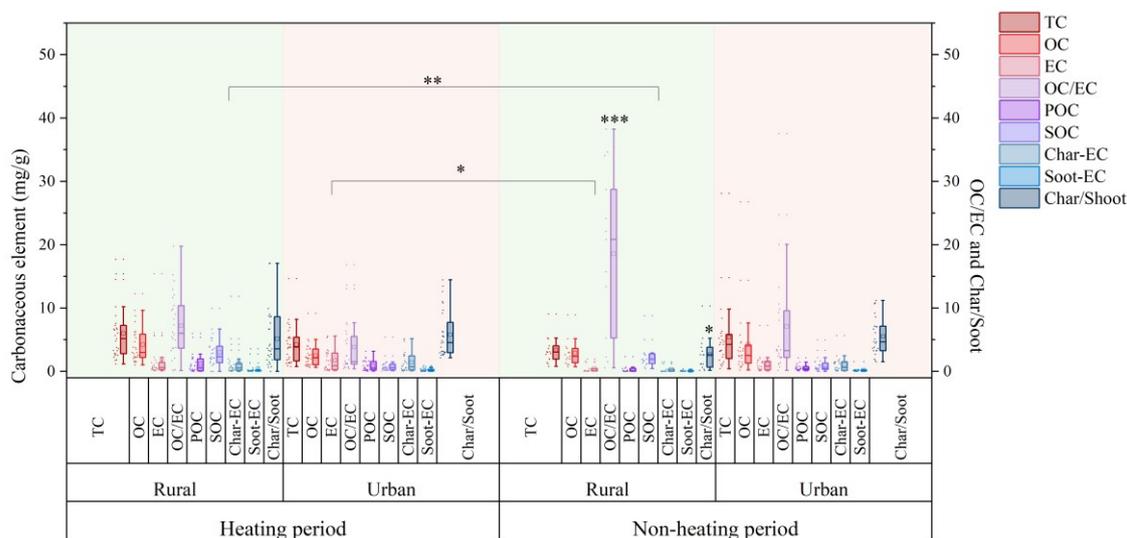
Figure 4 Concentrations of organic carbon (OC), elemental carbon (EC), secondary organic carbon (SOC), primary organic carbon (POC), char-EC, soot-EC and OC/EC, char/soot ratios in different sites (Rural, Urban) and seasonal variations (domestic heating and non-domestic heating period). Significant differences are indicated by asterisks (*$p < 0.05$; **$p < 0.01$; ***$p < 0.001$).

Seasonal analysis revealed elevated carbonaceous compound concentrations, specifically OC and EC, during the HP (not statistically significant). This increase is primarily due to local domestic heating activities coupled with adverse meteorological conditions, such as low temperature, weak winds (Oliveira et al., 2007; Gong et al., 2017), weak atmospheric turbulence, and frequent atmospheric inversions (Guo et al., 2016). Rural emissions primarily stem from coal and biomass burning for heating and cooking (Zhang et al., 2000; He et al., 2004), contributing to reduced OC and EC content in the NHP, whereas elevated EC levels in urban areas are primarily linked to vehicular and industrial sources. Spatiotemporal transport dynamics show EC depletion during rural ward pollutant migration due to atmospheric dispersion, particularly affecting coarse particulate fractions.

Notably, rural carbon emissions exceed urban levels in the southern basin, potentially

548 attributable to extended HP duration (7 months) compelling low-grade fuel (crop residues, wood,

549 raw coal and yak dung) utilization (Na et al., 2004). In contrast, urban areas benefit from solar/wind

550 energy infrastructure and government-led clean heating initiatives (suitable electricity for electricity

551 policy), achieving 66.63% clean heating penetration (Statistical Yearbook of Haixi Xizang

552 Autonomous Prefecture of Qinghai Province, 2023), leading to a comparatively lower TC content.

553　　　The OC/EC ratio is a valuable indicator of carbonaceous aerosol sources. In this study, Urban

554 areas exhibited stable OC/EC ratios ranging from 0.15 to 16.89 (mean = 3.97), whereas rural areas

555 showed significantly higher ratios during NHP (18.58 ± 12.80) compared to HP (7.20 ± 4.99) ($P <$

556 0.001) (Figure 4 and S11). Typically, the OC/EC ratio for vehicle emissions ranges from 0.7 to 2.4,

557 for coal combustion emissions from 0.3 to 7.6, and for biomass burning from 3.8 to 14.5 (Schmidl

558 et al., 2008; Gonçalves et al., 2010; Pio et al., 2011; Popovicheva et al., 2016).

559　　　These findings suggest that urban OC/EC ratios (0.15-16.89) are primarily associated with

560 vehicle and coal combustion, while rural ratios (0.14-38.25) are predominantly linked to coal and

561 biomass burning. The rural OC/EC ratios are significantly higher than those in urban areas ($P <$

562 0.001), which is consistent with the general distribution pattern of carbonaceous aerosols and

563 reflects a greater contribution of SOC (Zhang et al., 2008; Sandrini et al., 2014). The higher OC/EC

564 ratio typically indicates a greater contribution from biomass combustion; in this study, the OC/EC

565 ratio of rural was 10.99 ± 10.00, which is significantly lower than values recorded in Nam Co in

566 Xizang (16.3 ± 4.4) (Chen et al., 2015), yet higher than those observed in India (8.47) and Shanxi

567 (0.7-1.6), Beijing (1.9-2.7), and Tianjin rural (2.66) (Zhang et al., 2007; Saud et al., 2013; Cheng et

568 al., 2015; Wang et al., 2021). This finding indicates that carbonaceous aerosols in rural QDB derive

569 from both fossil fuel combustion and biomass burning, with a pronounced influence from the

570 burning of wood, yak dung, and similar biomass fuels, suggesting source specificity.

571

572 3.2.2 Char-EC and Soot-EC

573　　　Elemental carbon is classified into soot and char (Han et al., 2009b), with char-EC and soot-

574 EC defined as EC1 minus OPC and the sum of EC2 and EC3, respectively (Han et al., 2007). Char-

575 EC is typically produced from biomass burning at relatively low temperatures, whereas soot-EC

576 originates from high-temperature coal combustion and automotive emissions (Zhu et al., 2010; Cao

577 et al., 2013). The char-EC/soot-EC ratio, like the OC/EC ratio, serves as an indicator of carbon

578   aerosol sources. Since char and soot are mainly generated through combustion processes, their ratio

579   is typically influenced by two key factors: the primary emission source and the deposition removal

580   efficiency. For localized PM, such as in urban areas, the removal rate is generally negligible (Han

581   et al., 2009a).

582   Char-EC constitutes 75.88% of rural EC (74.71% HP; 78.84% NHP) and 85.00% of urban EC

583   (85.58% HP; 84.11% NHP) (Figure 4 and S10), demonstrating its dominance across spatial and

584   temporal scales (not statistically significant). Research suggests that char-EC constitutes a larger

585   proportion of coarse PM, while soot-EC is more predominant in fine particles, resulting in extended

586   atmospheric residence times for soot-EC due to reduced deposition velocities (Han et al., 2009b).

587   The increased levels of char-EC during the urban HP are linked to complex sources, including

588   biomass fuel usage and transportation emissions, resulting in elevated char concentrations in urban

589   areas and along busy roadways (Kim et al., 2011).

590   The char/soot ratios for automobile emissions, coal combustion, and biomass burning are 0.60,

591   1.9, and 11.6, respectively (Chow et al., 2004; Chuang et al., 2014). Generally, high-temperature

592   combustion (e.g., vehicle and industrial processes) yields lower char and soot concentrations, while

593   low-temperature combustion (e.g., household cooking and biomass burning) results in higher ratios

594   (Han et al., 2016; Han et al., 2012; Han et al., 2010; Han et al., 2009a). Differences in char/soot

595   ratios between urban and rural areas across seasons may be linked to wheat straw burning,

596   contrasting with minimal vegetation combustion impacts in cities like Xi'an (Cao et al., 2005). The

597   char/soot ratio for dust-fall observed in this study (4.97; Figure 4 and S11) is slightly higher than

598   those recorded in Jinchang (3.84) (Han et al., 2009a) and Daheihe, Inner Mongolia (3.2) (Han et al.,

599   2008). The relatively stable concentration of soot-EC in this study, along with the elevated char/soot

600   ratio, suggests a correlation with higher coal consumption among local residents and industries. This

601   indicates that, in comparison to other regions, carbon emissions in the remote QDB are

602   predominantly sourced from coal and biomass burning, supporting OC/EC ratio findings.

603   Furthermore, the char/soot ratio is elevated during HP (not statistically significant), highlighting the

604   predominant influence of coal and biomass burning in rural areas during HP, while fossil fuel

605   impacts are more pronounced in NHP.

606

607   3.2.3 Primary and secondary organic carbon

608   Aerosol samples with low OC/EC ratios typically exhibit low concentrations of POC, which

609   mainly comprises primary carbonaceous compounds. The MRS method enables discrimination of

610   OC into POC and SOC (Method 2.7.1) (Yoo et al., 2022; Liu et al., 2023). Secondary organic carbon

611   constitutes a dominant fraction of OC in atmospheric aerosols. Research on carbonaceous aerosols

612   in various Chinese cities indicates that SOC contributes 67% (53-83%) and 57% (48-62%) to rural

613   and urban OC, respectively (Zhang et al., 2008), marginally lower than the 72.61% observed in this

614   study (Figure 4 and S12). This is likely because SOC formation relies on solar radiation, the QDB

615   experiences high levels of solar energy (Liu et al., 2017), which may facilitate photochemical

616   oxidation of VOCs into SOC (Hama et al., 2022).

617   During the NHP, rural areas exhibit the highest SOC/OC ratio of 87.32% (Figure S13), while

618   urban areas record the lowest ratio of 52.94% during the HP. This trend reflects elevated potential

619   for photochemical activity and reduced contributions from POC, likely due to local emission sources,

620   such as traffic and coal combustion (Mbengue et al., 2018). The high SOC/OC ratio suggests that

621   SOC largely displaces OC. Our findings indicate that SOC levels are greater in rural areas (78.44%)

622   compared to urban regions (67.78%) (not statistically significant), which consistent with the

623   observation of higher OC/EC ratios in rural areas likely attributable to significant coal consumption

624   for domestic heating, which enhances emissions of semi-volatile organic compounds and organic

625   gases (Dan, 2004). As for seasonal variations, studies in California show an increase in SOC levels

626   during warmer months, which is consistent with our results (Na et al., 2004). This contrasts with the

627   broader observation that higher temperatures typically lead to lower SOC concentrations (Strader et

628   al., 1999; Sheehan and Bowman, 2001). This discrepancy may stem from varying sources of SOC

629   emissions throughout the seasons, necessitating further investigation in conjunction with other

630   carbonaceous indicators.

631   This study conducted a comparative analysis of carbonaceous element concentrations in

632   atmospheric dust-fall and road dust between the QDB and other global regions (Table S4). To ensure

633   data comparability, the selected road dust samples consisted of directly collected in-situ dust without

634   resuspension treatment. The results revealed that the concentrations of TC, OC, and EC in QDB

635   (4.87, 3.48, and 1.41 mg/g, respectively) were significantly lower than those in industrial or urban

636   areas such as Bolu, Turkey; New Delhi, India; and Ezhou, China, and were even lower than many

637   other Chinese cities (Table S4). The low concentrations of OC and EC in QDB indicate minimal

anthropogenic pollution influence in this region, and the data can represent the regional background values of carbonaceous components in atmospheric dust-fall in the arid inland areas of East Asia (Chen et al., 2019a). This is crucial for global models assessing the emission fluxes of carbonaceous aerosols from dust source regions. In contrast, extremely high values of carbonaceous elements were found primarily in urban road dust from locations like Bolu, Turkey (TC: 605.2 mg/g), Gwangju, South Korea (TC: 31.97 mg/g), and Xi'an, China (TC: 36.53 mg/g), indicating strong influences from traffic emissions (mainly non-exhaust emissions) (Wei et al., 2015; Lee et al., 2018; Demir et al., 2022). For atmospheric dust-fall in major cities like New Delhi, India, and Wuhan, China, the carbonaceous components are affected by the combination of traffic emissions (diesel vehicle emissions being a major source of EC), industrial activities, and emissions from dense populations (Deng et al., 2014; Zhang, 2014; Zhan et al., 2016; Mishra and Kulshrestha, 2017).

The OC/EC ratio in QDB (7.09) is an intermediate level. It is much lower than that in regions dominated by biomass burning, such as Kumasi, West Africa (17.07) and Huainan, China (21.4), but is higher to ratios found in cities like Gwangju, South Korea (5.63) and Ulaanbaatar, Mongolia (5.69)(Lee et al., 2018; Bandowe et al., 2019; Liu et al., 2020). We primarily analyzed the OC/EC ratios in cities across different regions of China to reveal the influence of varying economic development levels.

Figure 5 presents spatial variations in urban OC/EC ratios across China. The findings reveal that the Northwest region, represented by QDB urban and Xi'an (XA) (Han et al., 2009b), exhibits a significantly lower ratio (2.50 ± 1.47) compared to central regions, including Nanchang (NC) (Zhang, 2014), Huangshi (HS) (Zhan et al., 2016), Wuhu (WH) (Deng et al. 2014), Xiaogan (XG) (Zhan et al., 2022), and Huainan (HN) (Liu et al., 2020), where the ratio is 5.86 ± 7.81. This ratio is also lower than that observed in eastern cities such as Beijing (BJ) (Tang et al., 2013), Tianjin (TJ) (Ma et al., 2019), and Shijiazhuang (SJZ) (Guo et al., 2018), which have a ratio of 6.83 ± 2.77. This pattern is consistent with the trends in atmospheric PM OC/EC ratios (Xie et al., 2023), suggesting that the carbon in the dust of the QDB urban primarily results from coal combustion and industrial emissions, leading to elevated EC concentrations and lower OC/EC ratios (Liu et al., 2022). Conversely, cities with higher economic development, such as Beijing and Tianjin, characterized by greater population density and income levels, typically experience secondary pollution, resulting in higher OC/EC ratios.

668   While the MDCO sampler effectively captures dry deposition flux, the reported OC and EC

669   values must be interpreted with specific limitations in mind. First, passive sampling is governed by

670   aerodynamic drag and gravitational settling; therefore, the collected OC is likely skewed toward the

671   coarse fraction (e.g., re-suspended soil, biological debris) while potentially under-representing fine-

672   mode anthropogenic combustion aerosols which have negligible settling velocities. This implies

673   that the OC fluxes reported here should be interpreted as fluxes of deposited particulate OC, not as

674   a direct surrogate for total atmospheric OC. Second, the extended exposure period inherent to

675   passive sampling may lead to negative artifacts due to volatilization. Semi-volatile organic

676   compounds may partition from the particulate to the gas phase, a process accelerated in

677   environments with high solar radiation and ambient temperatures (Turpin et al., 1994).

678   Consequently, the OC fluxes reported here likely represent a conservative lower limit. Finally,

679   environmental factors such as wind speed and humidity affect collection efficiency. High wind

680   speeds can induce turbulence leading to the resuspension of lighter organic particles from the

681   collector, while high humidity may facilitate chemical or biological degradation of the organic

682   fraction prior to laboratory analysis (Chow et al., 2011). Taken together, these processes imply that

683   the OC collection efficiency of the MDCO sampler is not a fixed quantity but varies with

684   temperature, relative humidity, precipitation, wind direction and other environmental factors. The

685   role of these meteorological factors in atmospheric dust deposition is examined in detail in Section

686   3.5.

687   The char/soot ratio in QDB is notably high at 5.04, significantly exceeding that of other regions

688   such as Xi'an (0.99) and Wuhan (0.09) (Wei et al., 2015; Liu et al., 2021). Char-EC primarily

689   originates from incomplete combustion processes like biomass burning and coal combustion. Soot-

690   EC mainly derives from high-temperature combustion sources such as fuel oil and diesel vehicle

691   exhaust (Han et al., 2009). The exceptionally high char/soot ratio in QDB strongly indicates that its

692   limited carbonaceous components predominantly originated from relatively inefficient combustion

693   sources. These potentially included coal or small-scale biomass burning for local

694   residential/expedition activities (e.g., heating, cooking) and possibly long-range transported

695   biomass burning products (e.g., from forest/agricultural fires in South or Southeast Asia) (Han et al.,

696   2009; Han et al., 2006; Han et al., 2016). In contrast, the very low char/soot ratios observed in cities

697   like Wuhan and Xi'an clearly point to traffic source emissions as their primary contributor, a finding

698   likely influenced by the specific focus of those studies on road dust.

699
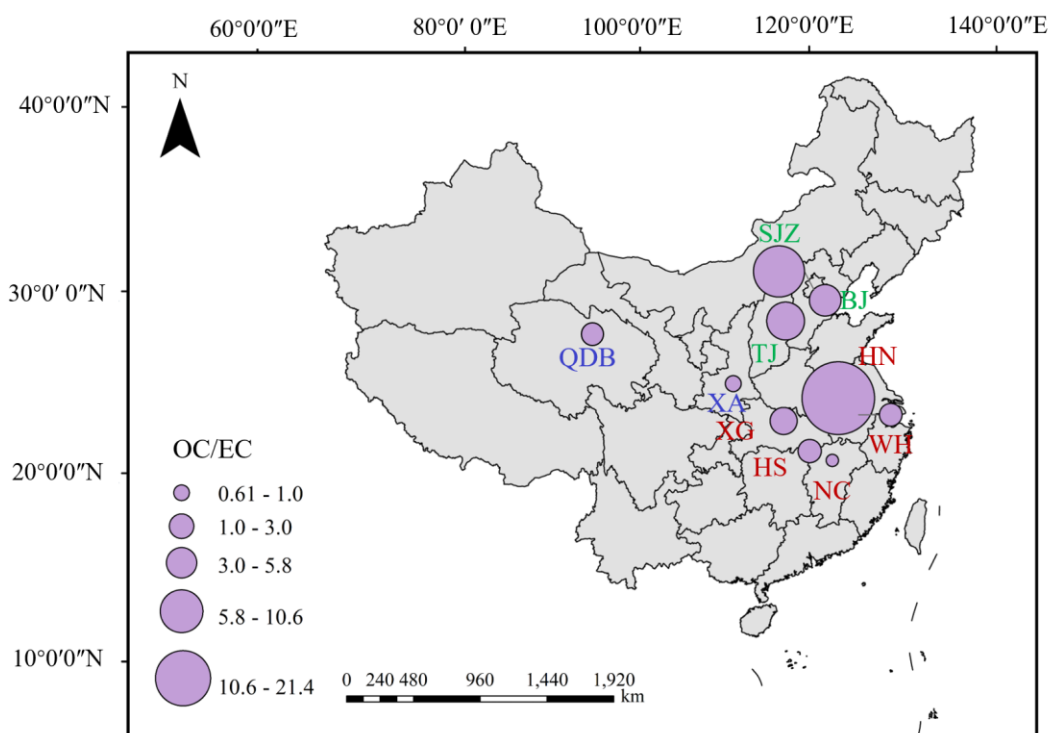
701   **Figure 5** Distribution of OC/EC ratios across various regions of China. Blue designations represent

702   the Northwest region, red indicates the Central region, and green denotes the Eastern region. The

703   circle size reflects the magnitude of the OC/EC ratios.

704

705   However, we fully recognize the fundamental differences in sources and composition between

706   road dust and atmospheric dust-fall. Road dust is primarily secondary dust formed from traffic

707   activities, construction dust, soil particles, and resuspended deposited atmospheric particles, with

708   its carbonaceous composition strongly reflecting intense local anthropogenic emissions (Casotti

709   Rienda and Alves, 2021). In contrast, atmospheric dust-fall integrates contributions from local

710   sources, regional transport, and even long-range transport. Therefore, direct comparison between

711   these two may introduce bias when interpreting regional pollution characteristics and the degree of

712   anthropogenic influence, which cannot be overlooked. Building on this analysis, the next phase of

713   this research will focus on the sampling and analysis of fine atmospheric particulate matter ($PM_{2.5}$

714   and PM_1) to more accurately elucidate the emission levels and environmental and climatic impacts

715   of carbonaceous aerosols in the QDB.

3.3 Trace elements concentration

The total concentration of major (Fe, Si, Al) and trace elements (Ti, Cr, Cd, Cu, Mn, Ni, Pb, V, Zn) was determined to be 8.74 ± 5.82 mg/g, while arsenic (As) remained below the detection limit in all analyzed samples. Crustally derived elements—Fe, Al, Si, and Ti—dominated the elemental profile, aligning with dust composition patterns reported in Ira, Singapore, and Beijing-Hebei regions, China (Joshi et al., 2009; Qiao et al., 2013; Eivazzadeh et al., 2021). In comparison to cities such as Beijing, Shanghai, Xi'an, and Lanzhou, and Junggar Basin the levels of heavy metals in dust from the QDB are relatively low (Jiang et al., 2018) (Supplementary Table S5).

The low heavy metal content in dust deposition within the QDB can be attributed to the following factors. The region has sparse human activity, lacks heavy industrial zones and dense urban clusters, resulting in low total anthropogenic emissions of heavy metals. Furthermore, the surface soil in the QDB itself has a low background level of heavy metals, primarily derived from natural sources with relatively weak influence from human activities (Nuralykyzy et al., 2021; Chen et al., 2021). From the meteorological perspectives, the basin's high altitude, strong winds, and arid conditions with minimal precipitation favor the dispersion of atmospheric pollutants. This makes the formation of prolonged stagnant weather conditions unlikely, thereby preventing the accumulation of pollutants and the occurrence of high concentrations near the ground. A particularly unique aspect of the QDB is its role as a significant source of salt dust. The recent study indicates that salt dust emitted from the playa lakes within the basin contributes substantially to atmospheric dust deposition (Zhu et al., 2025). These salt dust particles, composed mainly of soluble salts like NaCl and gypsum, may dilute the relative concentration of non-salt components, such as heavy metals, when released into the atmosphere in large quantities. The combined effect of these factors leads to the observed low heavy metal content in dust deposition in this region.

Throughout both the HP and NHP, trace elements concentrations in urban areas were consistently higher than in rural areas (not statistically significant), with the exception of Ti (Figure 6 and S14). During the HP, urban levels of Zn, Pb, and Cu were significantly elevated compared to rural areas ($P < 0.05$), and Pb also demonstrated a significant increase in urban during the NHP ($P < 0.01$). In rural, the differences in metal concentrations between HP and NHP were minimal. In

contrast, urban areas exhibited higher concentrations of all elements except for Ti, Cd, and Cr during the HP, with Fe and V showing notably elevated levels compared to other regions (not statistically significant). These variations in average concentrations indicate that coal combustion for domestic heating in urban areas contributes to increased atmospheric heavy metal levels (Duan and Tan, 2013; Meng et al., 2017). In contrast, Cd and Cr exhibited mixed anthropogenic sources with limited coal combustion contributions, while Ti concentrations remained stable across seasons, reflecting minimal anthropogenic influence.

Analysis of the carbonaceous components in QDB dust deposition reveals more intensive coal combustion in rural areas, yet the heavy metal concentrations in atmospheric deposition are lower than in urban area (not statistically significant). This observation can be explained by the following factors. First, pollution sources in rural areas are relatively singular, whereas urban areas are influenced by more complex heavy metal sources. During the heating period, heavy metals in the rural atmosphere of the QDB mainly originate from coal and biomass combustion. In contrast, urban areas are affected by a wider range of sources, including industrial activities, traffic emissions, and others (Liu et al., 2021; Huang et al., 2021a). Additionally, the dense building layout in urban areas hinders pollutant dispersion, leading to accumulation, while the open terrain in rural areas facilitates dilution and diffusion. This pattern, where rural heavy metal concentrations (particularly Pb, Cr, Cd, As, and other elements associated with coal combustion) are lower than those in urban areas during the heating season, has also been observed in studies conducted in Northeast China, Shanghai, Taiyuan, the Yangtze River Delta, and Southern Nigeria (Shi et al., 2012; Liu et al., 2021; Huang et al., 2021a; Liu et al., 2023b; Hilary et al., 2025).
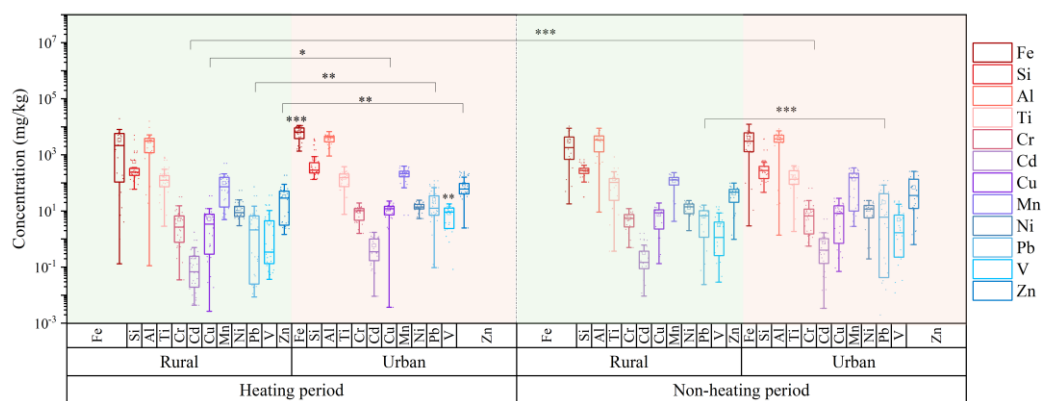
Figure 6 Concentration of heavy metals by rural and urban settings during domestic heating and

769   non-domestic heating periods. Significant differences are indicated by asterisks ($*p < 0.05$; $**p <$

770   0.01; $***p < 0.001$).

771

3.4 Source apportionment

773   We conducted a PMF source apportionment analysis on soluble ions, trace and carbonaceous

774   elements present in dust, specifically focusing on ps-SO_4^{2-}, ps-Ca^{2+}, ps-K^+, ps-Mg^{2+}, ps-Cl^-, ps-Na^+,

775   nps-SO_4^{2-}, nps-Ca^{2+}, nps-K^+, nps-Mg^{2+}, nps-Cl^-, nps-Na^+, Fe, Si, Al, Ti, Cr, Cd, Cu, Mn, Ni, Pb, V,

776   Zn, SOC, POC and char-EC, soot-EC. Seven source factors were identified based on prior research

777   and an understanding of potential local sources: salt lakes, soil, traffic emissions, secondary

778   inorganics, biomass and coal burning, and industrial activities (Figure 7 and S15. A plot of the time

779   series is provided in Figure S16. The generation of Figure 7a involved extracting factors identified

780   as the same source from the PMF factor profiles of each site (Urban and Rural) and each heating

781   season (HP and NHP) shown in Figure S15. The arithmetic mean of the contributions from

782   characteristic species (elements and ions) corresponding to each factor was calculated. Species with

783   average contributions exceeding 20% were defined as characteristic species of that source in

784   atmospheric dust over the QDB.

785   The factor profiles for each element in these source categories represent the arithmetic mean

786   of profiles from six stations, with detailed operational methods provided in Supplementary Text S1.

787   The uncertainty of the source contributions was calculated directly from the standard error of the

788   multiple regression coefficients between the deposition flux (independent variable) and the source

789   contribution (dependent variable) at different monitoring sites (Belis et al., 2015; Manousakas et al.,

790   2017). The regression method assumes that all factors explaining the mass have been identified;

791   however, if a significant portion of the mass not directly related to the species in the PMF analysis

792   is omitted, the source contributions may be overestimated, which could be an important additional

793   source of uncertainty. The results are shown in Table S6. It must be noted that this method captures

794   only a portion of the total uncertainty, as it does not include errors from profile uncertainty or

795   rotational ambiguity. The low errors calculated by this method indicate a good model fit. In this

796   study, the sample numbers used for PMF source apportionment were 690, 780, 480, and 750 for the

797   Urban-NHP, Urban-HP, Rural-NHP, and Rural-HP groups, respectively. Limited sample number can

increase the risk of model overfitting, reduce the representativeness of source profiles, and potentially lead to the merging of multiple sources into a mixed factor (Norris et al., 2014). Future research will extend the observation period and increase the sample number to further enhance the reliability of the source apportionment results.

The ions ss-Na$^+$, ss-Cl$^-$, ss-SO$_4^{2-}$, ss-Ca^{2+}, ss-K$^+$, and ss-Mg^{2+} are widely acknowledged as indicators of sea salt (Ambade et al., 2022; Aswini et al., 2022; Gluscic et al., 2023). In this study, we identified ps-Cl$^-$ (83.96%), ps-Ca^{2+} (83.71%), and ps-SO$_4^{2-}$ (83.71%), ps-Na$^+$ (83.70%), ps-Mg^{2+} (83.66%), ps-K$^+$ (82.35%) as key markers of salt lake sources. The contribution of salt lake sources in rural (12.29%) was higher than in urban (6.87%). During the HP, the proportion of salt lake sources in rural areas was 4.97%, compared to 19.61% in the NHP; urban showed contributions of 2.16% during the HP and 11.58% in the NHP, showing opposite seasonal trends. Backward trajectory simulations indicated that during the HP, air mass in both urban and rural areas mainly originated from the northwestern part of the basin and the eastern Tarim Basin, whereas during the NHP, they were broadly influenced by the salt lake regions within the basin (Figure S6). The minor wind direction differences and the inter-distributed sampling points (Figure 1), suggests no substantial geographical disparity between urban and rural sites. Additionally, the ion content derived from playa salts in dust deposits increased during the NHP in both areas. Therefore, we propose that the anomalous increase in salt lake contribution during the urban HP may be closely related to human activities. The enhanced Urban Heat Island (UHI) effect and temperature inversion structures during the HP can alter boundary layer height, turbulence, and deposition conditions, thereby increasing the residence time of externally transported particles within the urban boundary layer and elevating their measured contribution (Cichowicz and Bochenek, 2024). Urban heat sources and heating emissions may also modify local transport pathways, leading to more concentrated deposition of dust originating from playa regions over urban areas. Furthermore, dry road surfaces, increased traffic, and construction activities during the HP can promote the resuspension of previously deposited playa dust. The use and subsequent resuspension of road de-icing salts (e.g., NaCl, CaCl$_2$) may further amplify the contribution of tracer ions indicative of playa salts (Gertler et al., 2006; Casotti Rienda and Alves, 2021).

The second factor pertains to soil dust, characterized by trace element such as Fe (47.03%) and Si (36.22%), along with ions such as nps-Na$^+$ (54.21%), nps-Ca^{2+} (44.05%), nps-Mg^{2+} (32.30%),

(Pervez et al., 2018; Tian et al., 2021). Additionally, the proportions of elements such as SOC (32.58%) and POC (20.84%) suggest that the dust is likely mixed with fossil fuel emissions. Furthermore, V (24.62%) was detected at multiple sampling sites, indicating contributions from both soil dust and traffic emissions. Mg, Ca^{2+}, Al, Si, and Fe are typical tracers for soil dust (Liu et al., 2003; Heo et al., 2009). Notably, the contribution of soil dust in rural areas (21.14%) exceeded that in urban areas (12.97%), indicating that soil dust is a major source of atmospheric deposition. In urban areas, the contribution during the NHP was relatively low (6.84%), likely due to higher wind speeds and the effectiveness of frequent summer precipitation (Zhang et al., 2015a).

The third factor is traffic emissions, which are particularly pronounced in urban areas. Key characteristic elements and ions include nps-Cl^-(56.71%), Zn (50.13%), Cd (49.41%), Pb (47.84%), Ni(44.22%), Cu(37.61%), nps-Mg^{2+} (30.54%), V (29.63%), nps-K^+ (27.74%), NO_3^- (24.35%) and char-EC (46.71%), soot-EC (38.12%), SOC (32.25%), POC (23.72%) (Adeniran et al., 2017). In rural areas, traffic emissions contributed 8.52% to atmospheric deposition during the NHP, whereas in urban areas, the contribution was significantly higher at 46.83%, with 32.91% during the HP and 60.75% in the NHP. These findings correlate with previous studies on OC/EC and char/soot ratios, suggesting that carbonaceous elements in the NHP primarily derive from traffic emissions. The traffic emission factor in the QDB represents a mixture of vehicle exhaust and non-exhaust sources (e.g., tire and brake wear, and resuspended road dust). Elements and ions including V, NO_3^-, Ni, and carbonaceous components primarily associated with vehicle exhaust (Cong et al., 2011; Zhang et al., 2012). For instance, Ni can be emitted from fuel combustion and vehicle exhaust (Pacyna and Pacyna, 2001). In contrast, elements such as Cu, Zn, nps-Mg^{2+}, and nps-K^+ originate from non-exhaust vehicle emissions, including brake and tire wear, as well as the resuspension of road dust (Amato et al., 2014). For example, Zn may derive from the wear of rubber tires on roads (Rogge et al., 1993), Pb emissions may be related to wear (tires/brakes) (Smichowski et al., 2007), and Cu is associated with brake wear (Lin et al., 2015). Furthermore, the presence of crustal elements and ions such as Fe, Si, and nps-Mg^{2+} in the traffic emission factor for Urban-NHP, Urban-HP, and Rural-NHP suggests an additional contribution from resuspended road dust (Chen et al., 2019).
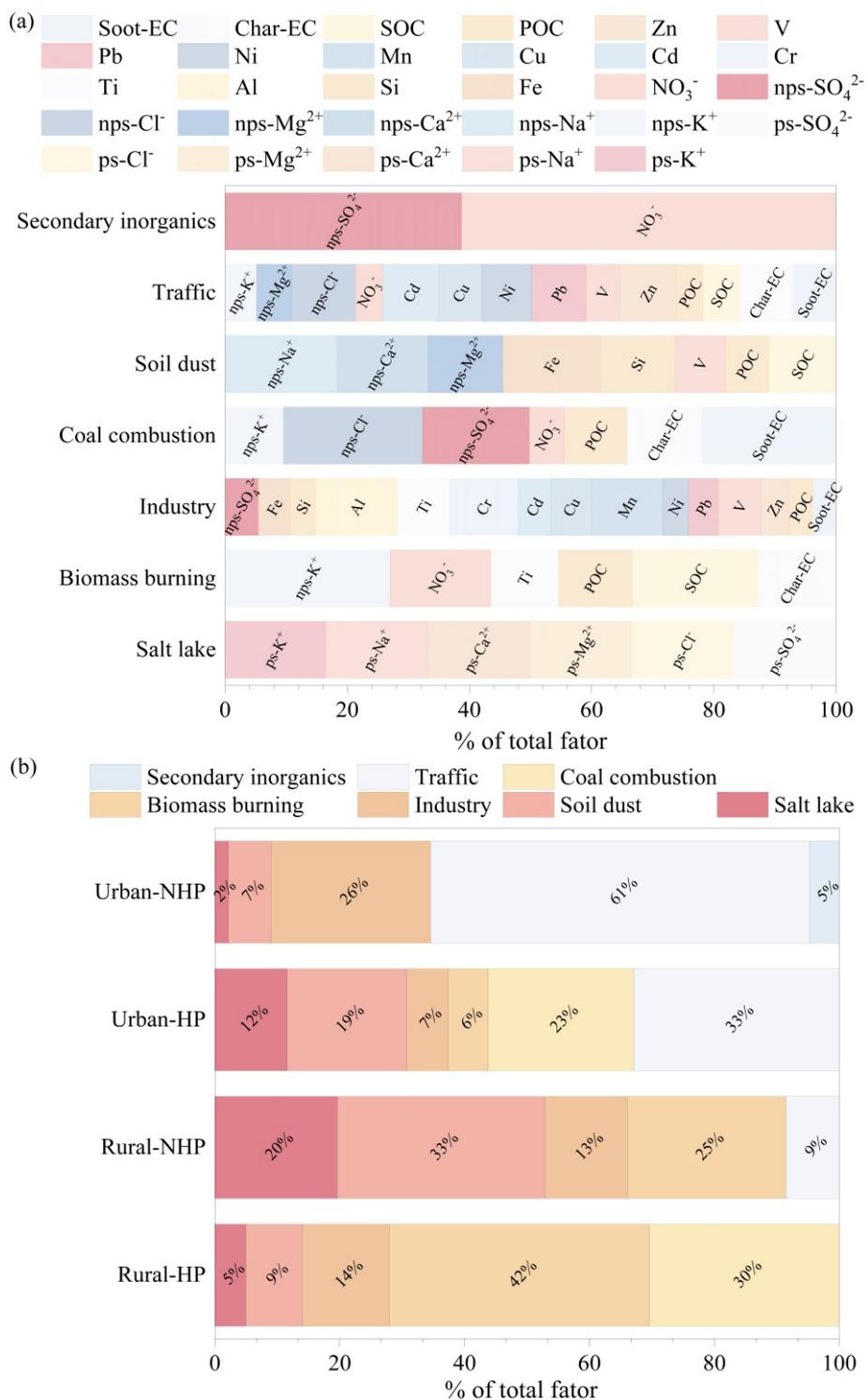
Figure 7 Factor profile and contributions in urban and rural area. (a) presents the factor profiles, represented as the arithmetic mean of individual elements across various locations, highlighting only those elements that constitute more than 20% of each profile. (b) illustrates the contributions of different sources at each location. [HP, domestic heating period; NHP, non-domestic heating period].

862

The fourth factor is coal combustion, characterized by high concentrations of nps-Cl⁻ (75.40%), nps-SO_4^{2-} (57.87%), nps-K^+ (31.75%), NO_3^- (19.10%), and soot-EC (72.54%), char-EC (40.63%), POC (34.10%) (Kundu and Stone, 2014; Contini et al., 2016). Zhang et al (2023) found that coal combustion emits particles rich in Cl⁻. Coal combustion was more intense at site LTC in rural areas and at site DLX in urban areas. Coal combustion occurs exclusively during the HP, contributing 30.38% in rural areas and 23.31% in urban areas. These results align with earlier studies on carbonaceous aerosols, indicating that the carbon content from coal combustion emissions is higher in rural than in urban aeras. Consistent with northern China, air pollution in QDB urban has declined due to the adoption of clean heating technologies (Zhang et al., 2021; Xue et al., 2023). However, rural coal combustion remains a major source of carbonaceous aerosols during the HP.

The fifth factor, biomass burning, is characterized by significant concentrations of non-precipitating species, including nps-K^+ (56.99%), NO_3^-(34.97%), Ti (23.26%) and SOC(43.68%), char-EC (26.78%), POC (25.60%) (Simoneit, 2002; Sulong et al., 2019). K^+ serves as an important tracer for biomass burning (Cachier and Ducret, 1991). Biomass burning contributes 33.55% to rural atmospheric dust deposition, with a higher proportion during the HP (41.67%) compared to NHP (25.43%). In urban, biomass burning is primarily observed during the HP, contributing only 6.41%. These findings underscore biomass burning as a major source of carbon emissions in rural settings, aligning with the prevalent use of biomass fuels for cooking and domestic heating in Northern China's rural areas (Meng et al., 2019), where 70% to 80% of energy demand are fulfilled by materials such as dung cakes, firewood, charcoal, and crop residues (Tao et al., 2018; Shi et al., 2019). Furthermore, increased biomass burning is also associated with the autumn harvest period (Chen et al., 2017; Li et al., 2021).

The sixth factor pertains to industrial emissions, which are characterized by high concentrations of Mn (61.98%), Cr (59.22%), Ti (44.90%), V (37.17%), Cu (34.95%), Cd (28.63%), Fe (27.47%) Pb (25.75%) and Zn (24.03%) (Almeida et al., 2015; Yao et al., 2016). These elements were consistently detected across all sampling sites, alongside Al (71.17%), nps-SO_4^{2-} (28.84%), Si (22.24%) and POC (20.95%), soot-EC (19.97%), which indicate potential contributions from soil dust. Zn, Cu, Fe, and Mn are major chemical components in industrial emission profiles; Cd is a trace element found in metallurgical industries (Xu et al., 2022), while Zn and Mn emitte from oil

combustion, metallurgy, and steel manufacturing processes (You et al., 2017). Pb and Cd are associated with metal smelting and processing (Fang et al., 2021). Industrial emissions showed greater contributions during the HP at XZH and at DLX. In rural areas, industrial emissions constitute 13.57% of carbon output, with contributions of 13.95% during the HP and 23.20% during the NHP. In urban areas, industrial emissions account for 16.12% overall, with 6.69% during the HP and 25.55% in the NHP. Due to the abundance of non-ferrous metal resources (e.g., lead-zinc ores), oil, natural gas, and saline minerals (e.g., potassium, lithium) in the QDB, the primary industrial activities are mining and associated chemical industries. Particularly around the GEM and DLX sites, the presence of numerous Pb-Zn, Fe, and Cu mining enterprises leads to significant contributions from industrial emissions to urban dust fallout, making it one of the major sources of air pollution in the basin.

The seventh factor is secondary inorganic aerosols, primarily composed of NO_3^- (72.46%), nps-SO_4^{2-} (45.79%), (Liu et al., 2015; Liu et al., 2016a). High mass loadings of NO_3^- and SO_4^{2-} are characteristic of typical secondary inorganic aerosols (Huang et al., 2021). Research indicates that NO_3^- and SO_4^{2-} primarily result from the conversion of gaseous precursors, such as SO_2 and NO_x, through photochemical reactions, predominantly sourced from local and regional emission (Liu et al., 2015; Tao et al., 2013). Secondary inorganic aerosols are predominantly observed in urban areas during the NHP, where they contribute 4.70% to total aerosol sources. This increase is likely due to elevated temperatures and enhanced solar radiation during this period, which promote photochemical activity (Pandolfi et al., 2010).

Dust deposition sources exhibit significant seasonal and spatial variations. In the QDB, coal combustion (26.85%) and biomass burning (24.04%) dominate during HP, transitioning to traffic emissions (34.64%), soil dust (20.04%) and industry emission (19.37%) as the primary contributor in NHP. Rural areas predominantly contribute to dust through biomass burning and coal combustion, as well as natural sources like windblown dust and salt lake emissions. This pattern aligns with increased coal usage for winter domestic heating and heightened biomass burning for cooking and heating in rural areas. In urban, dust deposition is briefly influenced by anthropogenic activities, including traffic and industrial emissions, with minimal contributions from domestic heating. Such differences can be attributed to varying economic development models, industrial and energy structures, and levels of human activity (Kataki et al., 2016).

Time series analysis (Figure S16) indicates that atmospheric dust deposition in rural areas primarily originates from natural processes and dispersed anthropogenic combustion due to sparse human activities. During the NHP, the contribution of salt-lake emissions increases in May and June. Strong winds in spring and summer in southern QDB transport saline soil particles, making them a key source of dust deposition (Zhu et al., 2025). Soil-derived dust shows variations highly synchronized with the salt-lake source, with elevated contributions also occurring in May and June, reflecting the natural erosion of exposed surfaces under high wind conditions (Zhang, 2010). Traffic contributions rise noticeably in July and August, likely linked to increased summer tourism and transportation. During the HP, contributions from biomass and coal combustion increase, peaking from November to January. This peak is attributed to the widespread use of biomass fuels such as livestock dung for decentralized heating in rural areas, leading to increased particulate matter emissions (Chen et al., 2023). In contrast, contributions from salt lakes and wind-blown dust decrease significantly, likely due to lower wind speeds and reduced natural source emissions in winter (Jiménez et al., 2018; Li et al., 2019a; Yang et al., 2024).

In urban areas, where human activities are more concentrated, pollution sources are dominated by centralized anthropogenic emissions (industry, traffic, and centralized heating), with temporal trends driven by both industrial activity and the heating cycle. During the NHP, industrial contributions increase, especially in towns such as GEM and DLX, where surrounding mining operations constitute a major anthropogenic source (Zhu et al., 2016). Traffic-related contributions follow a trend similar to that in rural NHP, also peaking in July and August, reflecting the common influence of increased vehicle flow during the tourism season. Meanwhile, precursors such as SO_2 and NO_x from industrial and traffic emissions undergo photochemical and gas-to-particle conversion under summer sunlight, enhancing the formation of secondary inorganic aerosols (e.g., SO_4^{2-}, NO_3^-) (Zhang et al., 2013; Ma et al., 2017). During the HP, trends in salt-lake emissions, soil dust, and coal/biomass combustion are generally similar to those in rural areas. However, unlike in rural regions, traffic contributions in urban areas continue to increase during the HP, highlighting the higher intensity and less seasonally-variable nature of human activities in towns (Peng et al., 2021).

This study observed that the contribution of biomass burning to atmospheric dust deposition in rural areas of the QDB during the HP was higher than that of soil dust. Given that the collected dust samples had particle sizes >10 μm, while biomass burning typically emits aerosols in the submicron

37

range, we propose several potential explanations. Firstly, during the HP, factors such as increased soil moisture and snow cover significantly suppress soil dust emission, resulting in a lower intensity than in other seasons (An et al., 2018; Yang et al., 2019). Simultaneously, biomass and coal burning for heating increases substantially, leading to intense, short-term emissions of fine particles. Although it was fine initially, these high-concentration ultrafine particles can undergo coagulation or coalescence, aggregating with each other or onto pre-existing coarse particles, thereby increasing their size (Butler and Mulholland, 2004; Kulmala et al., 2004; Li et al., 2020). Furthermore, fine particles from biomass burning (e.g., carbonaceous materials) may mix internally with coarse particles like soil dust or salt dust from the QDB, forming internally mixed particles (Li et al., 2003; Hand et al., 2010). During source apportionment, such coarse particles are more likely to be attributed to the biomass burning source. Additionally, the QDB is a significant source of salt dust (Zhu et al., 2025). Salt dust particles (e.g., halite, gypsum) provide excellent condensation nuclei for soluble substances emitted from biomass burning, greatly promoting hygroscopic growth (Li et al., 2003; Kumar, 2010; Wang, 2013). The basin's topography also favors stable inversion layers, inhibiting pollutant dispersion and allowing particles more time to grow, mix, and age in the atmosphere. Prevailing wintertime winds may also transport pollutants from surrounding regions into the basin.

Moreover, the dust in this study was collected using a passive sampler. Over 90% of the collected dust particles were smaller than 100 μm, with approximately 25% less than 10 μm (Figure S2), indicating the presence of fine particles (<10 μm), albeit in a relatively small proportion. The particle size distribution of atmospheric dust deposition is similar to that of TSP, with both primarily consisting of particles smaller than 100 μm. Using PMF source apportionment, this study identified a notably high contribution from biomass burning in rural areas, particularly during the heating period. Similarly, studies on atmospheric TSP in Iran (Ashrafi et al., 2018), the Qinghai-Xizang Plateau (Lulang) (Zhao et al., 2013), Northeast China (Jia et al., 2024), and Qingdao (Liu et al., 2022) have also reported significant contributions from biomass and coal combustion. This suggests that contributions from biomass and coal combustion can indeed be observed in particles larger than 10 μm. Finally, the PMF model may have uncertainties in resolving sources with similar chemical profiles. If the chemical compositions of local soil dust and biomass burning particles overlap after long-range transport and complex atmospheric reactions, the model might not fully separate them

982   (Cesari et al., 2016).

983

984   **3.5 Influence of meteorological factors**

985   Meteorological parameters critically influence the accumulation and dispersion of airborne

986   pollutants. To examine their impact on the chemical composition of dust deposition in this study,

987   monthly data for temperature, humidity, precipitation, wind speed and direction, sunshine duration,

988   frequency of visibility ≤10 km were obtained from four monitoring stations (XZH, GEM, NMH,

989   DLX) during the study period (Table 1 and Figure S17). Data from the LTC and BLX sites were

990   excluded from this analysis due to a lack of on-site meteorological instrumentation.

991   Based on ANOVA results, wind speed and temperature were significantly higher during the

992   NHP ($P < 0.05$), promoting dust emission and consequently increasing atmospheric dust flux

993   (Jiménez et al., 2018; Li et al., 2019b; Yang et al., 2024). However, at DLX, wind speed showed no

994   significant seasonal difference, while precipitation and relative humidity were significantly higher

995   in the NHP ($P < 0.05$). Since precipitation is a known suppressor of dust deposition (Li et al., 2019b),

996   meteorological factors were not the primary driver of the elevated dust flux at DLX during the NHP

997   (Figure S18); other factors, such as increased tourism, likely played a more important role.

998   Additionally, correlation analysis revealed that dust and salt dust flux were positively correlated

999   with the frequency of visibility ≤10 km and wind speed ($P < 0.05$) and negatively correlated with

1000   relative humidity ($P < 0.05$), consistent with previous findings (Wei et al., 2023).

1001   Pearson correlation analysis further elucidated the relationships between dust chemical

1002   components and meteorological parameters. Ions derived from salt lake (ps ions) and crustal

1003   elements (e.g., Al) showed significant correlations with wind direction and speed ($P < 0.05$, Figure

1004   S19), indicating the dominant control of wind on the emission and transport of both playa salt and

1005   soil dust. During the HP in both rural and urban areas, relative humidity was negatively correlated

1006   with ps ions and crustal elements ($P < 0.05$), suggesting that higher humidity promotes the removal

1007   of airborne particles (Deshmukh et al., 2011). Playa salt ions are hygroscopic, so higher relative

1008   humidity facilitates their deliquescence (Rörig-Dalgaard, 2021). The mean annual relative humidity

1009   in the QDB (about 34 %RH) is notably lower than Wuhan (75.4 %RH) (Zang et al., 2021), Handan

1010   (63.35 %RH) (Meng et al., 2016), Pearl River Delta region (67.05 %RH) (Yue et al., 2015), Jorhat,

India (80.29 %RH) (Rabha et al., 2021) and other regions, providing favorable conditions for the
long-range transport of salt-lake-derived particles.

Table 1 Meteorological conditions at the monitoring stations during the sampling periods.

Site	Period	Temperature (°C)	Relative humidity (%)	Precipitation (mm·d⁻¹)	Wind speed (m·s⁻¹)	Wind direction	Sunshine duration (h·m⁻¹)	Frequency of visibility ≤10 km
XZH	Whole	4.27 ± 10.58	33.56 ± 5.74	2.63 ± 3.64	3.29 ± 0.63	WNW	237.73 ± 26.86	36.52 ± 15.27
	HP	-3.16 ± 6.30	33.57 ± 6.36	1.47 ± 2.95	2.93 ± 0.49	WNW	240.58 ± 25.04	41.19 ± 16.61
	NHP	15.65 ± 2.86	33.54 ± 4.63	4.41 ± 3.97	3.83 ± 0.40	W	233.55 ± 28.82	29.36 ± 9.10
GEM	Whole	5.76 ± 9.80	31.22 ± 5.39	3.07 ± 4.03	1.94 ± 0.43	W	237.44 ± 30.10	65.89 ± 26.78
	HP	-0.91 ± 5.94	30.38 ± 5.58	1.78 ± 1.69	1.75 ± 0.35	W	233.03 ± 30.95	83.54 ± 14.18
	NHP	16.45 ± 2.83	32.57 ± 4.38	6.1 ± 4.77	2.24 ± 0.36	W	244.21 ± 27.40	37.65 ± 15.71
NMH	Whole	5.42 ± 10.01	33.03 ± 6.99	2.93 ± 4.05	1.53 ± 0.39	WNW	221.93 ± 23.79	78.58 ± 16.21
	HP	-1.57 ± 6.08	30.23 ± 6.09	0.54 ± 1.14	1.70 ± 0.37	W	218.58 ± 20.84	88.75 ± 8.04
	NHP	16.13 ± 2.77	37.32 ± 6.04	6.59 ± 4.17	1.29 ± 0.30	WNW	226.84 ± 26.79	62.99 ± 12.84
DLX	Whole	3.32 ± 9.07	38.24 ± 8.48	18.45 ± 23.90	2.40 ± 0.35	WNW	254.63 ± 56.83	33.69 ± 12.3
	HP	-3.08 ± 5.39	34.04 ± 6.26	7.12 ± 8.89	2.42 ± 0.33	WNW	260.09 ± 49.28	34.5 ± 11.45
	NHP	13.12 ± 2.78	44.68 ± 5.95	35.83 ± 29.34	2.38 ± 0.35	W	230.33 ± 32.44	32.45 ± 11.98

Note: HP = heating period; NHP = non-heating period.

For nps ions, nps-Cl⁻ (a tracer of coal combustion) during the HP was positively correlated
with wind direction ($P < 0.05$, Figure S19), indicating downwind transport. In contrast, nps-K⁺ (a
tracer of biomass burning) was negatively correlated with wind speed and solar radiation ($P < 0.05$),
consistent with the observed peak in combustion contributions during winter when solar radiation
is the lowest. Increased wind speed may suppress biomass-burning intensity (Zhang, 2024), while
higher solar radiation can reduce smoldering-phase nps-K⁺ emissions and enhance photochemical
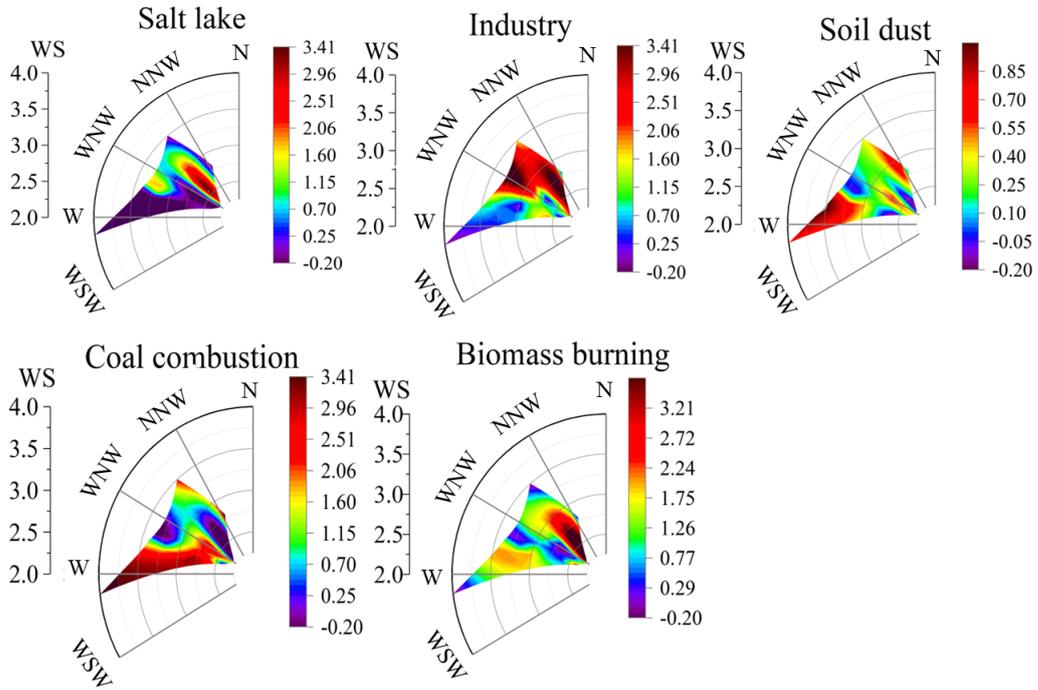removal of aerosols (Kuang et al., 2020; Huang and Gao, 2021).

For carbonaceous components (Figure S20), in the rural NHP, soot-EC, OC, and the char/soot
ratio were positively correlated with precipitation and negatively with the frequency of visibility

1026 ≤10 km ($P < 0.05$). In the rural HP, the char/soot ratio was positively correlated with precipitation.

1027 In the urban NHP, char-EC, soot-EC, and their ratios showed positive correlations with humidity

1028 and precipitation ($P < 0.01$), while POC was positively correlated with the frequency of visibility

1029 ≤10 km ($P < 0.01$). Total carbon, OC, and SOC were negatively correlated with wind speed ($P <$

1030 0.05). In the urban HP, EC and char-EC were negatively correlated with the frequency of visibility

1031 ≤10 km; POC was positively correlated with wind speed and solar radiation but negatively with the

1032 frequency of visibility ≤10 km ($P < 0.05$); and the char/soot ratio was positively correlated with

1033 wind speed and negatively with the frequency of visibility ≤10 km ($P < 0.01$).

1034   Overall, wind speed was negatively correlated with TC, OC, SOC, POC, and the char/soot ratio

1035 ($P < 0.05$). This pattern aligns with findings from Xi'an (Cao et al., 2009), New Delhi (Tiwari et al.,

1036 2015), and Karachi (Bibi et al., 2017), although it was not observed in rural areas (Sharma et al.,

1037 2002). Increased wind speed enhances ventilation, promoting aerosol dispersion and reducing

1038 carbonaceous aerosol concentrations (Saha and Despiau, 2009). The low mean wind speed (about

1039 2.30 m/s) may also indicate that carbon emissions are predominantly local rather than distant sources

1040 (Shen et al., 2021). Positive correlations of precipitation and relative humidity with soot-EC,

1041 char-EC, OC, and the char/soot ratio likely reflect the hygroscopic nature of carbonaceous aerosols:

1042 under humid conditions, particles absorb water, increase in mass, and undergo accelerated dry

1043 deposition. For instance, $PM_{2.5}$ deposition rates can increase 2-3 fold as relative humidity rises from

1044 30% to 70%, thereby shortening their atmospheric residence time (Wu et al., 2016). The negative

1045 correlations of EC, char-EC, and POC with the frequency of visibility ≤10 km align with findings

1046 in cities such as Suzhou (Zhang et al., 2010) and Beijing (Kong et al., 2021), attributable to the

1047 strong light-absorbing (EC) and light-scattering (OC) properties of these components, which jointly

1048 enhance atmospheric extinction and reduce visibility (Zhang et al., 2010; Kong et al., 2021). Weaker

1049 correlations in rural areas indicate that carbonaceous components are less influenced by local

1050 meteorological dilution and removal processes, pointing to more complex source influences.

1051   In summary, seasonal variations in atmospheric dust deposition result from the combined

1052 effects of meteorological conditions and anthropogenic emissions. In urban areas, meteorological

1053 factors, especially wind speed and relative humidity, play a dominant role in the dispersion and

1054 removal of local anthropogenic pollutants. In rural areas, dust composition is more strongly

1055 influenced by large-scale wind-driven dust transport and regional combustion activities.

Rural-HP

Salt lake

Industry

Soil dust

Coal combustion

Biomass burning

Rural-NHP
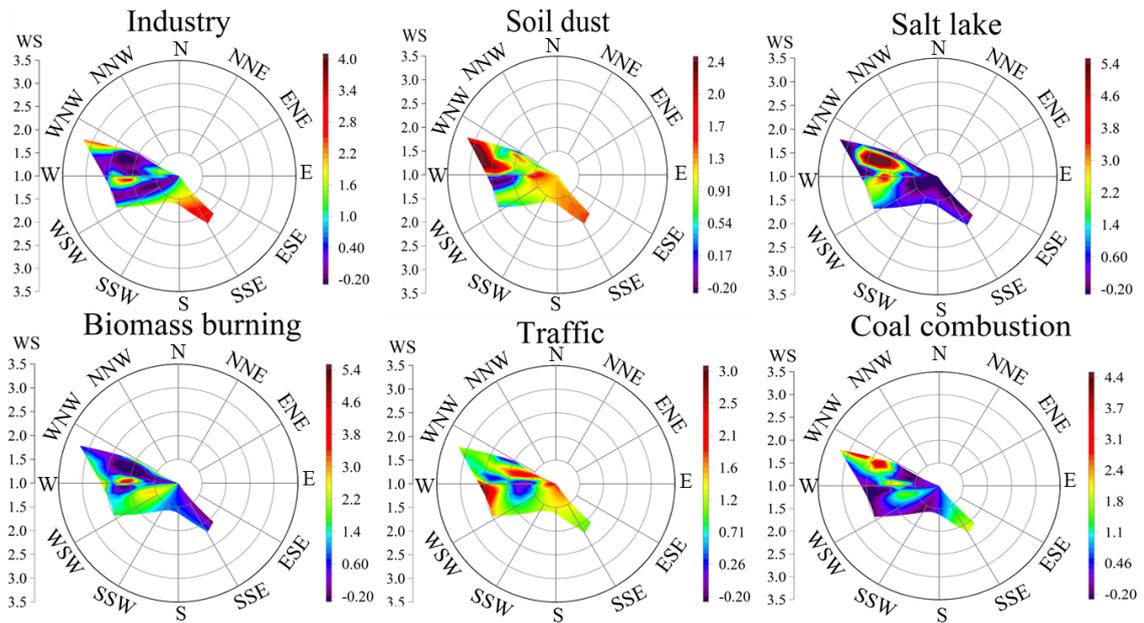
Salt lake
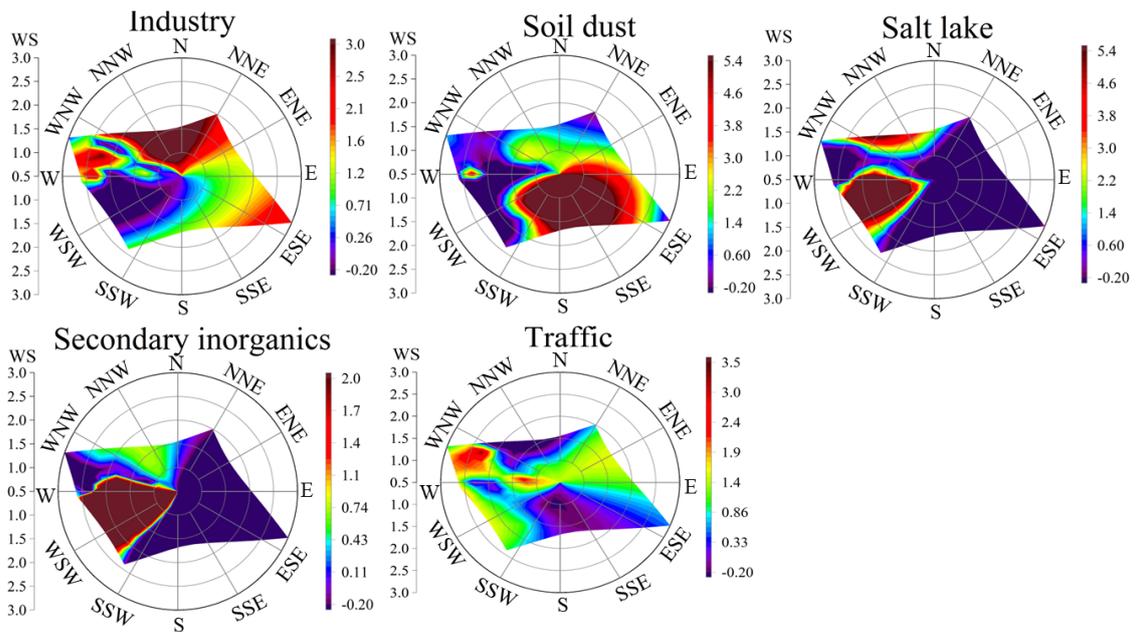
Industry

Soil dust

Traffic

Biomass burning
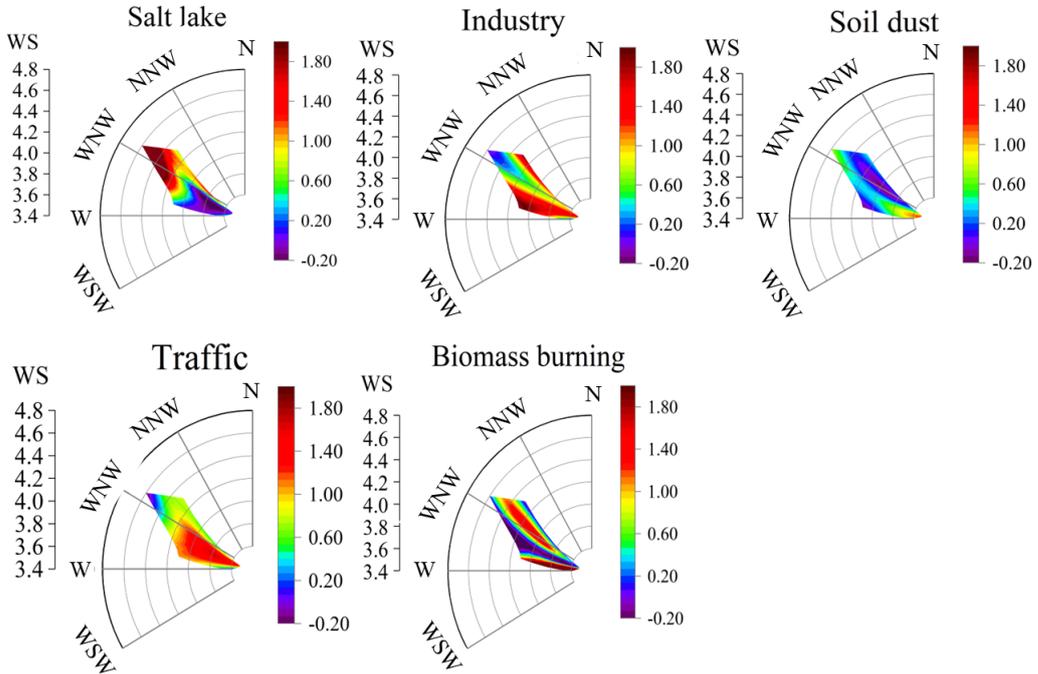
Figure 8 Relationship between wind speed, wind direction, and atmospheric dust deposition sources in rural of the Qaidam Basin during domestic heating (HP) and non-heating (NHP) periods.

Figure 9 Relationship between wind speed, wind direction, and atmospheric dust deposition sources in urban of the Qaidam Basin during domestic heating (HP) and non-heating (NHP) periods.

Wind direction analysis provides a valuable supplement to the PMF model (Watson et al., 2008). Studies have shown that emissions from sources such as traffic, biomass burning, coal combustion,

and salt lakes exhibit significant directional patterns, which can be effectively visualized using polar plots (Saraga et al., 2021). In this study, bivariate polar plots were generated for the concentrations of POC, SOC, char-EC, soot-EC, and selected ions/elements (Figure S21-S24), as well as for the source contributions resolved by the PMF model (Figure 8 and 9), to illustrate their directional provenance. Notably, the directional patterns of the various aerosol components exhibited distinct differences and did not fully align with the local prevailing wind directions.

The polar plots of key tracer ions and elements (Figure S21-S24) showed patterns consistent with the corresponding PMF-resolved source factors (Figure 8 and 9), supporting the validity of the source apportionment. Specifically, the following pairs showed similar directional distributions: Total-ps and the salt-lake source; nps-K^+, POC, and char-EC with biomass burning; nps-Ca^{2+} and Si with soil dust; nps-SO_4^{2-}, nps-Cl^-, and SOC with coal combustion; Fe and Cd with industry; Ni and Zn with vehicle combustion; Fe and Al with industry; and nps-SO_4^{2-} together with NO_3^- with secondary formation. These spatial consistencies reinforce that the selected chemical tracers are associated with their respective PMF-identified sources.

Wind speeds in rural areas are generally higher than those in urban environments, with predominant wind directions between west (W) and north (N), indicating the potential long-distance transport of pollutants. Specifically, emissions from saline lakes primarily originate from the west-northwest (WNW) direction. Back trajectory modeling suggests that HP levels are mainly attributed to salt lake emissions from the northwestern QDB, while in NHP, sources include long-distance transport from salt lakes in the Tarim Basin (Figure S6, S7). For industrial emissions during the HP, sources primarily originate from medium- to short-distance transport in the W direction, with NHP periods showing contributions from both the west (W) and northwest-northwest (NNW) directions. In contrast, soil dust in HP is predominantly sourced from long-distance transport from the W direction, whereas in NHP, it is largely of local origin. Biomass burning during HP mainly arises from local sources, while its contribution during NHP is minimal and comes from both local and long-distance transport, consistent with PMF results.

In urban areas, lower wind speeds and varying dominant wind directions between the HP and NHP lead to different sources of pollutants. During HP, emissions from saline lakes and coal combustion primarily originate from short-distance transport in the WNW direction, while biomass burning is sourced from the W. In contrast, industrial emissions, soil dust, and vehicle combustion

1098 are predominantly attributed to local sources. In NHP, pollutants demonstrate a dispersion trend

1099 from their sources to urban areas. Industrial emissions primarily come from the WNW to north-

1100 northeast (NNE) directions, soil dust from the southwest (SW), and vehicle emissions from the W

1101 direction. Notably, both salt lake and secondary formation sources exhibit similar directional

1102 patterns, indicating a common origin from the SW direction. The presence of processing enterprises

1103 near salt lakes suggests that secondary aerosols may form from emitted SO_2 and NO_2 (Hewitt, 2001).

1104 These findings align with previous analyses showing that urban industrial and traffic emissions

1105 mainly derive from local sources, while coal and biomass burning predominantly originate from

1106 surrounding rural areas, corroborating the role of nearby soil sources in salt lake and soil emissions.

1107

1108 **3.6 Environmental implication**

1109 The source apportionment analysis using the PMF model indicates that in the QDB, rural dust-

1110 fall predominantly originates from the combustion of solid fuels, including firewood, yak dung, and

1111 coal, accounting for approximately 72.05% of the total contribution. This proportion significantly

1112 exceeds contributions reported for rural areas in Beijing (41%) (Hua et al., 2018), Agra (54.3%)

1113 (Agarwal et al., 2020), and Beihai, Guangxi Province (66.7%) (Zhang et al., 2019).

1114 The higher contribution in this study likely reflects the local energy profile, as the sampling

1115 site in Haixi Mongol and Xizang Autonomous Prefecture, Qinghai Province, primarily relies on coal,

1116 yak dung, and firewood, constituting 58%, 23.5%, and 13% of rural energy consumption,

1117 respectively (Jiang et al., 2020; Shen et al., 2021). In contrast, solid biomass fuels, including wood

1118 and yak dung, account for over 70% of rural household energy consumption in Xizang, with yak

1119 dung alone representing 53% (Liu et al., 2008; Xiao et al., 2015). Similar patterns emerge in South

1120 and Central Asia, where biomass fuels dominate residential heating (firewood: 39%; dung: 29%)

1121 (Amacher et al., 1999; Heltberg et al., 2000; Hoeck et al., 2007; Foysal et al., 2012; Behera et al.,

1122 2015; Kerimray et al., 2018). In northern China, rural domestic heating primarily relies on coal

1123 (46%), firewood (23.8%), and electricity (15.1%) (Tao et al., 2018), further highlighting the unique

1124 energy composition of QDB.

1125 Recent studies have shown that South Asia, Central Asia, and Xizang contribute significantly

1126 to high concentrations of atmospheric PM, particularly BC, which accelerates glacier melting in the

QXP (Ming et al., 2010; Xia et al., 2011; Chen et al., 2015). The QDB is recognized as a significant dust source affecting the glacier surfaces on the QXP, although it is often overlooked (Dong et al., 2014; Wei et al., 2017; Zheng et al., 2021). Compared to other dust sources, the QDB exhibits higher emissions from coal combustion, giving it a unique influence on the QXP. The organic matter and pollutants, such as PAHs, released from household solid fuel combustion, particularly coal (98%) and dung (94%), are substantially higher than those from firewood (Leavey et al., 2017; Secrest et al., 2017; Ye et al., 2020). Consequently, the impact of PM from coal combustion in the QDB on the QXP is significant. Specifically, the presence of BC in PM increases glacier albedo, accelerating the melting of glaciers and snow in the region (Kang et al., 2020) and impacting global freshwater resources (Huss and Hock, 2018). Additionally, BC enhances cloud condensation nuclei, ice number concentration, and cloud cover (Zhou et al., 2025), thereby influencing global climate change. Furthermore, coal combustion releases harmful emissions, including CO_2, NO_x, CO, SO_2 and sulfur trioxide (Munawer, 2018), adversely affecting local human health and exacerbating climate warming on the QXP (Liu et al., 2006; Li et al., 2023), with broader implications for global climate. Therefore, the atmospheric pollutants emission of the QDB deserves considerable attention. However, this study focuses primarily on larger particles, indicating a need for further research on the environmental impacts of carbonaceous aerosols in atmospheric PM within the QDB.

In addition to the distinctive energy consumption structure in the rural QDB, which leads to significant contributions from coal and biomass burning during HP, atmospheric dust deposition in the QDB during the NHP primarily originates from traffic and industrial emissions. The contribution from traffic emissions during the NHP was twice that during the HP. Considering the larger particle size of the dust samples collected in this study, the traffic-related dust is likely derived mainly from vehicle non-exhaust emissions, such as road dust (Gondwal and Mandal, 2021). This indicates that NHP atmospheric conditions are significantly influenced by resource development and tourism. Sampling sites, such as Qarhan Salt Lake, along with GEM and LTC stations within approximately 100 km (Figure 1), suggest that salt lake resource extraction has a lower impact on regional aerosols than traffic emissions, despite salt lakes being the primary resource. This is likely because salt lake development mainly involves solar evaporation and chemical processes like extraction and adsorption, which emit fewer pollutants compared to other mining methods (Zhen, 2010). Consequently, salt lake resource exploitation exerts a relatively minor effect on local atmospheric

1157 carbonaceous aerosol.

1158 Similar salt lakes with comparable environments to QDB, such as Salar de Uyuni in Bolivia,

1159 the Atacama Salt Lake in Chile, and Ombre Muerto in Argentina, are rich in lithium resources (Li

1160 et al., 2014), making them focal points for resource development. Additionally, Salar de Uyuni, the

1161 Atacama Salt Lake, Junggar Basin, and the Great Salt Lake are renowned tourist destinations. This

1162 suggests that, in arid basin salt lakes with similar climates and intensive human activity, atmospheric

1163 carbonaceous aerosols are likely influenced by resource exploitation and tourism, especially tourism.

1164 The study's findings can inform policy decisions regarding unexploited salt lakes in South America,

1165 such as Ombre Muerto and Salar de Uyuni. However, while QDB also hosts mineral resources such

1166 as copper, iron, and tin, this research focused on larger particles (>100 μm), which are more

1167 indicative of local sources. Given that sampling was conducted around the salt lakes, potential

1168 impacts from other mineral resource developments may have been underestimated. Further research

1169 is necessary to fully assess the environmental effects of carbonaceous aerosols in QDB atmospheric

1170 particles.

1171 In conclusion, the localized source profiles developed in this study, such as OC/EC ratios for

1172 heating-period emissions and key heavy-metal tracers, provide critical input parameters for regional

1173 climate and air quality models. This enables more accurate simulation of the emission, transport,

1174 and deposition of carbonaceous aerosols in the QDB and supports quantitative assessment of their

1175 contribution to glacier retreat on the QXP. Based on that rural areas in arid and semi-arid basins

1176 such as QDB rely heavily on solid fuels for heating, with associated environmental impacts, we

1177 recommend that local governments implement targeted clean-energy transition policies. These

1178 should prioritize promoting clean heating alternatives (e.g., solar and electric heating) in rural

1179 regions, supported by financial subsidies and technical assistance. Simultaneously, the adoption of

1180 clean stoves and upgraded biomass fuels should be encouraged to reduce emissions from traditional

1181 biomass and coal combustion (Dickinson et al., 2015; Li et al., 2011; Shen et al., 2017). Given the

1182 close climatic and environmental linkage between QDB and QXP, we further propose integrating

1183 air pollution control in QDB into the broader environmental protection framework of QXP.

1184 Establishing a joint regional air pollution prevention and control mechanism for the "QDB–QXP"

1185 system would help align emission reduction in the basin with glacier protection goals on the plateau.

1186 To strengthen the scientific foundation of such a mechanism, future studies should focus on

1187 clarifying the key transport pathways, transformation processes, and quantitative impacts of air

1188 pollutants from QDB to QXP glaciers.

1189

4. Conclusion

1191   This study analyzed the composition of dust deposition at six sampling sites in the southern

1192 QDB from January 2020 to March 2023 and examined DF, soluble ions, trace and carbonaceous

1193 element content in urban and rural samples during both domestic heating and non-domestic heating

1194 periods. Through integrated application of backward trajectory modeling, PMF, and carbon

1195 speciation indices, we identified dominant dust sources and evaluated domestic heating impacts on

1196 atmospheric processes in remote regions.

1197   The findings revealed that DF and carbon emissions were significantly higher in rural than in

1198 urban areas. Among carbon indicators, urban areas exhibited elevated EC levels (1.46 ± 1.60 mg/g),

1199 while OC levels were higher in rural (3.73 ± 2.61 mg/g). Economic development increase OC/EC

1200 ratios, but they are driven by different intrinsic factors. Char-EC was the dominant contributor to

1201 EC (80.44%), with urban char-EC levels (85.00%) showing a notable increase compared to rural

1202 levels (75.88%). Secondary organic carbon was the principal contributor to OC (72.61%), with rural

1203 SOC levels surpassing (78.44%) those in urban areas (67.78%). The OC/EC and char-EC/soot-EC

1204 ratios, along with PMF results, indicated that during HP, dust deposition in the QDB was primarily

1205 derived from coal combustion (26.85%) and biomass burning (24.04%), while traffic emissions

1206 accounted for 34.64% of dust during NHP. Coal and biomass burning were the main contributors to

1207 rural dust, strongly influenced by domestic heating, whereas urban dust predominantly originated

1208 from traffic (46.83%) and industrial emissions (16.12%). Compared to other dust sources in the

1209 QXP, coal consumption in the QDB is higher during the domestic heating period. The resulting

1210 emissions of BC and greenhouse gases may exacerbate glacier melting in the region, warranting

1211 increased attention. Given the distinctive carbonaceous aerosol signatures identified in the QDB,

1212 we recommend prioritizing their radiative forcing effects in regional environmental policymaking

1213 and climate modeling frameworks. Furthermore, findings of this study offer a valuable scientific

1214 basis for understanding atmospheric carbonaceous aerosols in arid basins and salt lake regions with

1215 climates similar to QDB. They can particularly inform policy decisions regarding unexploited salt

1216   lakes in South America, such as Ombre Muerto and Salar de Uyuni.

1217   However, this study primarily focused on larger-scale PM and examined the effects of heating

1218   on carbonaceous aerosols in the QDB. It lacks an investigation of aerosols with smaller particle

1219   sizes (e.g., PM_{10}, $PM_{2.5}$, PM_1), which is essential for a comprehensive understanding of

1220   carbonaceous aerosol characteristics in this unique region. Furthermore, in addition to offline

1221   observations, future research should incorporate online observations with high spatiotemporal

1222   resolution and utilize numerical air quality models such as CMAQ, CAMx, WRF-CHEM, and

1223   NAQPMS to analyze the spatiotemporal distribution and future trends of carbon aerosols in the

1224   QDB.

1225

Author contribution

1227   HZ: Conceptualization, data curation, formal analysis, funding acquisition, investigation,

1228   methodology, project administration, validation, writing – original draft.

1229   LZ: Data curation, formal analysis, methodology.

1230   SZ: funding acquisition, validation, writing – review & edited.

1231   XZ: Supervision, conceptualization, funding acquisition, writing – review & edited.

1232

1239

Declaration of competing interest

1241   The authors declare that there is no conflict of interest.

1242

Data availability

1244   Datasets for this research has been uploaded in Zenodo and is available at

1245   https://doi.org/10.5281/zenodo.14382853 (Zhu, 2024).

Reference

Abdollahi, S., Karimi, A., Madadi, M., Eslamian, S., Ostad-Ali-Askari, K., and Singh, V. P.: Lead concentration in dust fall in Zahedan, Sistan and Baluchistan Province, Iran, Journal of Geography and Cartography, 4, 6, https://doi.org/10.24294/jgc.v4i2.601, 2021.

Adeniran, J. A., Yusuf, R. O., and Olajire, A. A.: Exposure to coarse and fine particulate matter at and around major intra-urban traffic intersections of Ilorin metropolis, Nigeria, Atmospheric Environment, 166, 383-392, https://doi.org/10.1016/j.atmosenv.2017.07.041, 2017.

Agarwal, A., Satsangi, A., Lakhani, A., and Kumari, K. M.: Seasonal and spatial variability of secondary inorganic aerosols in $PM_{2.5}$ at Agra: Source apportionment through receptor models, Chemosphere, 242, 125132, https://doi.org/10.1016/j.chemosphere.2019.125132, 2020.

Aiken, A. C., DeCarlo, P. F., Kroll, J. H., Worsnop, D. R., Huffman, J. A., Docherty, K. S., Ulbrich, I. M., Mohr, C., Kimmel, J. R., Sueper, D., Sun, Y., Zhang, Q., Trimborn, A., Northway, M., Ziemann, P. J., Canagaratna, M. R., Onasch, T. B., Alfarra, M. R., Prevot, A. S. H., Dommen, J., Duplissy, J., Metzger, A., Baltensperger, U., and Jimenez, J. L.: O/C and OM/OC ratios of primary, secondary, and ambient organic aerosols with High-Resolution Time-of-Flight Aerosol Mass Spectrometry, Environmental Science & Technology, 42, 4478-4485, https://doi.org/10.1021/es703009q, 2008.

Almeida, S. M., Lage, J., Fernández, B., Garcia, S., Reis, M. A., and Chaves, P. C.: Chemical characterization of atmospheric particles and source apportionment in the vicinity of a steelmaking industry, Science of The Total Environment, 521-522, 411-420, https://doi.org/10.1016/j.scitotenv.2015.03.112, 2015.

Alzahrani, A. J., Alghamdi, A. G., and Ibrahim, H. M.: Assessment of soil loss due to wind erosion and dust deposition: Implications for sustainable management in arid regions, Applied Sciences, 14(23), 10822, https://doi.org/10.3390/app142310822, 2024.

Amacher, G. S., Hyde, W. F., and Kanel, K. R.: Nepali fuelwood production and consumption: Regional and household distinctions, substitution and successful intervention, The Journal of Development Studies, 35, 138-163, https://doi.org/10.1080/00220389908422584, 1999.

Ambade, B., Sankar, T. K., Sahu, L. K., and Dumka, U. C.: Understanding sources and composition of black carbon and $PM_{2.5}$ in urban environments in East India, Urban Science, 6(3), 60, https://doi.org/10.3390/urbansci6030060, 2022.

Amato, F., Alastuey, A., de la Rosa, J., Gonzalez Castanedo, Y., Sánchez de la Campa, A. M., Pandolfi,

1276   M., Lozano, A., Contreras González, J., and Querol, X.: Trends of road dust emissions contributions

1277   on ambient air particulate levels at rural, urban and industrial sites in southern Spain, Atmospheric

1278   Chemistry and Physics, 14, 3533-3544, https://doi.org/10.5194/acp-14-3533-2014, 2014.

1279 Arimoto, R., Duce, R. A., Savoie, D. L., Prospero, J. M., Talbot, R., Cullen, J. D., Tomza, U., Lewis, N.

1280   F., and Ray, B. J.: Relationships among aerosol constituents from Asia and the North Pacific during

1281   PEM-West A, Journal of Geophysical Research: Atmospheres, 101, 2011-2023,

1282   https://doi.org/10.1029/95JD01071, 1996.

1283 Ashrafi, K., Fallah, R., Hadei, M., Yarahmadi, M., and Shahsavani, A.: Source apportionment of Total

1284   Suspended Particles (TSP) by Positive Matrix Factorization (PMF) and Chemical Mass Balance

1285   (CMB) modeling in Ahvaz, Iran, Archives of Environmental Contamination and Toxicology, 75,

1286   278-294, https://doi.org/10.1007/s00244-017-0500-z, 2018.

1287 Bandowe, B. A. M., Nkansah, M. A., Leimer, S., Fischer, D., Lammel, G., and Han, Y.: Chemical (C, N,

1288   S, black carbon, soot and char) and stable carbon isotope composition of street dusts from a major

1289   West African metropolis: Implications for source apportionment and exposure, Science of The Total

1290   Environment, 655, 1468-1478, https://doi.org/10.1016/j.scitotenv.2018.11.089, 2019.

1291 Barjoee, S. S., Abadi, S. Z. M., Elmi, M. R., Varaoon, V. T., and Nikbakht, M.: Evaluation of trace

1292   elements pollution in deposited dust on residential areas and agricultural lands around Pb/Zn

1293   mineral areas using modified pollution indices, Journal of Environmental Health Science and

1294   Engineering, 19, 753-769, https://doi.org/10.1007/s40201-021-00643-8, 2021.

1295 Behera, B., Rahut, D. B., Jeetendra, A., and Ali, A.: Household collection and use of biomass energy

1296   sources in South Asia, Energy, 85, 468-480, https://doi.org/10.1016/j.energy.2015.03.059, 2015.

1297 Belis, C. A., Pernigotti, D., Karagulian, F., Pirovano, G., Larsen, B. R., Gerboles, M., and Hopke, P. K.:

1298   A new methodology to assess the performance and uncertainty of source apportionment models in

1299   intercomparison exercises, Atmospheric Environment, 119, 35-44,

1300   https://doi.org/10.1016/j.atmosenv.2015.08.002, 2015.

1301 Bibi, S., Alam, K., Chishtie, F., Bibi, H., and Rahman, S.: Temporal variation of Black Carbon

1302   concentration using Aethalometer observations and its relationships with meteorological variables

1303   in Karachi, Pakistan, Journal of Atmospheric and Solar-Terrestrial Physics, 157-158, 67-77,

1304   https://doi.org/10.1016/j.jastp.2017.03.017, 2017.

1305 Bond, T. C. and Bergstrom, R. W.: Light absorption by carbonaceous particles: An investigative review,

Aerosol Science and Technology, 40, 27-67, https://doi.org/10.1080/02786820500421521, 2006.

Bond, T. C., Streets, D. G., Yarber, K. F., Nelson, S. M., Woo, J. H., and Klimont, Z.: A technology-based global inventory of black and organic carbon emissions from combustion, Journal of Geophysical Research: Atmospheres, 109, https://doi.org/10.1029/2003JD003697, 2004.

Bond, T. C., Doherty, S. J., Fahey, D. W., Forster, P. M., Berntsen, T., DeAngelo, B. J., Flanner, M. G., Ghan, S., Kärcher, B., Koch, D., Kinne, S., Kondo, Y., Quinn, P. K., Sarofim, M. C., Schultz, M. G., Schulz, M., Venkataraman, C., Zhang, H., Zhang, S., Bellouin, N., Guttikunda, S. K., Hopke, P. K., Jacobson, M. Z., Kaiser, J. W., Klimont, Z., Lohmann, U., Schwarz, J. P., Shindell, D., Storelvmo, T., Warren, S. G., and Zender, C. S.: Bounding the role of black carbon in the climate system: A scientific assessment, Journal of Geophysical Research: Atmospheres, 118, 5380-5552, https://doi.org/10.1002/jgrd.50171, 2013.

Boreddy, S. K. R., Kawamura, K., Okuzawa, K., Kanaya, Y., and Wang, Z.: Temporal and diurnal variations of carbonaceous aerosols and major ions in biomass burning influenced aerosols over Mt. Tai in the North China Plain during MTX2006, Atmospheric Environment, 154, 106-117, https://doi.org/10.1016/j.atmosenv.2017.01.042, 2017.

Bowen, H. J. M.: Environmental chemistry of the elements. Academic Press, https://doi.org/10.1002/9780470140451, 1979.

Brooks, J., Liu, D., Allan, J. D., Williams, P. I., Haywood, J., Highwood, E. J., Kompalli, S. K., Babu, S. S., Satheesh, S. K., Turner, A. G., and Coe, H.: Black carbon physical and optical properties across northern India during pre-monsoon and monsoon seasons, Atmospheric Chemistry and Physics, 19, 13079-13096, https://doi.org/10.5194/acp-19-13079-2019, 2019.

Butler, K. M. and Mulholland, G. W.: Generation and transport of smoke components, Fire Technology, 40, 149-176, https://doi.org/10.1023/B: FIRE.0000016841.07530.64, 2004.

Cachier, H. and Ducret, J.: Influence of biomass burning on equatorial African rains, Nature, 352, 228-230, https://doi.org/10.1038/352228a0, 1991.

Cao, J. J., Wang, Q. Y., Chow, J. C., Watson, J. G., Tie, X.-X., Shen, Z. X., Wang, P., and An, Z. S.: Impacts of aerosol compositions on visibility impairment in Xi'an, China, Atmospheric Environment, 59, 559-566, https://doi.org/10.1016/j.atmosenv.2012.05.036, 2012a.

Cao, J. J., Zhu, C. S., Chow, J. C., Watson, J. G., Han, Y. M., Wang, G. H., Shen, Z. X, and An, Z. S.: Black carbon relationships with emissions and meteorology in Xi'an, China, Atmospheric Research,

94, 194-202, https://doi.org/10.1016/j.atmosres.2009.05.009, 2009.

Cao, J.: Characteristics of carbonaceous aerosol in Pearl River Delta Region, China during 2001 winter period, Atmospheric Environment, 37, 1451-1460, https://doi.org/10.1016/s1352-2310(02)01002-6, 2003.

Cao, J. J., Shen, Z. X., Chow, J. C., Watson, J. G., Lee, S. C., Tie, X. X., Ho, K. F., Wang, G. H., and Han, Y. M.: Winter and summer $PM_{2.5}$ chemical compositions in fourteen Chinese cities, Journal of Air Waste Manage Association, 62, 1214-1226, https://doi.org/10.1080/10962247.2012.701193, 2012b.

Cao, J. J., Zhu, C. S., Tie, X. X., Geng, F. H., Xu, H. M., Ho, S. S. H., Wang, G. H., Han, Y. M., and Ho, K. F.: Characteristics and sources of carbonaceous aerosols from Shanghai, China, Atmospheric Chemistry and Physics, 13, 803-817, https://doi.org/10.5194/acp-13-803-2013, 2013.

Casotti Rienda, I. and Alves, C. A.: Road dust resuspension: A review, Atmospheric Research, 261, 105740, https://doi.org/10.1016/j.atmosres.2021.105740, 2021.

Cesari, D., Amato, F., Pandolfi, M., Alastuey, A., Querol, X., and Contini, D.: An inter-comparison of PM_{10} source apportionment using PCA and PMF receptor models in three European sites, Environmental Science and Pollution Research, 23, 15133-15148, https://doi.org/10.1007/s11356-016-6599-z, 2016.

Chen, L., Zhang, X. Y., Tang, Q. L., Geng, Y., Wang, E. L., and Li, J. Y.: Heavy metal pollution and source analysis of surface soil in the Qaidam Basin (in Chinese), Environmental Science, 42, 4880–4888, https://doi.org/10.13227/j.hjkx.202101052, 2021.

Chen, M., Li, M.-Y., Zhou, J. Y., Fu, R.-B., Wang, X. F., and Shen Z.: Characteristics and source analysis of heavy metal pollution in dust in a heavy industrial area of Northwest China (in Chinese), Environmental Science and Technology, 47(02), 155-164, https://doi.org/10.19672/j.cnki.1003-6504.1004.23.338, 2024.

Chen, P., Kang, S., Bai, J., Sillanpää, M., and Li, C.: Yak dung combustion aerosols in the Tibetan Plateau: Chemical characteristics and influence on the local atmospheric environment, Atmospheric Research, 156, 58-66, https://doi.org/10.1016/j.atmosres.2015.01.001, 2015.

Chen, W., Tong, D. Q., Dan, M., Zhang, S., Zhang, X., and Pan, Y.: Typical atmospheric haze during crop harvest season in northeastern China: A case in the Changchun region, Journal of Environmental Sciences, 54, 101-113, https://doi.org/10.1016/j.jes.2016.03.031, 2017.

53

1366   Cheng, X. and Lin, X.: Temporal and spatial distribution characteristics of dust in Shenyang and analysis

1367   of influencing factors (in Chinese). Environmental Protection Science 35(06), 1-3 + 58,

1368   https://doi.org/10.16803/j.cnki.issn.1004-6216.2009.06.001, 2009.

1369   Chow, J. C.: Measurement methods to determine compliance with ambient air quality standards for

1370   suspended particles, Journal of the Air & Waste Management Association, 45, 320-382,

1371   https://doi.org/10.1080/10473289.1995.10467369, 1995.

1372   Chow, J. C., Lowenthal, D. H., Chen, L. W. A., Wang, X., and Watson, J. G.: Mass reconstruction methods

1373   for $PM_{2.5}$: A review, Air Quality, Atmosphere & Health, 8, 243-263, https://doi.org/10.1007/s11869-

1374   015-0338-3, 2015.

1375   Chow, J. C., Watson, J. G., Kuhns, H., Etyemezian, V., Lowenthal, D. H., Crow, D., Kohl, S. D.,

1376   Engelbrecht, J. P., and Green, M. C.: Source profiles for industrial, mobile, and area sources in the

1377   Big Bend Regional Aerosol Visibility and Observational study, Chemosphere, 54, 185-208,

1378   https://doi.org/10.1016/j.chemosphere.2003.07.004, 2004.

1379   Christie, J. A., Elliott, H. E., O'Connell-Lopez, S. M. O., Perry, K., Pratt, K. A., Hallar, A. G., Hrdina,

1380   A., Murphy, J. G., Riedel, T. P., Long, R. W., Mitroo, D., Haskins, J. D., and Gaston, C. J.: Halogen

1381   production from playa dust emitted from the Great Salt Lake: Implications of the shrinking Great

1382   Salt Lake on regional air quality, ACS Earth and Space Chemistry, 9, 480-493,

1383   https://doi.org/10.1021/acsearthspacechem.4c00258, 2025.

1384   Chuang, M. T., Lee, C. T., Chou, C. C. K., Lin, N.-H., Sheu, G. R., Wang, J. L., Chang, S. C., Wang,

1385   S.MH., Chi, K. H., Young, C. Y., Huang, H., Chen, H. W., Weng, G -H., Lai, S. Y., Hsu, S. P., Chang,

1386   Y. J., Chang, J. H., and Wu, X. C.: Carbonaceous aerosols in the air masses transported from

1387   Indochina to Taiwan: Long-term observation at Mt. Lulin, Atmospheric Environment, 89, 507-516,

1388   https://doi.org/10.1016/j.atmosenv.2013.11.066, 2014.

1389   Cichowicz, R. and Bochenek, A. D.: Assessing the effects of urban heat islands and air pollution on

1390   human quality of life, Anthropocene, 46, 100433, https://doi.org/10.1016/j.ancene.2024.100433,

1391   2024.

1392   Cong, Z., Kang, S., Luo, C., Li, Q., Huang, J., Gao, S., and Li, X.: Trace elements and lead isotopic

1393   composition of PM_{10} in Lhasa, Tibet, Atmospheric Environment, 45, 6210-6215,

1394   https://doi.org/10.1016/j.atmosenv.2011.07.060, 2011.

1395   Dang, X., Chang, L., and Lu, N.: The impact of climatic warm-wet situation of the Tibetan Plateau on

1396   the water resources and environment in Qaidam Basin, Geology of China, 46, 359-368, 2019.

1397   Demir, T., Karakaş, D., and Yenisoy-Karakaş, S.: Source identification of exhaust and non-exhaust traffic

1398   emissions through the elemental carbon fractions and Positive Matrix Factorization method,

1399   Environmental Research, 204, 112399, https://doi.org/10.1016/j.envres.2021.112399, 2022.

1400   Deng Z. W., Fang, F. M., Jiang, P. L., Zhang J. Q. and Lin Y. S.: Distribution characteristics of black

1401   carbon content in surface dust in Wuhu city (in Chinese), Journal of Anqing Normal University

1402   (Natural Science Edition), 37(01), 58-62, https://doi.org/10.14182/j.cnki.1001-2443.2014.01.009,

1403   2014.

1404   Deshmukh, D. K., Deb, M. K., Tsai, Y. I., and Mkoma, S. L.: Water soluble ions in $PM_{2.5}$ and PM_1

1405   aerosols in Durg City, Chhattisgarh, India, Aerosol and Air Quality Research, 11, 696-708,

1406   https://doi.org/10.4209/aaqr.2011.03.0023, 2011.

1407   Dickinson, K. L., Kanyomse, E., Piedrahita, R., Coffey, E., Rivera, I. J., Adoctor, J., Alirigia, R.,

1408   Muvandimwe, D., Dove, M., Dukic, V., Hayden, M. H., Diaz-Sanchez, D., Abisiba, A. V., Anaseba,

1409   D., Hagar, Y., Masson, N., Monaghan, A., Titiati, A., Steinhoff, D. F., Hsu, Y. Y., Kaspar, R., Brooks,

1410   B. A., Hodgson, A., Hannigan, M., Oduro, A. R., and Wiedinmyer, C.: Research on emissions, air

1411   quality, climate, and cooking technologies in Northern Ghana (Reaccting): study rationale and

1412   protocol, BMC Public Health, 15, 126, https://doi.org/10.1186/s12889-015-1414-1, 2015.

1413   Donahue, N. M.: Chapter 3.2 - Air pollution and air quality, in: Green chemistry, Elsevier, 151-176,

1414   https://doi.org/10.1016/B978-0-12-809270-5.00007-8, 2018.

1415   Dong, Z., Qin, D., Kang, S., Ren, J., Chen, J., Cui, X., Du, Z., and Qin, X.: Physicochemical

1416   characteristics and sources of atmospheric dust deposition in snow packs on the glaciers of western

1417   Qilian Mountains, China, Tellus B: Chemical and Physical Meteorology, 66, 20956,

1418   https://doi.org/10.3402/tellusb.v66.20956, 2014.

1419   Duan, J. and Tan, J.: Atmospheric heavy metals and Arsenic in China: Situation, sources and control

1420   policies, Atmospheric Environment, 74, 93-101, https://doi.org/10.1016/j.atmosenv.2013.03.031,

1421   2013.

1422   Eivazzadeh, M., Hassanvand, M. S., Faridi, S., and Gholampour, A.: Source apportionment and

1423   deposition of dustfall-bound trace elements around Tabriz, Iran, Environmental Science and

1424   Pollution Research International, 28, 59403-59415, https://doi.org/10.1007/s11356-020-12173-1,

1425   2021.

Fan, Q., Cheng, Y., Chen, T., and Xu, N.: Influence of water replenishment of lakes in the Northern Qaidam Basin on salt lake resources and ecological environment, Journal of Salt Lake Research, 30, 11-18, https://doi.org/10.18307/2024.0344 2022.

Fang, B., Zeng, H., Zhang, L., Wang, H., Liu, J., Hao, K., Zheng, G., Wang, M., Wang, Q., and Yang, W.: Toxic metals in outdoor/indoor airborne $PM_{2.5}$ in port city of Northern, China: Characteristics, sources, and personal exposure risk assessment, Environmental Pollution, 279, 116937, https://doi.org/10.1016/j.envpol.2021.116937, 2021.

Fang, H., Lowther, S. D., Zhu, M., Pei, C., Li, S., Fang, Z., Yu, X., Yu, Q., Wang, Y., Zhang, Y., Jones, K. C., and Wang, X.: $PM_{2.5}$-bound unresolved complex mixtures (UCM) in the Pearl River Delta region: Abundance, atmospheric processes and sources, Atmospheric Environment, 226, https://doi.org/10.1016/j.atmosenv.2020.117407, 2020.

Feng, W., Guo, Z., Xiao, X., Peng, C., Shi, L., Ran, H., and Xu, W.: Atmospheric deposition as a source of cadmium and lead to soil-rice system and associated risk assessment, Ecotoxicology and Environmental Safety, 180, 160-167, https://doi.org/10.1016/j.ecoenv.2019.04.090, 2019.

Filonchyk, M., Yan, H., Yang, S., and Lu, X.: Detection of aerosol pollution sources during sandstorms in Northwestern China using remote sensed and model simulated data, Advances in Space Research, 61, 1035-1046, https://doi.org/10.1016/j.asr.2017.11.037, 2018.

Foysal, M., Hossain, M., Rubaiyat, A., Sultana, S., Uddin, M. K., Sayem, M., and Akhter, J.: Household energy consumption pattern in rural areas of Bangladesh, Indian Journal of Energy, 1, 72-85, 2012.

Fu, B.: Socio-economic data set of Qinghai-Tibet Plateau (1982-2018). National Tibetan Plateau / Third Pole Environment Data Center, http://data.tpdc.ac.cn, 2023.

Gao, G. S., Song, L. M., and Ma, Z. T.: Temporal and spatial distribution of dust-fall in Qinghai Province and analysis of its influencing factors (in Chinese), Chinese Journal of Desert Research, 33(04), 1124-1130, https://doi.org/10.7522/j.issn.1000-694X.2013.00153, 2013.

Gao, H. and Washington, R.: Arctic oscillation and the interannual variability of dust emissions from the Tarim Basin: a TOMS AI based study, Climate Dynamics, 35, 511-522, https://doi.org/10.1007/s00382-009-0687-4, 2010.

Gao, Y., Wang, H., Yuan, L., Jing, S., Yuan, B., Shen, G., Zhu, L., Koss, A., Li, Y., Wang, Q., Huang, D. D., Zhu, S., Tao, S., Lou, S., and Huang, C.: Measurement report: Underestimated reactive organic gases from residential combustion – insights from a near-complete speciation, Atmospheric

Chemistry and Physics, 23, 6633-6646, https://doi.org/10.5194/acp-23-6633-2023, 2023.

Garaga, R., Gokhale, S., and Kota, S. H.: Source apportionment of size-segregated atmospheric particles and the influence of particles deposition in the human respiratory tract in rural and urban locations of north-east India, Chemosphere, 255, https://doi.org/10.1016/j.chemosphere.2020.126980, 2020.

Gertler, A., Kuhns, H., Abu-Allaban, M., Damm, C., Gillies, J., Etyemezian, V., Clayton, R., and Proffitt, D.: A case study of the impact of Winter road sand/salt and street sweeping on road dust re-entrainment, Atmospheric Environment, 40, 5976-5985, https://doi.org/10.1016/j.atmosenv.2005.12.047, 2006.

Gholampour, A., Nabizadeh, R., Hassanvand, M. S., Taghipour, H., Nazmara, S., and Mahvi, A. H.: Characterization of saline dust emission resulted from Urmia Lake drying, Journal of Environmental Health Science & Engineering, 13, 82, https://doi.org/10.1186/s40201-015-0238-3, 2015.

Gonçalves, C., Alves, C., Evtyugina, M., Mirante, F., Pio, C., Caseiro, A., Schmidl, C., Bauer, H., and Carvalho, F.: Characterisation of PM_{10} emissions from woodstove combustion of common woods grown in Portugal, Atmospheric Environment, 44, 4474-4480, https://doi.org/10.1016/j.atmosenv, 2010.

Gondwal, T. K. and Mandal, P.: Review on classification, sources and management of road dust and determination of uncertainty associated with measurement of particle size of road dust, Mapan, 36, 909-924, https://doi.org/10.1007/s12647-021-00501-w, 2021.

Gong, M., Yin, S., Gu, X., Xu, Y., Jiang, N., and Zhang, R.: Refined 2013-based vehicle emission inventory and its spatial and temporal characteristics in Zhengzhou, China, Science of The Total Environment, 599-600, 1149-1159, https://doi.org/10.1016/j.scitotenv.2017.03.299, 2017.

Goossens, D. and Offer, Z. Y. J. Z. F. G.: Eolian deposition of dust over symmetrical hills: an evaluation of wind-tunnel data by means of terrain measurement, Zeitschrift für Geomorphologie, 37, 103-111, https://doi.org/10.1127/zfg/37/1993/103, 1993.Gray, H. A., Cass, G. R., Huntzicker, J. J., Heyerdahl, E. K., and Rau, J. A.: Characteristics of atmospheric organic and elemental carbon particle concentrations in Los Angeles, Environmental Science & Technology, 20, 580-589, https://doi.org/10.1021/es00148a006, 1986.

Griffin, D. W., Kellogg, C. A., Garrison, V. H., and Shinn, E. A.: The global transport of dust: An Intercontinental river of dust, microorganisms and toxic chemicals flows through the Earth's atmosphere, American Scientist, 90, 228-235, https://www.jstor.org/stable/27857658, 2002.

Guo, J., Miao, Y., Zhang, Y., Liu, H., Li, Z., Zhang, W., He, J., Lou, M., Yan, Y., Bian, L., and Zhai, P.: The climatology of planetary boundary layer height in China derived from radiosonde and reanalysis data, Atmosperic Chemistry and Physics, 16, 13309-13319, https://doi.org/10.5194/acp-16-13309-2016, 2016.

Guo, S., Wang, L., Zhou, P., Guo, S., Qin, W., An, S., Xiao, J. Y., Liu, J., and Ji, Y.: Characteristics and sources of organic carbon and elemental carbon in summer road dust in Shijiazhuang (in Chinese), Environmental Engineering, 36(04), 122-126, https://doi.org/10.13205/j.hjgc.201804025, 2018.

Guo, W. T., Zhao, F. Q., and Chang, H. L.: Analysis of the trend of environmental air quality changes in the main urban area of Changzhi City (in Chinese), Proceedings of Shanghai, China 3, 2010.

Gupta, A. and Dhir, A.: Assessment of air quality and chemical fingerprints for atmospheric fine aerosols in an Indian smart city, Environmental Pollutants and Bioavailability, 34, 21-33, https://doi.org/10.1080/26395940.2021.2024091, 2022.

Hahnenberger, M. and Nicoll, K.: Meteorological characteristics of dust storm events in the eastern Great Basin of Utah, U.S.A, Atmospheric Environment, 60, 601-612, https://doi.org/10.1016/j.atmosenv, 2012.

Hama, S., Ouchen, I., Wyche, K. P., Cordell, R. L., and Monks, P. S.: Carbonaceous aerosols in five European cities: Insights into primary emissions and secondary particle formation, Atmospheric Research, 274, https://doi.org/10.1016/j.atmosres, 2022.

Han, Y., Cao, J., An, Z., Chow, J. C., Watson, J. G., Jin, Z., Fung, K., and Liu, S.: Evaluation of the thermal/optical reflectance method for quantification of elemental carbon in sediments, Chemosphere, 69, 526-533, https://doi.org/10.1016/j.chemosphere, 2007a.

Han, Y., Cao, J., Chow, J. C., Watson, J. G., An, Z., Jin, Z., Fung, K., and Liu, S.: Evaluation of the thermal/optical reflectance method for discrimination between char- and soot-EC, Chemosphere, 69, 569-574, https://doi.org/10.1016/j.chemosphere, 2007b.

Han, Y. M., Lee, S. C., Cao, J. J., Ho, K. F., and An, Z. S.: Spatial distribution and seasonal variation of char-EC and soot-EC in the atmosphere over China, Atmospheric Environment, 43, 6066-6073, https://doi.org/10.1016/j.atmosenv, 2009a.

Han, Y. M., Cao, J. J., Chow, J. C., Watson, J. G., An, Z. S., and Liu, S. X.: Elemental carbon in urban soils and road dusts in Xi'an, China and its implication for air pollution, Atmospheric Environment, 43, 2464-2470, https://doi.org/10.1016/j.atmosenv, 2009b.

Han, Y. M., Han, Z. W., Cao, J. J., Chow, J. C., Watson, J. G., An, Z. S., Liu, S. X., and Zhang, R. J.: Distribution and origin of carbonaceous aerosol over a rural high-mountain lake area, Northern China and its transport significance, Atmospheric Environment, 42, 2405-2414, https://doi.org/10.1016/j.atmosenv, 2008.

Han, Y. M., Cao, J. J., Yan, B. Z., Kenna, T. C., Jin, Z. D., Cheng, Y., Chow, J. C., and An, Z. S.: Comparison of elemental carbon in lake sediments measured by three different methods and 150-year pollution history in Eastern China, Environmental Science & Technology, 45, 5287-5293, https://doi.org/10.1021/es103518c, 2011.

Han, Y. M., Chen, L. W. A., Huang, R. J., Chow, J. C., Watson, J. G., Ni, H. Y., Liu, S. X., Fung, K. K., Shen, Z. X., Wei, C., Wang, Q. Y., Tian, J., Zhao, Z. Z., Prévôt, A. S. H., and Cao, J. J.: Carbonaceous aerosols in megacity Xi'an, China: Implications of thermal/optical protocols comparison, Atmospheric Environment, 132, 58-68, https://doi.org/10.1016/j.atmosenv, 2016.

Hand, V. L., Capes, G., Vaughan, D. J., Formenti, P., Haywood, J. M., and Coe, H.: Evidence of internal mixing of African dust and biomass burning particles by individual particle analysis using electron beam techniques, Journal of Geophysical Research: Atmospheres, 115, https://doi.org/10.1029/2009JD012938, 2010.

He, L. Y., Hu, M., Huang, X. F., Yu, B. D., Zhang, Y. H., and Liu, D. Q.: Measurement of emissions of fine particulate organic matter from Chinese cooking, Atmospheric Environment, 38, 6557-6564, https://doi.org/10.1016/j.atmosenv, 2004.

Heltberg, R., Arndt, T. C., and Sekhar, N. U.: Fuelwood consumption and forest degradation: A household model for domestic energy substitution in rural India, Land Economics, 76, 213-232, https://doi.org/10.2307/3147225, 2000.

Heo, J. B., Hopke, P., Yi, S. M. J. A. C., Source apportionment of $PM_{2.5}$ in Seoul, Korea, Atmospheric Chemistry and Physics: 9, 4957-4971, https://doi.org/10.5194/acp-9-4957-2009, 2009.

Hewitt, C. N.: The atmospheric chemistry of sulphur and nitrogen in power station plumes, Atmospheric Environment, 35, 1155-1170, https://doi.org/10.1016/S1352-2310(00)00463-5, 2001.

Hilary, U., Efeoghene, E. A., Issac, A. O., Sami, R., Baakdah, F., and Pareek, S.: Exposure to airborne pollutants in urban and rural areas: levels of metals and microorganisms in PM_{10} and gaseous pollutants in ambient air, Air Quality, Atmosphere & Health, 18, 317-332, https://doi.org/10.1007/s11869-024-01644-w, 2025.

Hoeck, T., Droux, R., Breu, T., Hurni, H., and Maselli, D.: Rural energy consumption and land degradation in a post-Soviet setting – an example from the west Pamir mountains in Tajikistan, Energy for Sustainable Development, 11, 48-57, https://doi.org/10.1016/S0973-0826(08)60563-3, 2007.

Hu, Y. N. and Liu, Y. L.: Characteristics and source analysis of heavy metal pollution in indoor dust in Jinan (in Chinese). Environmental Science and Technology 45(06), 179-184, https://doi.org/10.19672/j.cnki.1003-6504.0043.22.338, 2022.

Hua, Y., Wang, S., Jiang, J., Zhou, W., Xu, Q., Li, X., Liu, B., Zhang, D., and Zheng, M.: Characteristics and sources of aerosol pollution at a polluted rural site southwest in Beijing, China, Science of The Total Environment, 626, 519-527, https://doi.org/10.1016/j.scitotenv, 2018.

Huang, H., Xu, Z. Q., Yan, J. X., Zhao, X. G., and Wang, D. L.: Characteristics of heavy metal pollution and ecological risk evaluation of indoor dust from urban and rural areas in Taiyuan City during the heating season (in Chinese), Journal of Environmrntal Science, 42, 2143-2152, https://doi.org/10.13227/j.hjkx.202008045, 2021a.

Huang, X. and Gao, J.: A review of near-limit opposed fire spread, Fire Safety Journal, 120, 103141, https://doi.org/10.1016/j.firesaf.2020.103141, 2021a.

Huang, X., Tang, G., Zhang, J., Liu, B., Liu, C., Zhang, J., Cong, L., Cheng, M., Yan, G., Gao, W., Wang, Y., and Wang, Y.: Characteristics of $PM_{2.5}$ pollution in Beijing after the improvement of air quality, Journal of Environmental Sciences, 100, 1-10, https://doi.org/10.1016/j.jes.2020.06.004, 2021b.

Ji, X., Xu, K., Liao, D., Chen, G., Liu, T., Hong, Y., Dong, S., Choi, S.-D., and Chen, J.: Spatial-temporal characteristics and source apportionment of ambient VOCs in Southeast Mountain Area of China, Aerosol And Air Quality Research, 22, 220016, https://doi.org/10.4209/aaqr. 220016, 2022.

Jia, H., Yan, C., and Xing, X.: Evaluation of eco-environmental quality in Qaidam Basin based on the Ecological Index (MRSEI) and GEE, Remote Sensing, 13, https://doi.org/10.3390/rs13224543, 2021.

Jia, S. M., Chen, M. H., Yang, P. F., Wang, L., Wang, G. Y., Liu, L. Y., and Ma, W. L.: Seasonal variations and sources of atmospheric EPFRs in a megacity in severe cold region: Implications for the influence of strong coal and biomass combustion, Environmental Research, 252, https://doi.org/10.1016/j.envres.2024.119067, 2024.

Jian, X., Guan, P., Fu, S. T., Zhang, D. W., Zhang, W., and Zhang, Y.-S.: Miocene sedimentary

environment and climate change in the northwestern Qaidam basin, northeastern Tibetan Plateau: Facies, biomarker and stable isotopic evidences, Palaeogeography Palaeoclimatology Palaeoecology, 414, 320-331, https://doi.org/10.1016/j.palaeo.2014.09.011, 2014.

Jiang, L., Xue, B., Xing, R., Chen, X., Song, L., Wang, Y., Coffman, D. M., and Mi, Z.: Rural household energy consumption of farmers and herders in the Qinghai-Tibet Plateau, Energy, 192, https://doi.org/10.1016/j.energy.2019.116649, 2020.

Jiang, Y., Shi, L., Guang, A. L., Mu, Z., Zhan, H., and Wu, Y.: Contamination levels and human health risk assessment of toxic heavy metals in street dust in an industrial city in Northwest China, Environmental Geochemistry and Health, 40, 2007-2020, https://doi.org/10.1007/s10653-017-0028-1, 2018.

Jiménez, L., Rühland, K. M., Jeziorski, A., Smol, J. P., and Pérez-Martínez, C.: Climate change and Saharan dust drive recent cladoceran and primary production changes in remote alpine lakes of Sierra Nevada, Spain, Global Change Biology, 24, e139-e158, https://doi.org/10.1111/gcb.13878, 2018.

Joshi, U. M., Vijayaraghavan, K., and Balasubramanian, R.: Elemental composition of urban street dusts and their dissolution characteristics in various aqueous media, Chemosphere, 77, 526-533, https://doi.org/10.1016/j.chemosphere, 2009.

Kang, S., Zhang, Y., Qian, Y., and Wang, H.: A review of black carbon in snow and ice and its impact on the cryosphere, Earth-Science Reviews, 210, https://doi.org/10.1016/j.earscirev.2020.103346, 2020.

Kataki, R., Goswami, K., Bordoloi, N. J., Narzari, R., Saikia, R., Sut, D., and Gogoi, L.: Biomass resources for biofuel production in Northeast India, in: Bioprospecting of indigenous bioresources of North-East India, Springer Singapore, Singapore, 127-151, https://doi.org/10.1007/978-981-10-0620-3_8, 2016.

Kerimray, A., Suleimenov, B., De Miglio, R., Rojas-Solórzano, L., Amouei Torkmahalleh, M., and Ó Gallachóir, B. P.: Investigating the energy transition to a coal free residential sector in Kazakhstan using a regionally disaggregated energy systems model, Journal of Cleaner Production, 196, 1532-1548, https://doi.org/10.1016/j.jclepro, 2018.

Khan, A. J., Swami, K., Ahmed, T., Bari, A., Shareef, A., and Husain, L.: Determination of elemental carbon in lake sediments using a thermal–optical transmittance (TOT) method, Atmospheric Environment, 43, 5989-5995, https://doi.org/10.1016/j.atmosenv.2009.08.030, 2009.

Kim, K. H., Sekiguchi, K., Kudo, S., and Sakamoto, K.: Characteristics of atmospheric elemental carbon (Char and Soot) in ultrafine and fine particles in a roadside environment, Japan, Aerosol and Air Quality Research, 11, 1-12, https://doi.org/10.4209/aaqr.2010.07.0061, 2011.

Kong, L., Xin, J., Gao, W., Tang, G., Wang, X., Wang, Y., Zhang, W., Chen, W., and Jia, S.: A comprehensive evaluation of aerosol extinction apportionment in Beijing using a high-resolution time-of-flight aerosol mass spectrometer, Science of The Total Environment, 783, 146976, https://doi.org/10.1016/j.scitotenv.2021.146976, 2021.

Kuang, Y., He, Y., Xu, W., Yuan, B., Zhang, G., Ma, Z., Wu, C., Wang, C., Wang, S., Zhang, S., Tao, J., Ma, N., Su, H., Cheng, Y., Shao, M., and Sun, Y.: Photochemical aqueous-phase reactions induce rapid daytime formation of oxygenated organic aerosol on the North China Plain, Environmental Science & Technology, 54, 3849-3860, https://doi.org/10.1021/acs.est.9b06836, 2020.

Kulmala, M., Vehkamäki, H., Petäjä, T., Dal Maso, M., Lauri, A., Kerminen, V. M., Birmili, W., and McMurry, P. H.: Formation and growth rates of ultrafine atmospheric particles: a review of observations, Journal of Aerosol Science, 35, 143-176, https://doi.org/10.1016/j.jaerosci.2003.10.003, 2004.

Kumar, A.: Chemical characterization of mineral aerosols: Sources, transport and atmospheric transformations, Mohanlal Sukhadia University Udaipur, 2010.

Kumar, N., Johnson, J., Yarwood, G., Woo, J. H., Kim, Y., Park, R. J., Jeong, J. I., Kang, S., Chun, S., and Knipping, E.: Contributions of domestic sources to $PM_{2.5}$ in South Korea, Atmospheric Environment, 287, 119273, https://doi.org/10.1016/j.atmosenv.2022.119273, 2022.

Lai, S., Zhao, Y., Ding, A., Zhang, Y., Song, T., Zheng, J., Ho, K. F., Lee, S. C., and Zhong, L.: Characterization of $PM_{2.5}$ and the major chemical components during a 1-year campaign in rural Guangzhou, Southern China, Atmospheric Research, 167, 208-215, https://doi.org/10.1016/j.atmosres, 2016.

Leavey, A., Patel, S., Martinez, R., Mitroo, D., Fortenberry, C., Walker, M., Williams, B., and Biswas, P.: Organic and inorganic speciation of particulate matter formed during different combustion phases in an improved cookstove, Environmental Research, 158, 33-42, https://doi.org/10.1016/j.envres, 2017.

Lee, K. Y., Batmunkh, T., Joo, H. S., and Park, K.: Comparison of the physical and chemical characteristics of fine road dust at different urban sites, Journal of the Air & Waste Management

Association, 68, 812-823, https://doi.org/10.1080/10962247.2018.1443855, 2018.

Li, J. K., Liu, X. F. and Wang, D. H.: Overview of mineralization laws of lithium deposits in China (in Chinese). Acta Geologica Sinica, 88: 2269-2283. https://doi.org/10.19762/j.cnki.dizhixuebao, 2014.

Li, L., Ni, W., Cheng, Y., Wang, H., Yuan, K., and Zhou, B.: Evaluation of the eco-geo-environment in the Qaidam Basin, China, Environmental Earth Sciences, 80, https://doi.org/10.1007/s12665-020-09312-9, 2021a.

Li, M., Liu, Z., Chen, J., Huang, X., Liu, J., Xie, Y., Hu, B., Xu, Z., Zhang, Y., and Wang, Y.: Characteristics and source apportionment of metallic elements in $PM_{2.5}$ at urban and suburban sites in Beijing: Implication of emission reduction, Atmosphere, 10, https://doi.org/10.3390/atmos10030105, 2019a.

Li, P. H., Wang, Y., Li, T., Sun, L., Yi, X., Guo, L. Q., and Su, R. H.: Characterization of carbonaceous aerosols at Mount Lu in South China: implication for secondary organic carbon formation and long-range transport, Environmental Science and Pollution Research, 22, 14189-14199, https://doi.org/10.1007/s11356-015-4654-9, 2015b.

Li, Q. L and Sha, Z. J.: Remote sensing monitoring of ecological environment quality in the Qaidam Basin under climate warming (in Chinese), Ecological Science, 41(06), 92-99, https://doi.org/10.14108/j.cnki.1008-8873, 2022.

Li, R., Li, C., Zhuang, J., Zhu, H., Fang, L., and Sun, D.: Mechanistic influence of chemical agglomeration agents on removal of inhalable particles from coal combustion, ACS Omega, 5, 25906-25912, https://doi.org/10.1021/acsomega.0c03263, 2020.

Li, Y., Ma, L., Ge, Y., and Abuduwaili, J.: Health risk of heavy metal exposure from dustfall and source apportionment with the PCA-MLR model: A case study in the Ebinur Lake Basin, China, Atmospheric Environment, 272, 118950, https://doi.org/10.1016/j.atmosenv, 2022.

Li, Y., Song, Y., Kaskaoutis, D. G., Chen, X., Mamadjanov, Y., and Tan, L.: Atmospheric dust dynamics in southern Central Asia: Implications for buildup of Tajikistan loess sediments, Atmospheric Research, 229, 74-85, https://doi.org/10.1016/j.atmosres.2019.06.013, 2019b.

Li, Z., Sjödin, A., Romanoff, L. C., Horton, K., Fitzgerald, C. L., Eppler, A., Aguilar-Villalobos, M., and Naeher, L. P.: Evaluation of exposure reduction to indoor air pollution in stove intervention projects in Peru by urinary biomonitoring of polycyclic aromatic hydrocarbon metabolites, Environment International, 37, 1157-1163, https://doi.org/10.1016/j.envint.2011.03.024, 2011.

Li, Z., Liu, J., Zhai, Z., Liu, C., Ren, Z., Yue, Z., Yang, D., Hu, Y., Zheng, H., and Kong, S.: Heterogeneous changes of chemical compositions, sources and health risks of $PM_{2.5}$ with the "Clean Heating" policy at urban/suburban/industrial sites, Science of The Total Environment, 854, 158871, https://doi.org/10.1016/j.scitotenv.2022.158871, 2023.

Li, Z., Yue, Z., Yang, D., Wang, L., Wang, X., Li, Z., Wang, Y., Chen, L., Guo, S., Yao, J., Lou, X., Xu, X., and Wei, J.: Levels, chemical compositions, and sources of $PM_{2.5}$ of rural and urban area under the impact of wheat harvest, Aerosol and Air Quality Research, 21, https://doi.org/10.4209/aaqr.210026, 2021.

Lin, Y., Mu, G., Chen, L., Wu, C., and Xu, L.: Sorting characteristics and implications indicated by the grain size of near-surface atmospheric dust fall in the Qira Oasis (in Chinese), Journal of Desert Research, 42, 139-146, https://doi.org/10.7522/j.issn.1000-694X, 2022a.

Lin, Y., Mu, G., and Xu, L.: Grain size and sedimentary sorting characteristics of atmospheric dust in the Cele Oasis, Southern Margin of Taklimakan Desert, 14(13), 8093, https://doi.org/10.3390/su14138093, 2022b.

Lin, Y. C., Tsai, C. J., Wu, Y. C., Zhang, R., Chi, K. H., Huang, Y. T., Lin, S. H., and Hsu, S. C.: Characteristics of trace metals in traffic-derived particles in Hsuehshan Tunnel, Taiwan: size distribution, potential source, and fingerprinting metal ratio, Atmospheric Chemistry and Physics, 15, 4117-4130, https://doi.org/10.5194/acp-15-4117-2015, 2015.

Liu, B., Song, N., Dai, Q., Mei, R., Sui, B., Bi, X., and Feng, Y.: Chemical composition and source apportionment of ambient $PM_{2.5}$ during the non-heating period in Taian, China, Atmospheric Research, 170, 23-33, https://doi.org/10.1016/j.atmosres, 2016a.

Liu, G., Lucas, M., and Shen, L.: Rural household energy consumption and its impacts on eco-environment in Tibet: Taking Taktse county as an example, Renewable and Sustainable Energy Reviews, 12, 1890-1908, https://doi.org/10.1016/j.rser, 2008.

Liu, G., Li, J., Wu, D., and Xu, H.: Chemical composition and source apportionment of the ambient $PM_{2.5}$ in Hangzhou, China, Particuology, 18, 135-143, https://doi.org/10.1016/j.partic, 2015.

Liu, G., Yin, G., Kurban, A., Aishan, T., and You, H.: Spatiotemporal dynamics of land cover and their impacts on potential dust source regions in the Tarim Basin, NW China, Environmental Earth Sciences, 75, 1477, https://doi.org/10.1007/s12665-016-6269-y, 2016b.

Liu, H., Hu, B., Zhang, L., Zhao, X. J., Shang, K. Z., Wang, Y. S., and Wang, J.: Ultraviolet radiation

1696   over China: Spatial distribution and trends, Renewable and Sustainable Energy Reviews, 76, 1371-

1697   1383, https://doi.org/10.1016/j.rser, 2017.

1698   Liu, H., Jia, M., Tao, J., Yao, D., Li, J., Zhang, R., Li, L., Xu, M., Fan, Y., Liu, Y., and Cheng, K.:

1699   Elucidating pollution characteristics, temporal variation and source origins of carbonaceous species

1700   in Xinxiang, a heavily polluted city in North China, Atmospheric Environment, 298, 119626,

1701   https://doi.org/10.1016/j.atmosenv.2023.119626, 2023a.

1702   Liu, P., Zhou, H., Chun, X., Wan, Z., Liu, T., Sun, B., Wang, J., and Zhang, W.: Characteristics of fine

1703   carbonaceous aerosols in Wuhai, a resource-based city in Northern China: Insights from energy

1704   efficiency   and   population   density,   Environmental   Pollution,   292,   118368,

1705   https://doi.org/10.1016/j.envpol, 2022.

1706   Liu, T., Zhao, C., Chen, Q., Li, L., Si, G., Li, L., and Guo, B.: Characteristics and health risk assessment

1707   of heavy metal pollution in atmospheric particulate matter in different regions of the Yellow River

1708   Delta   in   China,   Environmental   Geochemistry   and   Health,   45,   2013-2030,

1709   https://doi.org/10.1007/s10653-022-01318-5, 2023b.

1710   Liu, W., Hopke, P. K., Han, Y. J., Yi, S. M., Holsen, T. M., Cybart, S., Kozlowski, K., and Milligan, M.:

1711   Application of receptor modeling to atmospheric constituents at Potsdam and Stockton, NY,

1712   Atmospheric Environment, 37, 4997-5007, https://doi.org/10.1016/j.atmosenv.2003.08.036, 2003.

1713   Liu, X., Wang, Y., Liu, R., Zhang, Y., Shao, L., Han, K., and Zhang, Y.: Pollution characteristics, source

1714   identification and potential ecological risk of 50 elements in atmospheric particulate matter during

1715   winter in Qingdao, Arabian Journal of Geosciences, 15, https://doi.org/10.1007/s12517-022-09521-

1716   5, 2022b.

1717   Liu, Y., Liu, G., Yousaf, B., Zhang, J., and Zhou, L.: Carbon fractionation and stable carbon isotopic

1718   fingerprint of road dusts near coal power plant with emphases on coal-related source apportionment,

1719   Ecotoxicology and Environmental Safety, 202, 110888, https://doi.org/10.1016/j.ecoenv, 2020a.

1720   Liu, Y., Wu, G., Duan, A. and Zhang, Q.: New evidence that climate warming in the Tibetan Plateau is a

1721   result of intensified greenhouse gas emissions (in Chinese), Chinese Science Bulletin, 51(8), 989-

1722   992, https://doi.org/10.1360/csb2006-51-8-989, 2006.

1723   Liu, Y., Zhu, Q., Huang, J., Hua, S., and Jia, R.: Impact of dust-polluted convective clouds over the

1724   Tibetan   Plateau   on   downstream   precipitation,   Atmospheric   Environment,   209,   67-77,

1725   https://doi.org/10.1016/j.atmosenv, 2019.

Liu, Y., Zhu, Q., Hua, S., Alam, K., Dai, T., and Cheng, Y.: Tibetan Plateau driven impact of Taklimakan dust on northern rainfall, Atmospheric Environment, 234, 117583, https://doi.org/10.1016/j.atmosenv, 2020b.

Liu, Z. Y., Cheng, J. L., Li, C. Y., Gao, Y., Zhan, C. L., Liu, S., Zhang, J. Q., and Liu, H. X.: Pollution characteristics and source analysis of carbon components in road dust from Qingshan District, Wuhan (in Chinese), Environmental Chemistry, 40, 772–778, https://doi.org/10.7524/j.issn.0254-6108.2020061305, 2021.

Lonati, G., Ozgen, S., and Giugliano, M.: Primary and secondary carbonaceous species in $PM_{2.5}$ samples in Milan (Italy), Atmospheric Environment, 41, 4599-4610, https://doi.org/10.1016/j.atmosenv, 2007.

Löw, F., Navratil, P., Kotte, K., Schöler, H. F., and Bubenzer, O.: Remote-sensing-based analysis of landscape change in the desiccated seabed of the Aral Sea—a potential tool for assessing the hazard degree of dust and salt storms, Environmental Monitoring and Assessment, 185, 8303-8319, https://doi.org/10.1007/s10661-013-3174-7, 2013.

Luo, M., Liu, Y., Zhu, Q., Tang, Y., and Alam, K.: Role and mechanisms of black carbon affecting water vapor transport to Tibet, Remote Sensing, 12(2), 0231, https://doi.org/10.3390/rs12020231, 2020.

Ma, Q., Wu, Y., Tao, J., Xia, Y., Liu, X., Zhang, D., Han, Z., Zhang, X., and Zhang, R.: Variations of chemical composition and source apportionment of $PM_{2.5}$ during winter haze episodes in Beijing, Aerosol and Air Quality Research, 17, 2791-2803, https://doi.org/10.4209/aaqr.2017.10.0366, 2017.

Ma, Y., Ji, Y. Q., Guo, J. J., Zhao, J. Q., Li, Y. Y., Wang, S. B. and Zhang, L.: Characteristics of carbon components and source analysis of road dust during spring in Tianjin (in Chinese), Acta Scientiae Circumstantiae 40(06), 2540-2545, https://doi.org/10.13227/j.hjkx, 2019.

Mahowald, N. M., Engelstaedter, S., Luo, C., Sealy, A., Artaxo, P., Benitez-Nelson, C., Bonnet, S., Chen, Y., Chuang, P. Y., Cohen, D. D., Dulac, F., Herut, B., Johansen, A. M., Kubilay, N., Losno, R., Maenhaut, W., Paytan, A., Prospero, J. M., Shank, L. M., and Siefert, R. L.: Atmospheric iron deposition: Global distribution, variability, and human perturbations, Annual Review of Marine Science, 1, 245-278, https://doi.org/10.1146/annurev.marine.010908.163727, 2009.

Manousakas, M., Papaefthymiou, H., Diapouli, E., Migliori, A., Karydas, A. G., Bogdanovic-Radovic, I., and Eleftheriadis, K.: Assessment of $PM_{2.5}$ sources and their corresponding level of uncertainty in a coastal urban area using EPA PMF 5.0 enhanced diagnostics, Science of The Total Environment,

574, 155-164, https://doi.org/10.1016/j.scitotenv.2016.09.047, 2017.

Mbengue, S., Fusek, M., Schwarz, J., Vodička, P., Šmejkalová, A. H., and Holoubek, I.: Four years of highly time resolved measurements of elemental and organic carbon at a rural background site in Central Europe, Atmospheric Environment, 182, 335-346, https://doi.org/10.1016/j.atmosenv, 2018.Meng, C. C., Wang, L. T., Zhang, F. F., Wei, Z., Ma, S. M., Ma, X., and Yang, J.: Characteristics of concentrations and water-soluble inorganic ions in $PM_{2.5}$ in Handan City, Hebei province, China, Atmospheric Research, 171, 133-146, https://doi.org/10.1016/j.atmosres.2015.12.013, 2016.

Meng, J. H., Shi, X. F., Xiang, Y. and Ren, Y. F.: Current status and sources of heavy metal pollution in the atmosphere (in Chinese). Environmental Science and Management 42(08), 51-53, https://doi.org/10.3969/j.issn.1673-1212.2017.08.011, 2017.

Meng, W., Zhong, Q., Chen, Y., Shen, H., Yun, X., Smith, K. R., Li, B., Liu, J., Wang, X., Ma, J., Cheng, H., Zeng, E. Y., Guan, D., Russell, A. G., and Tao, S.: Energy and air pollution benefits of household fuel policies in northern China, Proceedings of the National Academy of Sciences, 116, 16773-16780, https://doi.org/10.1073/pnas.1904182116, 2019.

Meng, W., Shen, H., Yun, X., Chen, Y., Zhong, Q., Zhang, W., Yu, X., Xu, H., Ren, Y. a., Shen, G., Ma, J., Liu, J., Cheng, H., Wang, X., Zhu, D., and Tao, S.: Differentiated-rate clean heating strategy with superior environmental and health benefits in Northern China, Environmental Science & Technology, 54, 13458-13466, https://doi.org/10.1021/acs.est.0c04019, 2020.

Miller, M. B., Fine, R., Pierce, A. M., and Gustin, M. S.: Identifying sources of ozone to three rural locations in Nevada, USA, using ancillary gas pollutants, aerosol chemistry, and mercury, Science of The Total Environment, 530-531, 483-492, https://doi.org/10.1016/j.scitotenv, 2015.

Millet, D. B., Donahue, N. M., Pandis, S. N., Polidori, A., Stanier, C. O., Turpin, B. J., and Goldstein, A. H.: Atmospheric volatile organic compound measurements during the Pittsburgh Air Quality Study: Results, interpretation, and quantification of primary and secondary contributions, Journal of Geophysical Research: Atmospheres, 110, https://doi.org/10.1029/2004JD004601, 2005.

Ming, J., Xiao, C., Sun, J., Kang, S., and Bonasoni, P.: Carbonaceous particles in the atmosphere and precipitation of the Nam Co region, central Tibet, Journal of Environmental Sciences, 22, 1748-1756, https://doi.org/10.1016/S1001-0742(09)60315-6, 2010.

Mishra, M. and Kulshrestha, U.: Chemical characteristics and deposition fluxes of dust-carbon mixed coarse aerosols at three sites of Delhi, NCR, Journal of Atmospheric Chemistry, 74, 399-421,

https://doi.org/10.1007/s10874-016-9349-1, 2017.

Moravek, A., Murphy, J. G., Hrdina, A., Lin, J. C., Pennell, C., Franchin, A., Middlebrook, A. M., Fibiger, D. L., Womack, C. C., McDuffie, E. E., Martin, R., Moore, K., Baasandorj, M., and Brown, S. S.: Wintertime spatial distribution of ammonia and its emission sources in the Great Salt Lake region, Atmospheric Chemistry and Physics, 19, 15691-15709, https://doi.org/10.5194/acp-19-15691-2019, 2019.

Munawer, M. E.: Human health and environmental impacts of coal combustion and post-combustion wastes, Journal of Sustainable Mining, 17, 87-96, https://doi.org/10.1016/j.jsm, 2018.

Na, K., Sawant, A. A., Song, C., and Cocker, D. R.: Primary and secondary carbonaceous species in the atmosphere of Western Riverside County, California, Atmospheric Environment, 38, 1345-1355, https://doi.org/10.1016/j.atmosenv, 2004.

Noll, K. E. and Fang, K. Y. P.: Development of a dry deposition model for atmospheric coarse particles, Atmospheric Environment (1967), 23, 585-594, https://doi.org/10.1016/0004-6981(89)90007-3, 1989.

Norris, G., Duvall, R., Brown, S., and Bai, S.: EPA Positive Matrix Factorization (PMF) 5.0 fundamentals and user guide, The United States Environmental Protection Agency, https://www.epa.gov, 2014.Nuralykyzy, B., Wang, P., Deng, X., An, S., and Huang, Y.: Heavy metal contents and assessment of soil contamination in different land-use types in the Qaidam Basin, Sustainability, 13(21), 12020, https://doi.org/10.3390/su132112020, 2021.

Offer, Z. Y., Goossens, D., and Shachak, M.: Aeolian deposition of nitrogen to sandy and loessial ecosystems in the Negev Desert, Journal of Arid Environments, 23, 355-363, https://doi.org/10.1016/S0140-1963(18)30609-8, 1992.

Oliveira, T., Pio, C., Alves, C., Silvestre, A., Evtyugina, M., Afonso, J., Caseiro, A., and Legrand, M.: Air quality and organic compounds in aerosols from a coastal rural area in the Western Iberian Peninsula over a year long period: Characterisation, loads and seasonal trends, Atmospheric Environment, 41, 3631-3643, https://doi.org/10.1016/j.atmosenv, 2007.

Pacyna, J. M. and Pacyna, E. G.: An assessment of global and regional emissions of trace metals to the atmosphere from anthropogenic sources worldwide, Environmental Reviews, 9, 269-298, https://doi.org/10.1139/a01-012, 2001.

Pandolfi, M., Gonzalez-Castanedo, Y., Alastuey, A., de la Rosa, J. D., Mantilla, E., de la Campa, A. S.,

1816 Querol, X., Pey, J., Amato, F., and Moreno, T.: Source apportionment of PM_{10} and $PM_{2.5}$ at multiple

1817 sites in the strait of Gibraltar by PMF: impact of shipping emissions, Environmental Science and

1818 Pollution Research, 18, 260-269, https://doi.org/10.1007/s11356-010-0373-4, 2010.

1819 Parajuli, S. P., Stenchikov, G. L., Ukhov, A., Mostamandi, S., Kucera, P. A., Axisa, D., Gustafson Jr, W.

1820 I., and Zhu, Y.: Effect of dust on rainfall over the Red Sea coast based on WRF-Chem model

1821 simulations, Atmospheric Chemistry and Physics, 22, 8659-8682, https://doi.org/10.5194/acp-22-

1822 8659-2022, 2022.

1823 Peng, T., Sun, C., Zhang, Y., and Fan, F.: Spatiotemporal variation of anthropogenic heat emission

1824 landscape pattern in the central urban area of Guangzhou, Journal of South China Normal University

1825 (Natural Science Edition), 53, 92–102, https://doi.org/10.6054/j.jscnun.2021080, 2021.

1826 Pervez, S., Bano, S., Watson, J. G., Chow, J. C., Matawle, J. L., Shrivastava, A., Tiwari, S., and Pervez,

1827 Y. F.: Source profiles for $PM_{10\text{-}2.5}$ resuspended dust and vehicle exhaust emissions in Central India,

1828 Aerosol and Air Quality Research, 18, 1660-1672, https://doi.org/10.4209/aaqr, 2018.

1829 Phairuang, W., Hongtieab, S., Suwattiga, P., Furuuchi, M., and Hata, M.: Atmospheric Ultrafine

1830 Particulate Matter ($PM_{0.1}$)-bound carbon composition in Bangkok, Thailand, Atmosphere, 13,

1831 https://doi.org/10.3390/atmos13101676, 2022.

1832 Pio, C., Cerqueira, M., Harrison, R. M., Nunes, T., Mirante, F., Alves, C., Oliveira, C., Sanchez de la

1833 Campa, A., Artíñano, B., and Matos, M.: OC/EC ratio observations in Europe: Re-thinking the

1834 approach for apportionment between primary and secondary organic carbon, Atmospheric

1835 Environment, 45, 6121-6132, https://doi.org/10.1016/j.atmosenv, 2011.

1836 Pipal, A. S., Singh, S., and Satsangi, G. P.: Study on bulk to single particle analysis of atmospheric

1837 aerosols at urban region, Urban Climate, 27, 243-258, https://doi.org/10.1016/j.uclim.2018.12.008,

1838 2019.

1839 Popovicheva, O. B., Engling, G., Diapouli, E., Saraga, D., Persiantseva, N. M., Timofeev, M. A., Kireeva,

1840 E. D., Shonija, N. K., Chen, S. H., Nguyen, D. L., Eleftheriadis, K., and Lee, C. T.: Impact of smoke

1841 intensity on size-resolved aerosol composition and microstructure during the biomass burning

1842 season in Northwest Vietnam, Aerosol and Air Quality Research, 16, 2635-2654,

1843 https://doi.org/10.4209/aaqr, 2016.

1844 Qi, D. L., Zhao, Q. N., Zhao, H. F., Han, T. F. and Su, W. J.: Temporal and spatial characteristics and

1845 regional differences of dust-fall in Qinghai Province from 2004 to 2017 (in Chinese), Arid

1846   Meteorology, 36(06), 927-935, http://www.ghqx.org.cn/CN/Y2018/V36/I6/927, 2018.

1847 Qian, G. Q. and Dong, Z. B.: Research on methods and related issues of atmospheric dust collection (in

1848   Chinese), Chinese Journal of Desert Research, (06), 119-122, https://doi.org/1000-694X9(2004)06-

1849   0779-04, 2014.

1850 Qian, Y., Yasunari, T. J., Doherty, S. J., Flanner, M. G., Lau, W. K. M., Ming, J., Wang, H., Wang, M.,

1851   Warren, S. G., and Zhang, R.: Light-absorbing particles in snow and ice: Measurement and

1852   modeling of climatic and hydrological impact, Advances in Atmospheric Sciences, 32, 64-91,

1853   https://doi.org/10.1007/s00376-014-0010-0, 2015.

1854 Qiao, Q., Huang, B., Zhang, C., Piper, J. D. A., Pan, Y., and Sun, Y.: Assessment of heavy metal

1855   contamination of dustfall in northern China from integrated chemical and magnetic investigation,

1856   Atmospheric Environment, 74, 182-193, https://doi.org/10.1016/j.atmosenv, 2013.

1857 Rabha, S., Saikia, B. K., Singh, G. K., and Gupta, T.: Meteorological influence and chemical

1858   compositions of atmospheric particulate matters in an Indian Urban Area, ACS Earth and Space

1859   Chemistry, 5, 1686-1694, https://doi.org/10.1021/acsearthspacechem.1c00037, 2021.

1860 Ramanathan, V. and Carmichael, G.: Global and regional climate changes due to black carbon, Nature

1861   Geoscience, 1, 221-227, https://doi.org/10.1038/ngeo156, 2008.

1862 Rogge, W. F., Hildemann, L. M., Mazurek, M. A., Cass, G. R., and Simoneit, B. R. T.: Sources of fine

1863   organic aerosol. 3. Road dust, tire debris, and organometallic brake lining dust: roads as sources and

1864   sinks, Environmental Science & Technology, 27, 1892-1904, https://doi.org/10.1021/es00046a019,

1865   1993.

1866 Rörig-Dalgaard, I.: Direct measurements of the deliquescence relative humidity in salt mixtures

1867   including the contribution from metastable phases, ACS Omega, 6, 16297-16306,

1868   https://doi.org/10.1021/acsomega.1c00538, 2021.

1869 Safai, P. D., Raju, M. P., Rao, P. S. P., and Pandithurai, G.: Characterization of carbonaceous aerosols

1870   over the urban tropical location and a new approach to evaluate their climatic importance,

1871   Atmospheric Environment, 92, 493-500, https://doi.org/10.1016/j.atmosenv.2014.04.055, 2014.

1872 Saha, A. and Despiau, S.: Seasonal and diurnal variations of black carbon aerosols over a Mediterranean

1873   coastal zone, Atmospheric Research, 92, 27-41, https://doi.org/10.1016/j.atmosres.2008.07.007,

1874   2009.

1875 Sandrini, S., Fuzzi, S., Piazzalunga, A., Prati, P., Bonasoni, P., Cavalli, F., Bove, M. C., Calvello, M.,

1876   Cappelletti, D., Colombi, C., Contini, D., de Gennaro, G., Di Gilio, A., Fermo, P., Ferrero, L.,

1877   Gianelle, V., Giugliano, M., Ielpo, P., Lonati, G., Marinoni, A., Massabò, D., Molteni, U., Moroni,

1878   B., Pavese, G., Perrino, C., Perrone, M. G., Perrone, M. R., Putaud, J.-P., Sargolini, T., Vecchi, R.,

1879   and Gilardoni, S.: Spatial and seasonal variability of carbonaceous aerosol across Italy, Atmospheric

1880   Environment, 99, 587-598, https://doi.org/10.1016/j.atmosenv.2014.10.032, 2014.

1881 Saraga, D., Maggos, T., Degrendele, C., Klánová, J., Horvat, M., Kocman, D., Kanduč, T., Garcia Dos

1882   Santos, S., Franco, R., Gómez, P. M., Manousakas, M., Bairachtari, K., Eleftheriadis, K.,

1883   Kermenidou, M., Karakitsios, S., Gotti, A., and Sarigiannis, D.: Multi-city comparative $PM_{2.5}$

1884   source apportionment for fifteen sites in Europe: The ICARUS project, Science of The Total

1885   Environment, 751, 141855, https://doi.org/10.1016/j.scitotenv.2020.141855, 2021.

1886 Schepanski, K.: Transport of mineral dust and its impact on climate, Geosciences, 2018, 8(5), 151,

1887   https://doi.org/10.3390/geosciences8050151, 2018.

1888 Schmidl, C., Marr, I. L., Caseiro, A., Kotianová, P., Berner, A., Bauer, H., Kasper-Giebl, A., and Puxbaum,

1889   H.: Chemical characterisation of fine particle emissions from wood stove combustion of common

1890   woods growing in mid-European Alpine regions, Atmospheric Environment, 42, 126-141,

1891   https://doi.org/10.1016/j.atmosenv, 2008.

1892 Secrest, M. H., Schauer, J. J., Carter, E. M., and Baumgartner, J.: Particulate matter chemical component

1893   concentrations and sources in settings of household solid fuel use, Indoor Air, 27, 1052-1066,

1894   https://doi.org/10.1111/ina.12389, 2017.

1895 Seinfeld, J. H., Pandis, S. N., and Noone, K. J. J. P. T.: Atmospheric chemistry and physics: From air

1896   pollution to climate change, 51, 88-90, 1998.

1897 Shahram, N., Majid, K., Mehdi, F., Soodabeh, M., and Ahmad, Y.: The origins and sources of dust

1898   particles, their effects on environment and health, and control strategies: A review, Journal of Air

1899   Pollution and Health, 1(2):137-152, https://api.semanticscholar.org/CorpusID:56256748, 2016.

1900 Sharma, S., Brook, J. R., Cachier, H., Chow, J., Gaudenzi, A., and Lu, G.: Light absorption and thermal

1901   measurements of black carbon in different regions of Canada, Journal of Geophysical Research:

1902   Atmospheres, 107, AAC 11-11, https://doi.org/10.1029/2002JD002496, 2002.

1903 Sheehan, P. E. and Bowman, F. M.: Estimated effects of temperature on secondary organic aerosol

1904   concentrations, Environmental Science & Technology, 35, 2129-2135,

1905   https://doi.org/10.1021/es001547g, 2001.

Shen, J. and Dai, B. L.: Development and utilization of salt lake brine lithium resources and its prospects (in Chinese), Industrial Minerals & Processing, 38, 1–4+7, https://doi.org/10.16283/j.cnki.hgkwyjg.2009.04.004, 2009.

Shen, G. F., Xiong, R., Cheng, H. F. and Tao, S.: Estimation of residential energy structure and primary $PM_{2.5}$ emissions in rural Tibet (in Chinese), Science Bulletin, 66(15), 1900-1911, https://doi.org/10.1360/TB-2020-0408, 2021.

Shen, L., Wang, H., Kong, X., Zhang, C., Shi, S., and Zhu, B.: Characterization of black carbon aerosol in the Yangtze River Delta, China: Seasonal variation and source apportionment, Atmospheric Pollution Research, 12, 195-209, https://doi.org/10.1016/j.apr.2020.08.035, 2021.

Shen, Z., Arimoto, R., Cao, J., Zhang, R., Li, X., Du, N., Okuda, T., Nakao, S., and Tanaka, S.: Seasonal variations and evidence for the effectiveness of pollution controls on water-soluble inorganic species in total suspended particulates and fine particulate matter from Xi'an, China, Journal of the Air & Waste Management Association, 58, 1560-1570, https://doi.org/10.3155/1047-3289.58.12.1560, 2008.

Shen, Z., Zhang, Q., Cao, J., Zhang, L., Lei, Y., Huang, Y., Huang, R. J., Gao, J., Zhao, Z., Zhu, C., Yin, X., Zheng, C., Xu, H., and Liu, S.: Optical properties and possible sources of brown carbon in $PM_{2.5}$ over Xi'an, China, Atmospheric Environment, 150, 322-330, https://doi.org/10.1016/j.atmosenv.2016.11.024, 2017.

Shi, G., Chen, Z., Teng, J., Bi, C., Zhou, D., Sun, C., Li, Y., and Xu, S.: Fluxes, variability and sources of cadmium, lead, arsenic and mercury in dry atmospheric depositions in urban, suburban and rural areas, Environmental Research, 113, 28-32, https://doi.org/10.1016/j.envres.2012.01.001, 2012.

Shi, X., Zhao, Y., Dai, S., Xu, L., Li, Y., Jia, H., and Zhang, Q.: Research on climatic change of Qaidam Basin since 1961, Journal of Desert Research, 25, 123-128, http://www.desert.ac.cn/CN/Y2005/V25/I1/123, 2005.

Shi, Z., Vu, T., Kotthaus, S., Harrison, R. M., Grimmond, S., Yue, S., Zhu, T., Lee, J., Han, Y., Demuzere, M., Dunmore, R. E., Ren, L., Liu, D., Wang, Y., Wild, O., Allan, J., Acton, W. J., Barlow, J., Barratt, B., Beddows, D., Bloss, W. J., Calzolai, G., Carruthers, D., Carslaw, D. C., Chan, Q., Chatzidiakou, L., Chen, Y., Crilley, L., Coe, H., Dai, T., Doherty, R., Duan, F., Fu, P., Ge, B., Ge, M., Guan, D., Hamilton, J. F., He, K., Heal, M., Heard, D., Hewitt, C. N., Hollaway, M., Hu, M., Ji, D., Jiang, X., Jones, R., Kalberer, M., Kelly, F. J., Kramer, L., Langford, B., Lin, C., Lewis, A. C., Li, J., Li, W.,

1936   Liu, H., Liu, J., Loh, M., Lu, K., Lucarelli, F., Mann, G., McFiggans, G., Miller, M. R., Mills, G.,

1937   Monk, P., Nemitz, E., O'Connor, F., Ouyang, B., Palmer, P. I., Percival, C., Popoola, O., Reeves, C.,

1938   Rickard, A. R., Shao, L., Shi, G., Spracklen, D., Stevenson, D., Sun, Y., Sun, Z., Tao, S., Tong, S.,

1939   Wang, Q., Wang, W., Wang, X., Wang, X., Wang, Z., Wei, L., Whalley, L., Wu, X., Wu, Z., Xie, P.,

1940   Yang, F., Zhang, Q., Zhang, Y., Zhang, Y., and Zheng, M.: Introduction to the special issue "In-depth

1941   study of air pollution sources and processes within Beijing and its surrounding region (APHH-

1942   Beijing)", Atmospheric Chemistry and Physics, 19, 7519-7546, https://doi.org/10.5194/acp-19-

1943   7519-2019, 2019.

1944   Shrivastava, M., Lou, S., Zelenyuk, A., Easter, R. C., Corley, R. A., Thrall, B. D., Rasch, P. J., Fast, J. D.,

1945   Massey Simonich, S. L., Shen, H., and Tao, S.: Global long-range transport and lung cancer risk

1946   from polycyclic aromatic hydrocarbons shielded by coatings of organic aerosol, Proceedings of the

1947   National Academy of Sciences, 114, 1246-1251, https://doi.org/10.1073/pnas.1618475114, 2017.

1948   Simoneit, B. R. T.: Biomass burning — a review of organic tracers for smoke from incomplete

1949   combustion, Applied Geochemistry, 17, 129-162, https://doi.org/10.1016/S0883-2927(01)00061-0,

1950   2002.

1951   Smichowski, P., Gómez, D., Frazzoli, C., and Caroli, S.: Traffic-related elements in airborne particulate

1952   matter, Applied Spectroscopy Reviews, 43, 23-49, https://doi.org/10.1080/05704920701645886,

1953   2007.

1954   Smith, R. M. and Twiss, P. C.: Extensive gaging of dust deposition rates, Kansas Acad, 68:2,

1955   https://doi.org/10.2307/3626489, 1965.

1956   Song, P. S., Li, W., Sun, B., Nie, Z., Bu, L. Z., and Wang, Y. S.: Progress in the development and

1957   utilization of salt lake resources (in Chinese), Journal of Inorganic Chemistry, 27, 801–815, 2011.

1958   Sow, M., Goossens, D., and Rajot, J. L.: Calibration of the MDCO dust collector and of four versions of

1959   the inverted frisbee dust deposition sampler, Geomorphology, 82, 360-375,

1960   https://doi.org/10.1016/j.geomorph.2006.05.013, 2006.

1961   Strader, R., Lurmann, F., and Pandis, S. N.: Evaluation of secondary organic aerosol formation in winter,

1962   Atmospheric Environment, 33, 4849-4863, https://doi.org/10.1016/S1352-2310(99)00310-6, 1999.

1963   Sulong, N. A., Latif, M. T., Sahani, M., Khan, M. F., Fadzil, M. F., Tahir, N. M., Mohamad, N., Sakai,

1964   N., Fujii, Y., Othman, M., and Tohno, S.: Distribution, sources and potential health risks of

1965   polycyclic aromatic hydrocarbons (PAHs) in $PM_{2.5}$ collected during different monsoon seasons and

1966   haze episode in Kuala Lumpur, Chemosphere, 219, 1-14, https://doi.org/10.1016/j.chemosphere,

1967   2019.

1968   Tang, Y., Han, G. L. and Xu, Z. F.: Characteristics of black carbon content in atmospheric dust in Beijing

1969   and its northern regions (in Chinese), Acta Scientiae Circumstantiae, 33(02), 332-338,

1970   https://doi.org/10.13671/j.hjkxxb.2013.02.033, 2013.

1971   Tao, J., Cheng, T., Zhang, R., Cao, J., Zhu, L., Wang, Q., Luo, L., and Zhang, L.: Chemical composition

1972   of $PM_{2.5}$ at an urban site of Chengdu in southwestern China, Advances in Atmospheric Sciences, 30,

1973   1070-1084, https://doi.org/10.1007/s00376-012-2168-7, 2013.

1974   Tao, S., Ru, M. Y., Du, W., Zhu, X., Zhong, Q. R., Li, B. G., Shen, G. F., Pan, X. L., Meng, W. J., Chen,

1975   Y. L., Shen, H. Z., Lin, N., Su, S., Zhuo, S. J., Huang, T. B., Xu, Y., Yun, X., Liu, J. F., Wang, X. L.,

1976   Liu, W. X., Cheng, H. F., and Zhu, D. Q.: Quantifying the rural residential energy transition in China

1977   from 1992 to 2012 through a representative national survey, Nature Energy, 3, 567-573,

1978   https://doi.org/10.1038/s41560-018-0158-4, 2018.

1979   Tian, M., Gao, J., Zhang, L., Zhang, H., Feng, C., and Jia, X.: Effects of dust emissions from wind erosion

1980   of soil on ambient air quality, Atmospheric Pollution Research, 12,

1981   https://doi.org/10.1016/j.apr.2021.101108, 2021.

1982   Tian, S. L., Pan, Y. P., and Wang, Y. S.: Size-resolved source apportionment of particulate matter in urban

1983   Beijing during haze and non-haze episodes, Atmospheric Chemistry and Physics, 16, 1-19,

1984   https://doi.org/10.5194/acp-16-1-2016, 2016.

1985   Tiwari, S., Pandithurai, G., Attri, S. D., Srivastava, A. K., Soni, V. K., Bisht, D. S., Anil Kumar, V., and

1986   Srivastava, M. K.: Aerosol optical properties and their relationship with meteorological parameters

1987   during wintertime in Delhi, India, Atmospheric Research, 153, 465-479,

1988   https://doi.org/10.1016/j.atmosres.2014.10.003, 2015.

1989   Turpin, B. J. and Huntzicker, J. J.: Identification of secondary organic aerosol episodes and quantitation

1990   of primary and secondary organic aerosol concentrations during SCAQS, Atmospheric Environment,

1991   29, 3527-3544, https://doi.org/10.1016/1352-2310(94)00276-Q, 1995.

1992   Turpin, B. J., Huntzicker, J. J., and Hering, S. V.: Investigation of organic aerosol sampling artifacts in

1993   the los angeles basin, Atmospheric Environment, 28, 3061-3071, https://doi.org/10.1016/1352-

1994   2310(94)00133-6, 1994.

1995   VanCuren, R. and Gustin, M. S.: Identification of sources contributing to $PM_{2.5}$ and ozone at elevated

sites in the western U.S. by receptor analysis: Lassen Volcanic National Park, California, and Great Basin National Park, Nevada, Science of The Total Environment, 530-531, 505-518, https://doi.org/10.1016/j.scitotenv, 2015.

Venkataraman, C., Brauer, M., Tibrewal, K., Sadavarte, P., Ma, Q., Cohen, A., Chaliyakunnel, S., Frostad, J., Klimont, Z., Martin, R. V., Millet, D. B., Philip, S., Walker, K., and Wang, S.: Source influence on emission pathways and ambient $PM_{2.5}$ pollution over India (2015–2050), Atmospheric Chemistry and Physics, 18, 8017-8039, https://doi.org/10.5194/acp-18-8017-2018, 2018.

Wang, F.: The mechanism and timescales of soil formation in the hyper-arid Atacama Desert, Chile, Purdue University, 2013.

Wang, F., Michalski, G., Seo, J.-h., and Ge, W.: Geochemical, isotopic, and mineralogical constraints on atmospheric deposition in the hyper-arid Atacama Desert, Chile, Geochimica et Cosmochimica Acta, 135, 29-48, https://doi.org/10.1016/j.gca, 2014.

Wang, M., Duan, Y., Xu, W., Wang, Q., Zhang, Z., Yuan, Q., Li, X., Han, S., Tong, H., Huo, J., Chen, J., Gao, S., Wu, Z., Cui, L., Huang, Y., Xiu, G., Cao, J., Fu, Q., and Lee, S.: Measurement report: Characterisation and sources of the secondary organic carbon in a Chinese megacity over 5 years from 2016 to 2020, Atmospheric Chemistry and Physics, 22, 12789-12802, https://doi.org/10.5194/acp-22-12789-2022, 2022.

Watson, J. G., Antony Chen, L. W., Chow, J. C., Doraiswamy, P., and Lowenthal, D. H.: Source apportionment: Findings from the U.S. supersites program, Journal of the Air & Waste Management Association, 58, 265-288, https://doi.org/10.3155/1047-3289.58.2.265, 2008.

Wei, C., Bandowe, B. A. M., Han, Y., Cao, J., Zhan, C., and Wilcke, W.: Polycyclic aromatic hydrocarbons (PAHs) and their derivatives (alkyl-PAHs, oxygenated-PAHs, nitrated-PAHs and azaarenes) in urban road dusts from Xi'an, Central China, Chemosphere, 134, 512-520, https://doi.org/10.1016/j.chemosphere.2014.11.052, 2015.

Wei, T., Dong, Z., Kang, S., Qin, X., and Guo, Z.: Geochemical evidence for sources of surface dust deposited on the Laohugou glacier, Qilian Mountains, Applied Geochemistry, 79, 1-8, https://doi.org/10.1016/j.apgeochem, 2017.

Wei, Y., Xie, Y., Dang, X., Guo, J., Liu, M., and Wu, H.: Characteristics of atmospheric dust deposition and influencing factors in different protection functional areas of the Jilantai Salt Lake Protection system, Research of Soil and Water Conservation, 30, 201-208,

2026   https://doi.org/10.13869/j.cnki.rswc.2023.05.027, 2023.

2027   Wu, C. and Yu, J. Z.: Determination of primary combustion source organic carbon-to-elemental carbon

2028   (OC/EC) ratio using ambient OC and EC measurements: secondary OC-EC correlation

2029   minimization method, Atmospheric Chemistry and Physics, 16, 5453-5465,

2030   https://doi.org/10.5194/acp-16-5453-2016, 2016.

2031   Wu, C., Wu, D., and Yu, J. Z.: Quantifying black carbon light absorption enhancement with a novel

2032   statistical approach, Atmospheric Chemistry and Physics, 18, 289-309, https://doi.org/10.5194/acp-

2033   18-289-2018, 2018a.

2034   Wu, Y., Zhang, R., Tian, P., Tao, J., Hsu, S. C., Yan, P., Wang, Q., Cao, J., Zhang, X., and Xia, X.: Effect

2035   of ambient humidity on the light absorption amplification of black carbon in Beijing during January

2036   2013, Atmospheric Environment, 124, 217-223, https://doi.org/10.1016/j.atmosenv.2015.04.041,

2037   2016.

2038   Xia, X., Zong, X., Cong, Z., Chen, H., Kang, S., and Wang, P.: Baseline continental aerosol over the

2039   central Tibetan plateau and a case study of aerosol transport from South Asia, Atmospheric

2040   Environment, 45, 7370-7378, https://doi.org/10.1016/j.atmosenv.2011.07.067, 2011.

2041   Xiao, Q., Saikawa, E., Yokelson, R. J., Chen, P., Li, C., and Kang, S.: Indoor air pollution from burning

2042   yak dung as a household fuel in Tibet, Atmospheric Environment, 102, 406-412,

2043   https://doi.org/10.1016/j.atmosenv, 2015.

2044   Xie, F., Guo, L., Wang, Z., Tian, Y., Yue, C., Zhou, X., Wang, W., Xin, J., and Lu, C.: Geochemical

2045   characteristics and socioeconomic associations of carbonaceous aerosols in coal-fueled cities with

2046   significant seasonal pollution pattern, Environmental International, 179, 108179,

2047   https://doi.org/10.1016/j.envint.2023.108179, 2023.

2048   Xu, L., Chen, X., Chen, J., Zhang, F., He, C., Zhao, J., and Yin, L.: Seasonal variations and chemical

2049   compositions of PM2.5 aerosol in the urban area of Fuzhou, China, Atmospheric Research, 104-

2050   105, 264-272, https://doi.org/10.1016/j.atmosres, 2012.

2051   Xu, M., Liu, Z., Hu, B., Yan, G., Zou, J., Zhao, S., Zhou, J., Liu, X., Zheng, X., Zhang, X., Cao, J., Guan,

2052   M., Lv, Y., and Zhang, Y.: Chemical characterization and source identification of $PM_{2.5}$ in Luoyang

2053   after the clean air actions, Journal of Environmental Sciences, 115, 265-276,

2054   https://doi.org/10.1016/j.jes.2021.06.021, 2022.

2055   Xu, R., Tie, X., Li, G., Zhao, S., Cao, J., Feng, T., and Long, X.: Effect of biomass burning on black

carbon (BC) in South Asia and Tibetan Plateau: The analysis of WRF-Chem modeling, Science of The Total Environment, 645, 901-912, https://doi.org/10.1016/j.scitotenv.2018.07.165, 2018b.

Xu, Z., Wang, J., and Han, J.: Ecological vulnerability assessment of the Qaidam Basin based on the SRP Model, Salt Lake Research, 32, 53-60, https://doi.org/10.3724/j.yhyj.2024009, 2024.

Xu, Z.: Airborne particles in outdoor air: Atmospheric dust, in: Fundamentals of air cleaning technology and its application in cleanrooms, Springer Berlin Heidelberg, 47-132, https://doi.org/10.1007/978-3-642-39374-7_2, 2014.

Xue, W., Wang, L., Yang, Z., Xiong, Z., Li, X., Xu, Q., and Cai, Z.: Can clean heating effectively alleviate air pollution: An empirical study based on the plan for cleaner winter heating in northern China, Applied Energy, 351, 121923, https://doi.org/10.1016/j.apenergy, 2023.

Yan, B., Zheng, M., Hu, Y., Ding, X., Sullivan, A. P., Weber, R. J., Baek, J., Edgerton, E. S., and Russell, A. G.: Roadside, urban, and rural comparison of primary and secondary organic molecular markers in ambient $PM_{2.5}$, Environmental Science & Technology, 43, 4287-4293, https://doi.org/10.1021/es900316g, 2009.

Yang, F., He, K., Ye, B., Chen, X., Cha, L., Cadle, S. H., Chan, T., and Mulawa, P. A.: One-year record of organic and elemental carbon in fine particles in downtown Beijing and Shanghai, Atmospheric Chemistry and Physics, 5, 1449-1457, https://doi.org/10.5194/acp-5-1449-2005, 2005.

Yang, Q. L., Wang, J. X. and Zhao, Z. X.: Temporal and spatial distribution characteristics and source analysis of heavy metals in atmospheric dust in typical industrial cities in Northeast China during winter and spring (in Chinese), Acta Scientiae Circumstantiae, 1-9, https://doi.org/10.13671/j.hjkxxb.2024.0254, 2024.

Yao, L., Yang, L., Yuan, Q., Yan, C., Dong, C., Meng, C., Sui, X., Yang, F., Lu, Y., and Wang, W.: Sources apportionment of $PM_{2.5}$ in a background site in the North China Plain, Science of the Total Environment, 541, 590-598, https://doi.org/10.1016/j.scitotenv, 2016.

Ye, W., Saikawa, E., Avramov, A., Cho, S. H., and Chartier, R.: Household air pollution and personal exposure from burning firewood and yak dung in summer in the eastern Tibetan Plateau, Environmental Pollution, 263, 114531, https://doi.org/10.1016/j.envpol, 2020.

Yoo, H. Y., Kim, K. A., Kim, Y. P., Jung, C. H., Shin, H. J., Moon, K. J., Park, S. M., and Lee, J. Y.: Validation of SOC estimation using OC and EC concentration in $PM_{2.5}$ measured at Seoul, Aerosol and Air Quality Research, 22, 210388, https://doi.org/10.4209/aaqr.210388, 2022.

You, S., Yao, Z., Dai, Y., and Wang, C. H.: A comparison of PM exposure related to emission hotspots in a hot and humid urban environment: Concentrations, compositions, respiratory deposition, and potential health risks, Science of The Total Environment, 599-600, 464-473, https://doi.org/10.1016/j.scitotenv.2017.04.217, 2017.

Yu, H., Yang, W., Wang, X., Yin, B., Zhang, X., Wang, J., Gu, C., Ming, J., Geng, C., and Bai, Z.: A seriously sand storm mixed air-polluted area in the margin of Tarim Basin: Temporal-spatial distribution and potential sources, Science of The Total Environment, 676, 436-446, https://doi.org/10.1016/j.scitotenv, 2019.

Yu, L. P., Li, D., Meng, L., Du, C. Y. and Zhao, P.: Observation and data processing methods for atmospheric dust deposition (in Chinese), Anhui Agricultural Sciences, 44: 185-186, https://doi.org/10.13989/j.cnki.0517-6611.2016.31.064, 2016.

Yu, L., Wang, G., Zhang, R., Zhang, L., Song, Y., Wu, B., Li, X., An, K., and Chu, J.: Characterization and source apportionment of $PM_{2.5}$ in an urban environment in Beijing, Aerosol and Air Quality Research, 13, 574-583, https://doi.org/10.4209/aaqr.2012.07.0192, 2013.

Yue, D., Zhong, L., Zhang, T., Shen, J., Zhou, Y., Zeng, L., Dong, H., and Ye, S.: Pollution properties of water-soluble secondary inorganic ions in atmospheric $PM_{2.5}$ in the Pearl River Delta Region, Aerosol and Air Quality Research, 15, 1737-1747, https://doi.org/10.4209/aaqr.2014.12.0333, 2015.

Zan, J., Maher, B. A., Fang, X., Stevens, T., Ning, W., Wu, F., Yang, Y., Kang, J., and Hu, Z.: Global dust impacts on biogeochemical cycles and climate, Nature Reviews Earth & Environment, 6, 789-807, https://doi.org/10.1038/s43017-025-00734-2, 2025.

Zang, L., Zhang, Y., Zhu, B., Mao, F., Zhang, Y., and Wang, Z.: Characteristics of water-soluble inorganic aerosol pollution and its meteorological response in Wuhan, Central China, Atmospheric Pollution Research, 12, 362-369, https://doi.org/10.1016/j.apr.2021.01.003, 2021.

Zhan, C., Han, Y., Cao, J., Wei, C., Zhang, J., and An, Z.: Validation and application of a thermal–optical reflectance (TOR) method for measuring black carbon in loess sediments, Chemosphere, 91, 1462-1470, https://doi.org/10.1016/j.chemosphere.2012.12.011, 2013.

Zhan, C. L., Zhan, J. W., Ke, Z. D., Liu, S., Zhang, J. Q. and Liu, H. X.: Pollution characteristics and source analysis of black carbon in different types of dust in Xiaogan, Hubei (in Chinese), Environmental Pollution and Control 44(01), 14-19＋26, https://doi.org/10.15985/j.cnki.1001-3865, 2022.

Zhan, C. L., Zhang, J. Q., Zheng, J. G., Yao, R. Z., Xiao, W. S. and Cao, J. J.: Pollution characteristics and source analysis of black carbon in atmospheric dust along National Highway 316 (in Chinese), Environmental Science and Technology, 39(04), 154-160, https://doi.org/10.3969-j.issn.1003-6504.20169, 2016.

Zhang, B., Shen, Z., Sun, J., He, K., Zou, H., Zhang, Q., Li, J., Xu, H., Liu, S., Ho, K.-F., and Cao, J.: County-level of particle and gases emission inventory for animal dung burning in the Qinghai–Tibetan Plateau, China, Journal of Cleaner Production, 367, https://doi.org/10.1016/j.jclepro.2022.133051, 2022.

Zhang, F.: Study on the dry deposition of organic carbon and elemental carbon in the atmosphere of Nanchang (in Chinese), Master's Thesis, 2014.

Zhang, F., Wang, Z. W., Cheng, H. R., Lv, X. P., Gong, W., Wang, X. M., and Zhang, G.: Seasonal variations and chemical characteristics of $PM_{2.5}$ in Wuhan, central China, Science of the Total Environment, 518-519, 97-105, https://doi.org/10.1016/j.scitotenv, 2015a.

Zhang, J., Liu, H. N., Zheng, Q. P., and Tang, L. J.: Correlation study between particulate matter and visibility in Suzhou, Proceedings of the 7th Annual Conference of Chinese Society of Particuology cum Symposium on Particle Technology across Taiwan Straits, Xi'an, Shaanxi, China, 1, 2010.

Zhang, H. and Han, F.: The preliminary remote sensing interpretation of salt lake and its environments in the Central Qaidam Basin, Northwest China, Journal of Salt Lake Research, 10, 28-34, 2002.

Zhang, J., Smith, K. R., Ma, Y., Ye, S., Jiang, F., Qi, W., Liu, P., Khalil, M. A. K., Rasmussen, R. A., and Thorneloe, S. A.: Greenhouse gases and other airborne pollutants from household stoves in China: a database for emission factors, Atmospheric Environment, 34, 4537-4549, https://doi.org/10.1016/S1352-2310(99)00450-1, 2000.

Zhang, J., Huang, X., Li, J., Chen, L., Zhao, R., Wang, R., Sun, W., Chen, C., Su, Y., Wang, F., Huang, Y., and Lin, C.: Chemical composition, sources and evolution of $PM_{2.5}$ during wintertime in the city cluster of southern Sichuan, China, Atmospheric Pollution Research, 14, 101635, https://doi.org/10.1016/j.apr.2022.101635, 2023.

Zhang, K., Shang, X., Herrmann, H., Meng, F., Mo, Z., Chen, J., and Lv, W.: Approaches for identifying $PM_{2.5}$ source types and source areas at a remote background site of South China in spring, Science of The Total Environment, 691, 1320-1327, https://doi.org/10.1016/j.scitotenv, 2019.

Zhang, N., Cao, J., Liu, S., Zhao, Z., Xu, H., and Xiao, S.: Chemical composition and sources of $PM_{2.5}$

and TSP collected at Qinghai Lake during summertime, Atmospheric Research, 138, 213-222, https://doi.org/10.1016/j.atmosres, 2014.

Zhang, P. X.: Salt lakes in the Qaidam Basin (in Chinese), Beijing: Science Press, 1987.

Zhang, R., Wang, H., Qian, Y., Rasch, P. J., Easter, R. C., Ma, P. L., Singh, B., Huang, J., and Fu, Q.: Quantifying sources, transport, deposition, and radiative forcing of black carbon over the Himalayas and Tibetan Plateau, Atmospheric Chemistry and Physics, 15, 6205-6223, https://doi.org/10.5194/acp-15-6205-2015, 2015b.

Zhang, R., Jing, J., Tao, J., Hsu, S. C., Wang, G., Cao, J., Lee, C. S. L., Zhu, L., Chen, Z., Zhao, Y., and Shen, Z.: Chemical characterization and source apportionment of $PM_{2.5}$ in Beijing: seasonal perspective, Atmospheric Chemistry and Physics, 13, 7053-7074, https://doi.org/10.5194/acp-13-7053-2013, 2013.

Zhang, S.: Spatial and temporal variation characteristics of atmospheric dust deposition flux in Hebei Province over the Recent 20 Years, Master's thesis, Hebei Normal University, 2010.

Zhang, X. Y., Wang, Y. Q., Zhang, X. C., Guo, W., and Gong, S. L.: Carbonaceous aerosol composition over various regions of China during 2006, Journal of Geophysical Research: Atmospheres, 113, https://doi.org/10.1029/2007jd009525, 2008.

Zhang, X. Y., Wang, Y. Q., Wang, D., Gong, S. L., Arimoto, R., Mao, L. J., and Li, J.: Characterization and sources of regional-scale transported carbonaceous and dust aerosols from different pathways in coastal and sandy land areas of China, Journal of Geophysical Research: Atmospheres, 110, https://doi.org/10.1029/2004jd005457, 2005.

Zhang, Y.: Satellite Observation and ground validation of volatile organic compounds emissions from biomass combustion, Master's thesis, Yunnan University, https://doi.org/10.27456/d.cnki.gyndu.2024.002784, 2024.

Zhang, Z., Zhou, Y., Zhao, N., Li, H., Tohniyaz, B., Mperejekumana, P., Hong, Q., Wu, R., Li, G., Sultan, M., Zayan, A. M. I., Cao, J., Ahmad, R., and Dong, R.: Clean heating during winter season in Northern China: A review, Renewable and Sustainable Energy Reviews, 149, 111339, https://doi.org/10.1016/j.rser, 2021.

Zhang, Z. C., Xie, Y. Q., Zhang, Z. J., Gao, G. S., Xu, B., Tian, X., Xu, H., Wie, Y. T., Shi, G. L. and Feng, Y. C.: Source analysis and seasonal variation characteristics of atmospheric dust deposition in Taiyuan City based on two receptor models (in Chinese), China Environmental Science, 42, 2577-

2586, https://doi.org/10.3969/j.issn.1000-6923, 2022.

Zhao, Z., Cao, J., Shen, Z., Xu, B., Zhu, C., Chen, L. W. A., Su, X., Liu, S., Han, Y., Wang, G., and Ho, K.: Aerosol particles at a high-altitude site on the Southeast Tibetan Plateau, China: Implications for pollution transport from South Asia, Journal of Geophysical Research: Atmospheres, 118, https://doi.org/10.1002/jgrd.50599, 2013.

Zheng, J., Hu, M., Du, Z., Shang, D., Gong, Z., Qin, Y., Fang, J., Gu, F., Li, M., Peng, J., Li, J., Zhang, Y., Huang, X., He, L., Wu, Y., and Guo, S.: Influence of biomass burning from South Asia at a high-altitude mountain receptor site in China, Atmospheric Chemistry and Physics, 17, 6853-6864, https://doi.org/10.5194/acp-17-6853-2017, 2017.

Zheng, K., Li, Y., Li, Z., and Huang, J.: Provenance tracing of dust using rare earth elements in recent snow deposited during the pre-monsoon season from mountain glaciers in the central to northern Tibetan Plateau, Environmental Science and Pollution Research, 28, 45765-45779, https://doi.org/10.1007/s11356-021-13561-x, 2021.

Zheng, M. P.: Geological report on salt lake resources and ecological environment in China (in Chinese), Acta Geologica Sinica, 84: 1613-1622. https://doi.org/10.19762/j.cnki.dizhixuebao, 2017.

Zhou, Y., Gao, X., and Lei, J.: Characteristics of dust weather in the Tarim Basin from 1989 to 2021 and its impact on the atmospheric environment, https://doi.org/10.3390/rs15071804, 2023.

Zhou, Y., Yang, J., Kang, S., Hu, Y., Chen, X., Xu, M., and Ma, M.: Black carbon aerosols impact snowfall over the Tibetan Plateau, Geoscience Frontiers, 16, 101978, https://doi.org/10.1016/j.gsf, 2025.

Zhu, C. S., Chen, C. C., Cao, J. J., Tsai, C. J., Chou, C. C. K., Liu, S. C., and Roam, G. D.: Characterization of carbon fractions for atmospheric fine particles and nanoparticles in a highway tunnel, Atmospheric Environment, 44, 2668-2673, https://doi.org/10.1016/j.atmosenv, 2010.

Zhu, H., Li, W., Kong, X., and Zhang, X.: Overlooked contribution of salt lake emissions: A case study of dust deposition from the Qinghai-Xizang Plateau, Journal of Geophysical Research: Atmospheres, 130, e2024JD042693, https://doi.org/10.1029/2024JD042693, 2025.

Zhu, H. X.: The dust deposition data of the Qaidam Basin [Dataset]. Zenodo. https://doi.org/10.5281/zenodo.14382853, 2024.

Zhu, X., Zhu, K., Xie, M., Huang, A., Ouyang, Y., Chen, F., and Zhao, W.: Analysis of current situation and future trend of anthropogenic heat emissions in Jiangsu Province, Climatic and Environmental

2206   Research, 21, 306-312, https://doi.org/10.3878/j.issn.1006-9585.2016.15171, 2016.